ISSN 2960-284X

Journal of Biosciences and Experimental Pharmacology

Volume 1, Number 1, December 2023

Published by
Dr. Nusrat Subhan

In association with School of Health and Life Sciences, North South University

Mailing Address:
Dr. Nusrat Subhan and Son's Science Publisher
Dr. Nusrat Subhan, House 229, Road 2, Block-B, Bashundhara, Dhaka, 1229

ISSN 2960-284X

Journal of Biosciences and Experimental Pharmacology

Journal of Biosciences and Experimental Pharmacology

ISSN- 2960-284X

Journal of Biosciences and Experimental Pharmacology
ISSN- 2960-284X

CONTENT Volume 1, 2023

Message from the Chief Editor

Welcome to the inaugural volume and issue of the Journal of Biosciences and Experimental Pharmacology (JBEP). We are pleased to share with our readers six brand-new papers from writers who have kindly shared their research findings on a range of pharmacy and pharmacology-related topics in this issue. The biosciences and pharmacology are very dynamic fields. For the creation of new drugs and drug delivery systems, research and development of new instruments, strategies, and processes are needed. Research conducted by academicians at different universities bridges the gap between industrial requirements for drug development and drug delivery systems and those of the academic curriculum.

Papers in the areas of pharmaceutical formulation development, phytochemistry, nanodrug delivery, and pharmaceutical analysis are included in this issue. Despite our best efforts, some of the articles and papers could not be included in the current edition due to decisions made by the editorial board and the referee review board. None of the writers should be discouraged from submitting their original works, case studies, research reviews, or empirical contributions to our journal in the future, though.

We would like to express our gratitude to all of our authors for making this issue possible as well as to our reviewers for helping us guarantee that JBEP is of the high caliber we aim to maintain. We sincerely hope that all parties involved—from authors to reviewers—will keep firmly backing our publication.

Dr. Md. Ashraful Alam
Chief Editor
Journal of Biosciences and Experimental Pharmacology

JBEP

Journal of Biosciences and Experimental Pharmacology
ISSN-2960-284X

Original Article

Comparative HPLC Analysis of Flavonoid Content and Antioxidant Activity of *Ginkgo biloba* Products Available in the Bangladeshi Market

Raushanara Akter[1]*, Sarin Ahmed[1], Md. Tanvir Kabir[1]

[1]*Department of Pharmacy, BRAC University, 66 Mohakhali, Dhaka 1212, Bangladesh*

Correspondence *E-mail: raushanara@bracu.ac.bd

Citation: Akter R.; Ahmed S..; Kabir M. T.; Comparative HPLC analysis of flavonoid content and antioxidant activity of *Ginkgo biloba* products available in the Bangladeshi market. *J. Bio. Exp. Pharm.* 2023, 1:01–15.

Received: October 8, 2023
Accepted: December 3, 2023
Published: December 15, 2023

Publisher's Note: JBEP stays neutral with regard to jurisdictional claims in published maps and institutional affiliations.

Abstract: Different brands of *Ginkgo biloba* standardized extract available in the Bangladeshi market are widely used for the symptomatic treatment of cognitive dysfunction, dementia, Alzheimer's disease, etc. This study was conducted to evaluate the quality of two *Ginkgo biloba* capsule dosage forms; one is from a mainstream pharmaceutical company (sample 2) and another is from a recognized herbal drug manufacturing company (sample 1). To assess their quality, the qualitative and quantitative analysis of the flavonoid content of the selected products were performed by HPLC followed by antioxidant activity determination using different antioxidant activity study methods. HPLC analysis of them identified the presence of two principal flavonoids; quercetin and kaempferol in the quantity of 6.01 and 0.29 mg in sample 2; and 1.34 and 0.28 mg in sample 1. Thus, the HPLC analysis revealed that the quantity of quercetin and kaempferol present in sample 2 was higher than in sample 1. In the DPPH assay, sample 2 showed higher DPPH free radical scavenging power with an IC_{50} of 0.34 mg/mL than sample 1 with an IC_{50} of 0.57 mg/mL Moreover, sample 2 showed higher TPC, TFC, and TAC than sample 1.

Keywords*: Ginkgo biloba*; Phytochemical screening; HPLC; Flavonoids; Antioxidant activity

1. Introduction

According to the World Health Organization (WHO), a total of 55 brands of herbal products are registered which are mentioned in the database of the Directorate General of Drug Administration (DGDA), Bangladesh as of 2012 [1,2]. A total of 25 Pharmaceutical companies (herbal division) and Herbal drug manufacturing companies in Bangladesh are producing herbal medicines [3]. Several brands of *Ginkgo biloba* extracts are manufactured by Bangladeshi Pharmaceutical companies and herbal drug manufacturing companies. The quality of products is of utmost priority for the drugs to be effective and safe [3,4]. Drugs may be collected from multiple sources, and the quality of the drugs can be varied accordingly. Thus, there might be a possibility of the presence of some substandard drugs along with standard

drugs [5]. This raises a concern regarding the safety, efficacy, and price of the medicines available in the market, and therefore physicians and patients must be extremely conscious while selecting medicines [4]. Post-market monitoring performs as a confidential mechanism to assess the quality, therapeutic efficacy, and safety of commercially available drug products [6]. Findings of such monitoring help accelerate product development and improve existing regulations to ensure the desired quality of the drug products [7].

Ginkgo biloba belongs to the Ginkgoaceae family and has a long history of use in traditional Chinese medicines. Extracts of *Ginkgo biloba* are well-documented with therapeutic effects to improve cognitive function and increase blood circulation in the brain and the entire body. It has been reported to be effective in mild to moderate cerebrovascular insufficiency, in the reduction of depression and thrombosis, and inhibition of platelet aggregation. Most importantly, *Ginkgo biloba* extract can improve concentration, and thinking problems, combat short-term memory loss, and thus, improve symptoms of Alzheimer's disease and dementia. It has also been found effective in treating Raynaud's disease, peripheral vascular disease, arterial occlusive disease, blood disorders, COPD symptoms, vision problems, vertigo, and tinnitus [8,9,10]. High-quality standardized *Ginkgo biloba* extract contains 24 % flavones glycosides namely, kaempferol, quercetin, and isorhamnetin along with 6 % terpene lactones such as bilobalide and Ginkgolides A, B, and C. Between these two main constituents of *Ginkgo biloba*, flavone glycosides are responsible for antioxidant activity while Ginkgolide is responsible for neuroprotection, improves choline uptake in the brain synapses, and reduces blood clotting [8,11]. Quercetin, a flavonol is abundantly present in the standardized *Ginkgo biloba* extract and exerts potent antioxidant effects by free radical scavenging activity which is attributed to the right molecular structure of quercetin [12].

After going through an in-depth literature review on *Ginkgo biloba*, it was found that post-market HPLC analysis of flavonoid content and *in-vitro* antioxidant potential of marketed samples containing standardized *Ginkgo biloba* extract had never been performed before in Bangladesh. This fact led us to assess the quality of commercially available *Ginkgo biloba* capsules in the Bangladeshi market where one of them (sample 1) was from a nationally recognized herbal drug manufacturing company and the other one (sample 2) was from a top-ranked mainstream pharmaceutical company. This study was devised to perform phytochemical screening and qualitative and quantitative HPLC analysis of flavonoids (quercetin and kaempferol) of the selected commercial products followed by determination of their antioxidant activity to compare their quality. These two products are commercially available in capsule dosage forms of 60 and 120 mg and are therapeutically used to treat cerebral insufficiency, and dementia syndromes:

memory deficit, poor concentration, Alzheimer's disease, depression, cognitive dysfunction, etc. **(Table 1)**.

2. Materials and Methods

2.1 Sample Collection

Selected two *Ginkgo biloba* brands were bought from a local authorized pharmacy shop in Mohakhali, Dhaka, Bangladesh. A general description of these two marketed samples is listed in **Table 1** and this information on the selected products was extracted from the websites of the selected companies.

Table 1. Description of the selected *Ginkgo biloba* products available in Bangladesh market

Sample no.	Dosage form (Dose)	Dosage and administration	Indications
Sample 1	Capsule (60 mg)	1 capsule twice daily	Cognitive dysfunction, Dementia, Alzheimer's disease, loss of memory and concentration, tinnitus, vertigo and cochlear deafness, senile macular degeneration and diabetic retinopathy, Raynaud's disease and acrocyanosis, intermittent claudication, varicose vein and bronchial asthma
Sample 2	Capsule (60 mg)	For adults: 120-240 mg/day. 1 or 2 capsules 2 to 3 times daily or as advised by the physician.	Cerebral insufficiency: memory deficit, depression, attention, and memory loss that occur with Alzheimer's disease and multi-infarct dementia. Vertigo and tinnitus, Peripheral vascular disease: improvement of pain-free walking distance in, Peripheral Arterial Occlusive Disease in Stage II according to Fontaine (intermittent claudication) in a regimen of physical therapeutic measures, walking exercise, acute cochlear deafness, and sexual dysfunction associated with SSRI use.

2.2 Preliminary phytochemical screening

A preliminary phytochemical screening was performed on the methanolic leaf extract of *Ginkgo biloba* from two commercial products according to the methods described by [13,14] to determine its qualitative chemical compositions, namely, the presence/absence of flavonoids, terpenoids, glycosides, alkaloids, sterols, coumarin, resins, phenolic compounds, tannin, saponins, etc.

2.3 High-performance liquid chromatography (HPLC) employed metabolite profiling of two Ginkgo biloba commercial products

HPLC analysis of *Ginkgo biloba* capsules containing standardized extract was performed to quantitatively identify two flavonoids; kaempferol and quercetin using the method explained in the United States Pharmacopoeia [15]. Alcohol, hydrochloric acid (HCl), and distilled water (H_2O) were added to a 100 mL volumetric flask at the ratio of 25:4:10 to prepare the extraction solvent. On the other hand, methanol, water, and phosphoric acid were mixed in a 100 mL volumetric flask at the ratio of 100:100:1 to prepare the mobile phase. Standard solution A (Quercetin standard solution) was prepared by measuring and dissolving 0.02 mg of USP Quercetin RS (Reference standard) in 1 mL methanol. Standard solution B (Kaempferol standard solution) was prepared by measuring and dissolving 0.02 mg of USP Kaempferol RS in 1 mL methanol. Approximately 1g of *Ginkgo biloba* fine powder from both *Ginkgo biloba* capsules (Marketed samples) was transferred to a 250 mL reflux condenser and round bottom flask fitted and 78 mL of the extraction solvent was added to the reflux condenser. The reflux condenser was placed in a hot water bath for a duration of 35 minutes until the solution turned into a deep red color and then the solution was allowed to cool at room temperature and decanted to a 100 mL volumetric flask. 20 mL of methanol was added again to the 250 mL flask and sonication was performed for 30 minutes. The solution was then filtered, and the filtrate was collected in a 100 mL volumetric flask. The residue on the filter was washed with methanol and collected in the same 100 mL volumetric flask which was later diluted with methanol to volume up to 100 mL and mixed. The extraction of flavonoids from the commercial *Ginkgo biloba* capsule powder was performed separately. Then, 20 µL of the solution was taken and injected into the HPLC column to obtain the HPLC chromatogram and detect the desired flavonoids at UV 370 nm at a flow rate of 1.5 mL/min on LC mode through 4.6 mm×25 cm (packing L1) column (Luna, Phenomenex) and the total run time was 50 minutes. It is important to note that the relative retention times (RTs) for Quercetin in standard solution A, and Kaempferol in standard solution B, are approximately 25.627 and 45.560 minutes, respectively. Finally, the percentage of Quercetin and Kaempferol present in the portion of *Ginkgo biloba* powder taken from the two samples was calculated

using the equation, quantity of flavonoid (mg) = (r_u/r_s) ×(Cs/W) ×F×10 Where r_u = Peak area of the relevant analyte of the Sample solution; r_s = Peak area of the relevant analyte of the Standard solution A/ Standard solution B; Cs = Concentration of the relevant analyte in Standard solution A/ Standard solution B; W = Weight of sample powder taken to prepare the Sample solution and F = Mean molecular mass factor used to convert each analyte into flavone glycoside with a mean molecular mass of 756.7: 2.504 for Quercetin and 2.588 for Kaempferol.

2.4 In-vitro antioxidant activity screening of two commercial Ginkgo biloba products

In-vitro antioxidant activity of the aqueous extracts of the two *Ginkgo biloba* commercial products was estimated using four methods were such as: DPPH free radical scavenging assay, total phenolic content (TPC), total flavonoid content (TFC), and total antioxidant capacity (TAC).

2.5 DPPH (1, 1-diphenyl-2-picryl hydrazyl) free radical scavenging assay

The DPPH free radical scavenging assay of aqueous extract of *Ginkgo biloba* from two marketed samples was determined using the method described by [16] and L-ascorbic acid was used as the standard. Different concentrations of sample solutions: 50-1200 µg/mL were prepared by serial dilution. The absorbance of the sample solutions and control (DPPH and methanol) were measured at 517 nm using U-2910 UV-Vis spectrophotometer (U-1800 SHIMADZU, Japan). The percentage inhibition of DPPH free radicals and the IC_{50} values were calculated.

2.6 Determination of total phenolic content (TPC)

The TPC of aqueous extracts of samples 1 and 2 was determined by the modified Folin Ciocalteu method [17]. Different concentrations of solutions of two samples ranging from 200 to 1200 µg/mL were prepared by serial dilution of stock solution with a concentration of 12 mg/mL. Gallic acid was used as a standard. The absorbance of standard and sample solutions was measured against a blank at 765 nm using a spectrophotometer (U-1800 SHIMADZU, Japan). TPC was expressed as gallic acid equivalent (GAE in mg) per gram of crude extracts.

2.7 Determination of total flavonoid content (TFC)

The total flavonoid content of the aqueous extract of two *Ginkgo biloba* products was determined according to the method described by [18]. TFC was also determined using the same concentration range as used for the TPC estimation of both samples. Quercetin was used as the standard and the stock solution was prepared in the same manner as the extract resulting in four serially diluted concentrations,

ranging from 1200, 800, 400, and 200 µg/mL. The absorbance of each of the sample and standard solutions was measured at 415nm against a blank using UV-Vis spectrophotometer (U-1800 SHIMADZU, Japan). The TFC of each of the samples was expressed as quercetin equivalents (QE) per gram of extracts.

2.8 Determination of total antioxidant capacity (TAC)

The total antioxidant capacity of two commercial products containing *Ginkgo biloba* standardized extracts was determined by using the method described by [19]. The sample and the standard ascorbic acid solutions ranging from 1200 to 200 µg/mL were prepared by serial dilution. Finally, the absorbance of the sample and standard solutions was measured against a blank at 695 nm using a UV-Vis spectrophotometer (U-1800 SHIMADZU, Japan). The total antioxidant capacity, A, for each of the fractions were expressed as ascorbic acid equivalents (AAE) in mg per gram of extracts.

3. Results

3.1 Preliminary phytochemical screening

Preliminary phytochemical screening of two commercial samples was conducted using methods described by [13,14] to detect the presence of different classes of phytoconstituents such alkaloids, flavonoids, coumarins, glycosides, terpenoids, tannins, saponins, phenolics, etc. The result is evident that both the samples contain flavonoids, coumarins, terpenoids, tannins, and phenolics **(Table 2)**. However, alkaloids, glycosides, sterols, saponins and resins were absent in both products.

Table 2. Results of preliminary phytochemical screening of sample 1 and sample 2

	Class of compound	**Result**	
		Sample 1	**Sample 2**
1.	Alkaloids	-	-
2.	Flavonoids	++++	++++
3.	Terpenoids	+	+
4.	Phenols/Phenolic compounds	++	++
5.	Glycosides	-	-
6.	Tannins	+++	+++
7.	Coumarins	++	++
8.	Resins	-	-
9.	Phytosterols	-	-
10.	Saponins	-	-

(+) means presence in a single method test, (++) means presence experimented in two methods, (+++) means presence experimented in three methods, (++++) means presence experimented in four methods and (-) means absence.

3.2 Identification and quantification of quercetin and kaempferol in sample 1 and sample 2 using the HPLC method

HPLC analysis of the selected samples was performed at 370 nm following standard protocol [15]. The standard Quercetin and Kaempferol produced peaks at 25.627 and 45.560 minutes in the HPLC chromatograms, respectively **(Figure 1 and 2)**. From the chromatogram of two samples, the presence of two flavonoids; quercetin and kaempferol in both samples were identified and quantified with comparison to retention time and peak area of two standards, respectively. In the case of the samples, sample 1 contained 1.34 mg of quercetin per capsule with a retention time of 25.500 minutes and 0.28 mg of kaempferol per capsule with a retention time of 45.727 minutes **(Figure 3 and 5).** On the other hand, sample 2 contained 6.01 mg of quercetin per capsule with a retention time of 25.793 minutes and 0.29 mg of kaempferol per capsule with a retention time of 45.847 minutes **(Figure 4 and 5).**

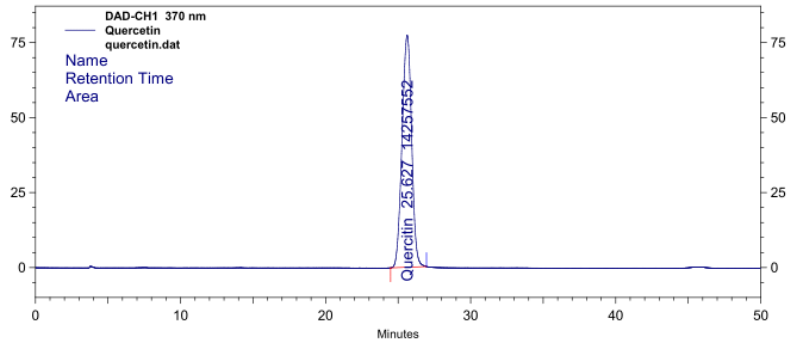

Figure 1. Identification of standard Quercetin by HPLC analysis

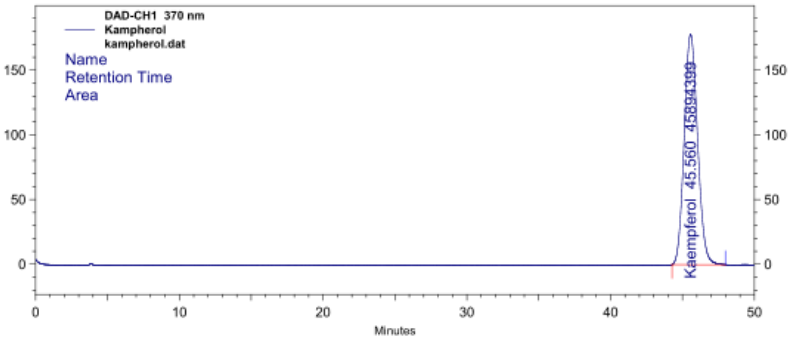

Figure 2. Identification of standard Kaempferol by HPLC analysis

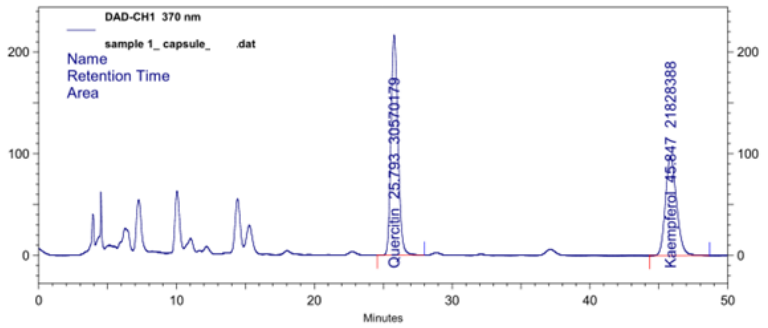

Figure 3. Identification of Quercetin and Kaempferol present in sample 1 by HPLC analysis

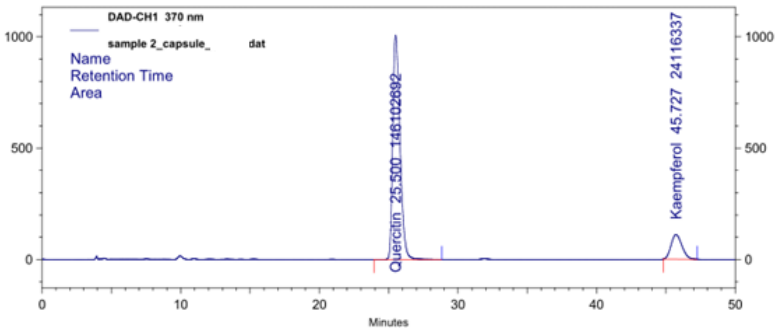

Figure 4. Identification of quercetin and kaempferol present in Sample 2 by HPLC analysis

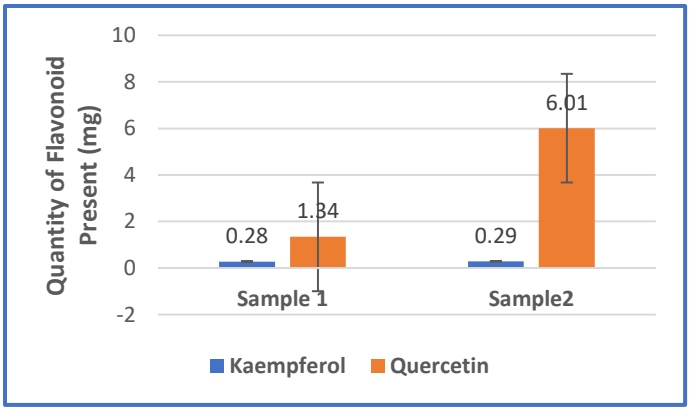

Figure 5. Quantity of two flavonoids; quercetin and kaempferol present in samples 1 and 2

3.3 Evaluation of antioxidant activity

3.3.1 DPPH ((1, 1-diphenyl-2-picryl hydroxyl) free radical scavenging potential of sample 1 and sample 2

DPPH free radical scavenging potential of both samples was found to increase with increased concentrations and at the highest concentration of 1200 µg/mL, both products exhibited the highest % of DPPH free radical inhibition which was 88.022±0.36 and 96.892±0.45 % for sample 1 and sample 2, respectively. IC_{50} values were found to be 566.00 and 333.99 µg/mL for sample 1 and sample, respectively. IC_{50} value of the standard ascorbic acid was found to be 300.50 µg/mL which was comparable to that of sample 2 **(Table 3)**.

Table 3. DPPH free radical scavenging activity of sample 1, sample 2, and the standard (Ascorbic acid).

Concentration (µg/mL)	**DPPH free radical scavenging assay (% of inhibition)**		
	Sample 1	**Sample 2**	**Standard (Ascorbic acid)**
50	15.706±0.25	15.367±0.22	27.797
100	32.005±0.41	25.124±0.41	39.661
200	35.706±0.21	55.367±0.30	52.542
400	47.005± 0.57	74.124± 0.23	60.790
800	58.757± 0.44	80.451± 0.25	76.723
1200	88.022± 0.36	96.892± 0.45	85.650
IC_{50} (µg/mL)	566.00	333.99	300.50

The values are the average of triplicates of experiments and are represented as mean ± % of relative standard deviation.

3.4 Total phenolic content (TPC) of sample 1 and sample 2

TPC of the samples was calculated using the standard curve of gallic acid ($y = 0.0002x + 0.0393$; R^2=0.988) and expressed as gallic acid equivalent (mg) per gram of standard extracts of sample 1 and sample 2. Sample 1 was found to have 837.88± 2.62 mg/g phenolic content whereas sample 2 was found to have 970.76 ± 1.66 mg/g phenolic content. It was evident from the result that sample 2 contained higher TPC than of sample 1 **(Table 4)**.

3.5 Total flavonoid content (TFC) of sample 1 and sample 2

TFC of both samples was calculated using the standard curve of quercetin ($y = 0.0002x + 0.0853$; $R^2 = 0.959$) and expressed as quercetin equivalent (mg) per gram of standard extracts of sample 1 and sample 2. Sample 1 and sample 2 were

found to have 778.39±2.10 and 896.83± 1.78 mg/g flavonoid content, respectively. It was evident from the result that sample 2 contained higher TFC than that of sample 1 **(Table 4)**.

3.6 Total antioxidant capacity (TAC) of sample 1 and sample 2

TAC of both samples was calculated using the standard curve of ascorbic acid ($y = 0.0002x + 0.0846$; $R^2 = 0.989$) and expressed as ascorbic acid equivalent (mg) per gram of standard extracts of sample 1 and sample 2. Sample 1 and sample 2 were found to have 822.24±1.08 mg/g and 960.42±0.57 total antioxidant capacity, respectively. It was evident from the result that sample 2 contained higher TAC than that of sample 1 **(Table 4)**.

Table 4. TPC, TFC, and TAC of *Ginkgo biloba* commercial products: sample 1 and sample 2 were expressed in mg gallic acid equivalent (GAE), quercetin equivalent (QE), and ascorbic acid equivalent (AAE) per g of dry extracts, respectively.

Antioxidant assay methods	**Sample 1**	**Sample 2**
TPC	837.88± 2.62	970.76 ± 1.66
TFC	778.39±2.10	896.83± 1.78
TAC	822.24±1.08	960.42±0.57

The values are the average of triplicates of experiments and are represented as mean ± % of relative standard deviation.

4. Discussion

The study was performed to evaluate the phytochemical screening, HPLC analysis of flavonoid content, and antioxidant activity of the aqueous standard extracts of *Ginkgo biloba* from two commercially available marketed products manufactured by Bangladeshi companies.

Post-market qualitative and quantitative HPLC analysis of flavonoid content of commercial *Ginkgo biloba* products manufactured by Bangladeshi companies has not been performed before. Qualitative analysis of two products by HPLC identified the presence of two main flavonoids; quercetin and kaempferol, and the quantitative analysis of the selected products by HPLC exhibited that product 1 contained 1.34 mg of quercetin and 0.28 mg kaempferol whereas product 2 contained 6.01 mg of quercetin and 0.29 mg of kaempferol per capsule containing 60 mg of standardized extracts. It is noted that in the total 25 % of ginkgo flavone glycosides present in the plant, the percentage of quercetin is 64.8-81.5 % (16.2-20.38 mg) of the total content (dominant), the percentage of kaempferol is 13.3-28.9 % (3.33-7.23 mg) of the total content and 2-8.4 % for isorhamnetin which is very low compared to the other two constituents [20]. Our study findings showed that sample 1 contained 2.23 %

quercetin and 0.47 % kaempferol and sample 2 contained 10.01 % quercetin and 0.48 % kaempferol. This means the content of the constituents present in these two samples is much lower than that found in the natural plant sources. However, the result shows that the contents of flavonoids present in sample 2 were higher than in sample 1 **(Figure 5).** Previously *Ginkgo biloba* five solid dosage forms available in the local market of South Africa were analyzed by HPLC-UV to determine flavonoid contents such as rutin, quercitrin, quercetin, kaempferol and isorhamnetin [21]. Quantitative analysis of flavonoid glycosides and terpene trilactones from the extracts of 11 commercial samples (tablet dosage forms) available in the local market of China by UPLC-UV has been reported previously [22].

As aqueous extract of *Ginkgo biloba* products available in the Bangladeshi local market was never used before to estimate the antioxidant activity, *in-vitro* antioxidant tests were carried out to examine the antioxidant potential of aqueous standard extracts of the selected *Ginkgo biloba* products. DPPH free radical scavenging assay, TFC, and TAC tests were used to evaluate the antioxidant capacity of aqueous extract of the two marketed products where data provided the evidence that they possess strong antioxidant capacity.

A wide number of diseases such as neurodegenerative diseases, Alzheimer's disease, aging, cancer, and cardiovascular diseases are induced by reactive oxygen species [23]. Free radicals-induced lipids or protein damage cause cell death. Endogenous neurotoxins are produced by the reaction between free radicals with neurotransmitters and these neurotoxins are responsible for dementia of Alzheimer's disease [24]. Plants' secondary metabolites particularly flavonoids are well-documented for their ability to neutralize free radicals and to possess a wide array of therapeutic activities such as antioxidative, antihypertensive, antimicrobial, anticancer, anti-inflammatory, diuretic, and antimicrobial [23,25]. These two commercial products manufactured by Bangladeshi companies contain standardized extracts of *Ginkgo biloba* leaf and are used for the treatment of Alzheimer's disease, loss of memory, cognitive dysfunction, memory loss, dementia, etc. which belong to neurodegenerative diseases primarily induced by free radicals generated in the biological system. Standardized extracts of *Ginkgo biloba* contain 24 % flavones glycosides; quercetin, kaempferol, and isorhamnetin and 6 % terpene lactones; Ginkgolides A, B, C and bilobalide [8,11]. Preliminary phytochemical screening of two products revealed the presence of flavonoids, phenolic compounds, terpenoids, coumarins, and tannins **(Table 2)**.

The DPPH free radical scavenging assay of two commercial products exhibited a concentration-dependent % of DPPH free radical scavenging **(Table 3)**. Product 2 showed much higher DPPH free radical scavenging potential (IC_{50}: 333.99 µg/mL) than that of product 1 (IC_{50}: 566.00 µg/mL) **(Table 3)**. This high quantity of

quercetin in product 2 found in HPLC analysis could be responsible for the higher DPPH free radical scavenging activity compared to product 1. Between these two main constituents of *Ginkgo biloba*, flavone glycosides (quercetin, kaempferol, and isorhamnetin) are responsible for antioxidant activity [11]. Previous studies reported good DPPH free radical scavenging activity of *Ginkgo biloba* leaf extract [26, 27]. The highest inhibition of DPPH free radical scavenging was produced by both *Ginkgo biloba* methanolic and ethanol extracts compared to stevia and parthenium [23]. Strong DPPH activity could be attributed to the electron transfer ability or hydrogen donating capacity of identified flavonoids; quercetin and kaempferol in the selected samples which is also reported by a previous study [25]. In addition to that, the antioxidant activity of the flavonoids also depends greatly on their chemical structure and the relative orientation of different groups present in the molecule, particularly the number and position of hydroxyl groups within the molecule.

The presence of a hydroxyl group in position three (3-OH) of the C ring is crucial for the antioxidant activity exerted by flavonoids [28]. For example, the flavonoid aglycones, such as quercetin, fisetin, (+)-catechin, myricetin, and morin, are more potent inhibitors of LPO than those lacking a 3-OH substitution such as diosmetin, apigenin (flavones), hesperetin, and naringenin (flavanones) [29].

TPC, TFC, and TAC determination of two samples exhibited antioxidant activity in a concentration-dependent manner. In total phenolic content determination, sample 2 had a higher TPC (970.76 ± 1.66 mg GAE/g of dry extract) than that of sample 1 (837.88± 2.62 mg GAE/g of dry extract). Antioxidant activity screening of crude methanol extract found TPC was 76.0±5.2 mg GAE/g dry weight [30]. Since our marketed samples were manufactured using standardized extract, they showed much higher TPC compared to this crude extract. Another study by found the phenolic content of aqueous ethanolic extracts was 75.74 mg g^{-1} GAE for the *Ginkgo biloba* leaf, and TPC ranged from 85.51 to 147.14 mg g^{-1} GAE for the commercial tea drugs they used [31].

Similarly, in total phenolic content determination, sample 2 contained more TFC (896.83± 1.78 mg QE/g of dry extract than that of sample 1 (778.39±2.10 mg QE/g of dry extract). This result is supported by the quantitative HPLC analysis of both samples where sample 2 was found to have 6.01 mg quercetin, a flavonoid whereas sample 1 had only 1.34 mg quercetin. It is noteworthy to mention that the sources of the two samples were different; sample 2 was from a mainstream top-ranked pharmaceutical company and sample 1 was from an herbal product manufacturing company. This high antioxidant activity in terms of TFC may be contributed partly by another flavanone glycoside, isorhamnetin found in the GB extract which was not identified and quantified in our study.

In the case of total antioxidant capacity determination, sample 2 exhibited

higher TAC (960.42±0.57 mg AAE/g of dry extract) than that of sample 1 (822.24±1.08 mg AAE/g of dry extract). Finally, it is noteworthy to mention that the total antioxidant capacity of both samples was found to be much higher than the standard Ascorbic acid. A previous study showed that the aqueous ethanolic extract of *Ginkgo biloba* leaf had 69.12 mmol/g AAE [31].

.

5. Conclusions

The phytochemical screening of two commercial *Ginkgo biloba* products indicated the presence of phytochemical constituents namely, flavonoids, terpenoids, phenolic compounds, coumarin, and tannins. Qualitative HPLC analysis of both samples detected the presence of two main flavonoids; quercetin and kaempferol, however quantitative HPLC analysis of them evident that sample 2 was found to have more quercetin and kaempferol content than sample 1. In all assay methods, the antioxidant potential determination of both samples revealed that sample 2 had stronger antioxidant properties than sample 1.

Author Contributions:

Conceptualization, DRA.; methodology, DRA, and SA.; data curation, SA.; writing—original draft preparation, DRA, SA, and MTK.; writing—review and editing, DRA and MTK.; Supervision, DRA. All authors have read and agreed to the published version of the manuscript."

Conflict of interest statement

Authors declare no conflict of interest

Funding

This research did not receive any specific grant from any funding agency in the public, commercial, or not-for-profit sectors.

Ethical approval

This article does not contain any studies with human participants or animals performed by any of the authors.

References

1. WHO global report on traditional and complementary medicine 2019 by the World Health Organization. pp147. Available Online: 2023; https://www.who.int/publications/i/item/978924151536
2. The Directorate General of Drug Administration (DGDA), Bangladesh, 2020. Available Online: 2023; https://www.dgda.gov.bd/index.php/2013-03-31-05-16-29/drug-manufacturers/herbal
3. Das, P., Das, S., Akhter, R., Huque, S., Akter, R., Shahriar, M. Comparative *in vitro* equivalence evaluation of some spironolactone generic tablets, commercially available in the Bangladesh drug market. *Indo American J. Pharm. Res.* 2017; *7*, 544-551.

4. Elghnimi, T.Y., El-Majri, M.A., Bennouh, R., Enkessa, A., Siam, M.M. Comparative in-vitro evaluation of commercial simvastatin tablets (20 mg). *Int. J. Pharm. Sci. Res.* 2016; *7*: 2402-2409.
5. Oishi, T.M., Munna, S., Noor, Z., Das, S., Akhter, R., Huque S., Shahriar, M. Comparative *in vitro* equivalence evaluation of some loratadine generic tablets marketed in Bangladesh. *IOSR J. Pharm. Biol. Sci.* 2017; *12*: 76-81.
6. Hailu, G.S., Gutema, G.B., Hishe, H.Z., Ali, Y.S., Asfaw, A.A. Comparative *in vitro* bioequivalence evaluation of different brands of amoxicillin capsules marketed in Tigray, Ethiopia. *Int. J. Pharm. Sci. Nanotechnol.* 2013; 6: 1966-1971.
7. Chandrasekaran, A R., Han C.Y., Chung A.C.Y., Cheang L.W., Ping, L.S. Post–market *in vitro* equivalency evaluation of paracetamol tablets in Kedah, Malaysia. *Int. J. Pharm. Sci. Nanotechnol.* 2011; *4*: 1403-1407.
8. Belwal, T., Giri, T., Bahukhandi, A., Tariq, M., Kewlani, P., Bhatt, I.D., Rawal, R.S. *Ginkgo biloba*. In: Nonvitamin and Nonmineral Nutritional Supplements, 1st ed., Nabavi, S.Y., Silva, A.S., Academic Press: Cambridge, Massachusetts, United States of America, 2019; Volume 1, pp. 241-250.
9. Fermino, B.L., Milanez, M.C., Freitas, G.B.L.D., Silva, W.C.F.N.D., Pereira, R.P., Rocha, J.B.T.D., Bonini, J.S. *Ginkgo biloba* L.: phytochemical components and antioxidant activity. *Afr. J. Pharm. Pharmacol.* 2015; *9:* 950-955.
10. Mullaicharam, AR. A Review on evidence-based practice of *Ginkgo biloba* in brain health. *Int. J. Chem.Pharm. Anal.* 2013; 1: 24-30.
11. Talbott, S.M., Hughes, K. *The health professional's guide to dietary supplements*, 1st ed., Lippincott Williams & Wilkins: 530 Walnut Street, Philadelphia, United States of America, 2007.
12. Pal, D., Sannigrahi, S., Mazumdar, U.K. Analgesic and anticonvulsant effects of saponin isolated from the leaves of Clerodendrum infortunatum Linn. in mice. *Indian J. Exp. Biol.* 2009; 47: 743-747.
13. Hossain, M.A., AL-Raqmi, K.A.S, AL-Mijizy, Z.H., Weli, A.M., Al-Riyami, Q. Study of total phenol, flavonoids contents and phytochemical screening of various leaves crude extracts of locally grown *Thymus vulgaris*. *Asian Pac. J. Trop. Biomed.* 2013; *3*: 705-710.
14. Gul, R., Jan, S.U., Faridullah, S., Sherani, S., Jahan, N. Preliminary phytochemical screening, quantitative analysis of alkaloids, and antioxidant activity of crude plant extracts from Ephedra intermedia indigenous to Balochistan. *Sci. World J.* 2017; *2017*: 1-7.
15. The United States Pharmacopeia. Vol. 4. United States Pharmacopeial Convention, 2018.
16. Lalhminghlui, K., Jagetia, G.C. Evaluation of the free-radical scavenging and antioxidant activities of *Chilauni, schima* wallichii Korth *in vitro*. *Future Sci. OA* 2018; 4: FSO272.
17. Chandra, S., Khan, S., Avula, B., Lata, H., Yang, M.H., ElSohly, M.A., Khan, I.A. Assessment of total phenolic and flavonoid content, antioxidant properties, and yield of aeroponically and conventionally grown leafy vegetables and fruit crops: a comparative study. *Evid. Based Complement. Alternat. Med.* 2014; 2014: 1-9.
18. Rebaya, A., Belghith, S.I., Baghdikian, B., Leddet, V.M., Mabrouki, F., Olivier, E., Cherif, J.K., Ayadi, M.T. Total phenolic, total flavonoid, tannin content, and antioxidant capacity of *Halimium halimifolium* (*Cistaceae*). *J. Appl. Pharm. Sci*. 2015; *5*: 052–057.

19. Prieto, P., Pineda, M., Aguilar, M. Spectrophotometric quantitation of antioxidant capacity through the formation of a phosphomolybdenum complex: specific application to the determination of vitamin E. *Anal. Biochem.* 1999; 269: 337-341.
20. Van Beek, T.A. Chemical analysis of *Ginkgo biloba* leaves and extracts. *J. Chromatogr. A* 2002; 967: 21-55.
21. Dubber, MJ., Kanfer, I. High-performance liquid chromatographic determination of selected flavonols in *Ginkgo biloba* solid oral dosage forms. *J. Pharm. Pharmaceut. Sci.* 2004; *7*: 303-309.
22. Xie, H., Wang, JR., Yau, LF., Liu, Y., Liu, L., Han, QB., Zhao, Z., Jiang, ZH. Quantitative analysis of the flavonoid glycosides and terpene trilactones in the extract of *Ginkgo biloba* and evaluation of their inhibitory activity towards fibril formation of β-amyloid peptide. *Molecules* 2014; *19*: 4466-4478.
23. Ahmed, Z.S., Nowrin, T., Hossain, M.H., Nasrin, T., Akter, R. Metabolite profiling of Crotalaria verrucosa leaf extract and evaluation of its antioxidant and cytotoxic potency. *Res. J. Phytochem.* 2018; 12: 60-70.
24. Volicer, L., Crino, P.B. Involvement of free radicals in dementia of the Alzheimer type: a hypothesis. *Neurobiol. Aging* 1990; 11: 567-571.
25. Srinivasan, S., Wankhar, W., Rathinasamy, S., Rajan, R. Free radical scavenging potential and HPTLC analysis of *Indigofera tinctoria* Linn (Fabaceae). *J. Pharm. Anal.* 2016; 6: 125-131.
26. Lugasi, A., Horvahovich, P., Dworschák, E. Additional information to the *in vitro* antioxidant activity of *Ginkgo biloba* L. *Phytother Res.* 1999; 13: 160–162.
27. Ahmad, N., Fazal, H., Abbasi, B.H, Farooq, S. Efficient free radical scavenging activity of *Ginkgo biloba*, *Stevia rebaudiana* and *Parthenium hysterophorous* leaves through DPPH (2, 2-diphenyl-1-picrylhydrazyl). *Int. J. Phytomedicine.* 2010; 2: 231-239.
28. Teixeira, S., Siquet, C., Alves, C., Boal, I., Marques, M.P., Borges, F., Lima, J.L., Reis, S. Structure–property studies on the antioxidant activity of flavonoids present in diet. *Free Radic. Biol. Med.* 2005; 39: 1099-1108.
29. Goh, L.M., Barlow, P.J., Yong, C.S. Examination of antioxidant activity of *Ginkgo biloba* leaf infusions. *Food Chem*. 2003; 82: 272-282.
30. Maltas, E., Vural, H.C., Yildiz, S. Antioxidant activity and fatty acid composition of *Ginkgo biloba* from Turkey. *J. Food Biochem.* 2011, 35; 803-818.
31. Koczka, N., Ombódi, A., Móczár, Z., Stefanovits-Bányai, E. Total phenolic content and antioxidant capacity of ginkgo teas. *Acta Aliment.* 2016; *45*: 77–84.

JBEP

Journal of Biosciences and Experimental Pharmacology
ISSN-2960-284X

Review Article

Harnessing the Medicinal Properties of *Premna esculenta* for Diseases and Beyond: A Review of Its Phytochemistry and Pharmacology

Jannatul Ferdous Shaily[1], Md. Abdul Motaleb Bhuiya[2], Md. Sohel Rana[3], Taslima Begum[1] and Pritesh Ranjan Dash[2*]

[1]*Department of Pharmacy, Primeasia University, Banani, Dhaka.*
[2]*Department of Pharmacy, University of Science and Technology Chittagong (USTC), Chittagong, Bangldesh,*
[3]*Department of Pharmacy, Jahangirnagar University, Savar, Dhaka*

Correspondence *E-mail: pritesh@ustc.ac.bd

Citation: Shaily, J. F.; Bhuiya, M. A. M.; Rana, M. S., Begum, T.; Dash, P. T. Harnessing the medicinal properties of Premna esculenta for diseases and beyond: a review of its phytochemistry and pharmacology, *J. Bio. Exp. Pharm.* 2023, 1: 16–24.

Received: November 21, 2023
Accepted: December 5, 2023
Published: December 15, 2023

Publisher's Note: JBEP stays neutral with regard to jurisdictional claims in published maps and institutional affiliations.

Abstract: *Premna esculenta* is a shrub from the *Verbenaceae* family that has historically been utilized by tribal people to cure a variety of inflammatory disorders. All of the pharmacological and phytochemical research done on the significant medicinal plant *Premna esculenta* has been attempted to be compiled in the current review. Traditional uses of *Premna esculenta* include the treatment of rheumatism, asthma, eye diseases, cough, fever, boils, and scrofulous disorders. The various plant components, including the leaves, stem, barks, roots, barks, and wood, have all been employed for extraction. Alkaloids, terpenoids, phenolic compounds, flavonoids, and amino acids make up the majority of the chemical components or secondary metabolites identified. Pharmacological activities like analgesic, antioxidant, anti-inflammatory, anti-hyperlipidemic, sedative, and hepatoprotective are mostly observed during *in-vitro* and *in-vivo* evaluation. Through a review of various studies conducted on *Premna esculenta*, this study has primarily focused on various pharmacological actions and medicinal uses.

Keywords: *Premna esculenta*; Phytochemistry; Pharmacology.

1. Introduction

Traditional pharmacological treatment for a variety of common liver problems, such as viral hepatitis and nonalcoholic fatty liver disease, has a poor success rate and adverse effects that could be fatal. Contrarily, traditional treatments have been used by many individuals around the world for a long time to cure liver problems without having any discernible adverse effects [1]. As a result, in order to replace the medications now in use and achieve greater efficacy and safety, it is required to look into different and supplementary medicine (CAM), particularly a natural remedy for liver disease illness [2]. World health has benefited greatly from medicinal plants. Many different botanicals have had their healing powers identified by science, and their active ingredients have been taken

out and examined. Today, many plant components are produced in sizable labs for use in medicinal treatments. However, the potential of many plant species as a source of novel medications is still largely untapped. *Premna esculenta Roxb*, a member of the Lamiaceae family of shrubs, is one of the covered shrubs that Bangladeshi tribal people have traditionally utilized to cure a variety of inflammatory illnesses. A thorough examination was conducted to check the phytochemical and pharmacological activity of various fractions of *Premna esculenta* in light of the extensive potential for using plants as sources for medications as well as the traditional usage prevalent in the area. In the forests of Bangladesh specially in Chittagong and Chittagong Hill Tracts, A shrub with short stems and branching is called *Premna esculenta Roxb*. (Family *Verbenaceae*) [3]. The herb often referred to as "Lelompata," has long been used by tribal people in Bangladesh to cure Jock worm and appetite infection, frenzy, hepatic, yellow fever, fluoralbus, tumor, swelling, serpent bite, abdomen ailments, and kidney stones. Consequently, for the treatment of bacterial and fungal infections, arthritis, and other conditions, the plant's leaves are applied directly to the area. That is afflicted in traditional medicine. To treat gout, edema, andjaundice, roots are frequently combined with other plants. In Khagrachari in Bangladesh, the leaves are one of the components of amedication used to treat jaundice. For jaundice patients in the Chittagong Hill Tracts, leaves boiled with a Nappi-a fermented paste made from different marine fish species are a crucial part of their diet [4]. The purpose of this review is to provide support for research work to explore the plant's uses, importance, phytochemistry and pharmacology.

2. Materials and Methods

2.1 Literature search strategy

The literature survey on *Premna esculenta* was carried out in the following databases: Google Scholar, PubMed, Research Gate, Science Direct and other applicable distributed materials. The data extraction and the selection criteria are mentioned in **Figure 1**.

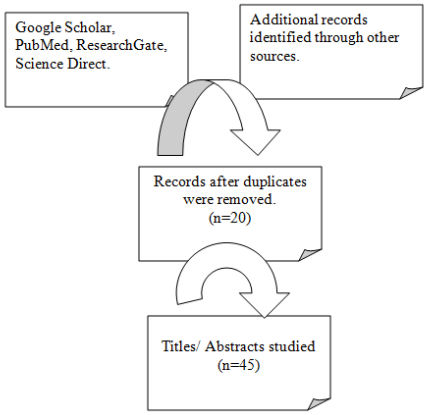

Figure 1: Flow chart of data extraction

3. Results

3.1 Botanical Description

The *Premna esculenta* shrub grows to a height of 6 to 8 feet, with a short, hair less stem, and thin, sharply four-edged branches and branch lets. Flowers are produced in corymbs made up between 4–8 opposing cymes that are velvet-hairy, measuring around 4-6 cm wide, and have four-edged stalks that are 1-2 cm long. They are present in the leaf axils and where a branch ceases to grow. Flowers are heterosexual, numerous, emerald green, and cream-colored, with 3 sprigs of flowers, cup-shaped sepals, 5 teeth, blunt teeth, and a pointed tip. The outside of the flowers is velvet-hairy. Funnel-shaped flower with two lips, 4 lobes, and lobes that are ovate to oblong in shape with blunt tips. Stamens are four, didynamous, and slightly protruding, and their filaments are thread-like and without hair, and roughly 1.5 to 2.5 mm in length. The blooming tube is slender and heavily velvet-haired at the neck, and around 3 to 4 mm in length. Simple opposite leaves are obovate-elliptic, elliptic-lance-shaped, 6–16 x 3–8 cm in size, with 4–7 on either side of the midvein, lateral veins. When young, the underside of the hair is pale yellowish velvet, and when fully grown, bald. The 0.4-0.7 cm long leaf stalks are thin. A drupe is a kind of fruit that is smooth, purple, and roughly 3 mm in diameter and has five lobed sepals that are used for fruiting.

3.1.1 Scientific Classification

Class: Magnoliopsida; Subclass: Lamiidae; Order: amiales; Family: Lamiaceae; Genus: *Premna;* Species: *Premna esculenta Roxb*. [5]

3.1.2 Typical Name

Common Name: Edible Premna; Bengali Name/Verncular: Lemon pata, Lalana, Lalong; Mizo: Lei-dum; Tamil: Atomukam, Tichamitam, Tichamitamaram; Telugu: Gabbunelli

3.1.3 Synonyms:

Gumira esculenta

There are several more names for it, including Lahanashak (Marma), Lamur (Marma), Angklung-gam (Khumi), Unarei (Bawm), Orai (Tripura), Kamrah (Marma), and Kramer-Rauh some of the Chakma people (Marma). Ailments are treated using leaf paste, leaf curry, or leaf boiling.

Figure 2: *Premna esculenta leaves*

4. Discussion

4.1 Phytoconstituents

The freshly acquired crude extract was qualitatively analyzed for the existence of several phytochemical components including alkaloids, tannins, reducing sugar, flavonoids, steroids, terpenoids, and saponins using known phytochemical methods [6, 7].

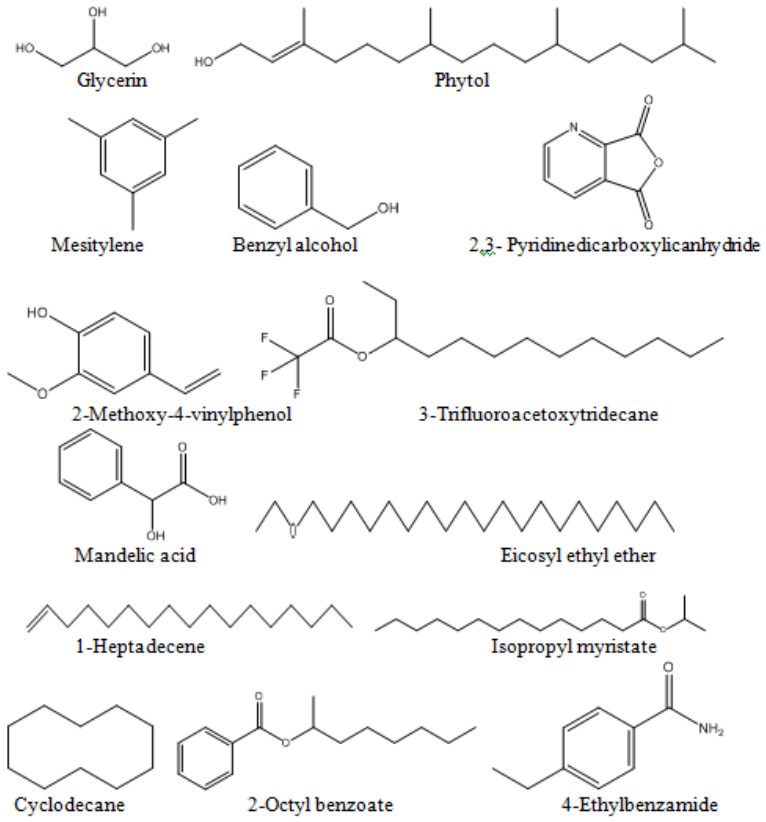

Figure 3: Reported chemical constituents of GC-MS analysis from methanolic extract of *Premna esculenta* [8]

4.*2 Pharmacological Activity*

Table 1: Reported pharmacological activity with possible mechanism of action of *P. esculenta*

Dose	Type of Activity	Type of assay	Mechanism of action	Ref.
In vitro and *In vivo* study 200 and 400 mg/kg	Hepatoprotective	Experimental animals (rat)	By reducing the elevated levels of serum enzyme, albumin, total protein, ALP	17
4.846±0.81 µg/ml	Thrombolytic	Clot disruption	Selectively bind to platelet thrombi Broad spectrum activity against human and plant pathogen	15, 16
500 µg/mL ± 0.977 µg/ml	Anti-oxidant	DPPH radical scavenging	Scavenging free radical	18
(20 µg/mL)	Anti-oxidant	DPPH	Free radical scavenging	18

4.2.1 Analgesic, anti-inflammatory, and anti-nociceptive properties

Animal models were used to assess the analgesic and anti-inflammatory effects of *P. esculenta* alcohol extract. Rats and mice were used in the radiant heat tail-flick method to assess the analgesic activity [9, 10]. To test the effectiveness of the anti-inflammatory, carrageenan-induced rat paw edema was utilized [11]. In the acetic acid-induced writhing test, chloroform and the ethyl acetate fraction of the ethanolic extract at a dose of 200 mg/kg showed a significant ($p< 0.001$) reduction in the number of writhes with 85.96 % and 61.98 % of inhibition, respectively. The extract of ethanol extended the tail-flicking period such as

88.49 % ($p< 0.001$) in the radiant heat tail-flick technique 90 minutes following oral administration of the same dosage rate. The ethanolic extract performed well in the carrageenan-induced edema test at a concentration of 200 mg/kg shown in the first and third hours of the research period, respectively, and saw significant suppression of paw edema with 22.68 % and 17.24 % inhibition [12].

4.2.2 Sedative Activity

The ethanolic extracts of root (200 mg/kg) similar leaf (200 mg/kg) of *P. esculenta* showed a substantial ($p< 0.05$ and $p <0.001$) decrease in the start and length of thiopental sodium-induced sleepiness. Administration such as 200 mg/kg *p.o.* of *P. esculenta* leaf extract of ethanolic. Pentobarbitone substantially ($p<0.01$) increased the length of produced sleep by 178 %. Pentobarbitone's ability to prolong the time spent sleeping caused by barbiturates and a considerable reduction in spontaneous motor activity (reduced locomotion) both pointed to the existence of substances in *P. esculenta* leaves that have a central nervous system (CNS) depressive effect [13, 14].

4.2.3 Thrombolytic Activity

By using an *in vitro* clot lysis model, the thrombolytic activity was assessed [15, 16]. The capability of an *in vitro* ethanolic extract from *P. esculenta* roots to dissolve blood clots. The ethanolic extract at 5 mg/mL significantly increased the amount of clot lysis activity (37.69 %, $p< 0.001$) in the clot lysis model. The plant extract's thrombolytic action was quick and dose-related, demonstrating that the impact was real and targeted. It is significant that *P. esculenta* has thrombolytic activity since it might significantly affect cardiovascular health.

4.2.4 Hepatoprotective Activity

The anti-hepatoprotective activity of *P. esculenta* was tested against rat liver damage brought by only carbon tetrachloride and assessed using the methodology outlined in [17]. Against the CCl_4-treated control group, oral administration of the ethanolic extract at a dose of 400 mg/kg/day for seven days substantially ($p<0.001$) decreased the elevated levels of serum alkaline phosphatase, glutamyl oxaloacetate transaminase, and glutamic pyruvic transaminase.

4.2.5 Anti-oxidant Activity

Anti-oxidant activity of the *P. esculenta* plant had already determined ethanolic preparations of plant leaves and roots have free radical scavenging properties that include the 1-diphenyl-2-picrylhydrazyl 1,1-diphenyl-2-picrylhydrazyl, a stable radical (DPPH). Extracting leaves with ethanol and roots has been observed to have Potential free radical scavengers: DPPH, superoxide, and NO using the *in vitro* extracts from plants with antioxidant properties[18]. The extract substantially ($p<0.001$) decreased the very high rate of SGPT, SGOT, and ALP and

enhanced the lowered amounts of albumin and total protein compared to the CCl_4-treated rats at dosages of 200 and 400 mg/kg p.o. Superoxide dismutase (SOD), catalase, and peroxidase decreased levels were also significantly increased (p<0.001) inside the extracts.

4.2.6 Anti-hyperlipidemic Activity

Premna esculenta (Roxb.) leaves and roots were used to create hyperlipidemic rats and mice, and their antihyperlipidemic efficacy was tested using ethanolic extracts of the plant's leaves and roots [19]. After a 24-hour treatment period, the ethanolic extract of leaves caused a significant (p<0.05) decrease in serum levels of triglycerides (TG), low-density lipoprotein (LDL), very low-density lipoprotein (VLDL), total cholesterol (TC), and atherogenic index when compared to the P-407-induced hyperlipidemic control mice. At a dosage of 250 mg/kg/day p.o., the leaf and root extracts significantly (p<0.05) decreased the blood levels of TC, TG, VLDL, and LDL as well as the atherogenic index as compared to P-407-induced hyperlipidemic control rats after 4 days of pretreatment.

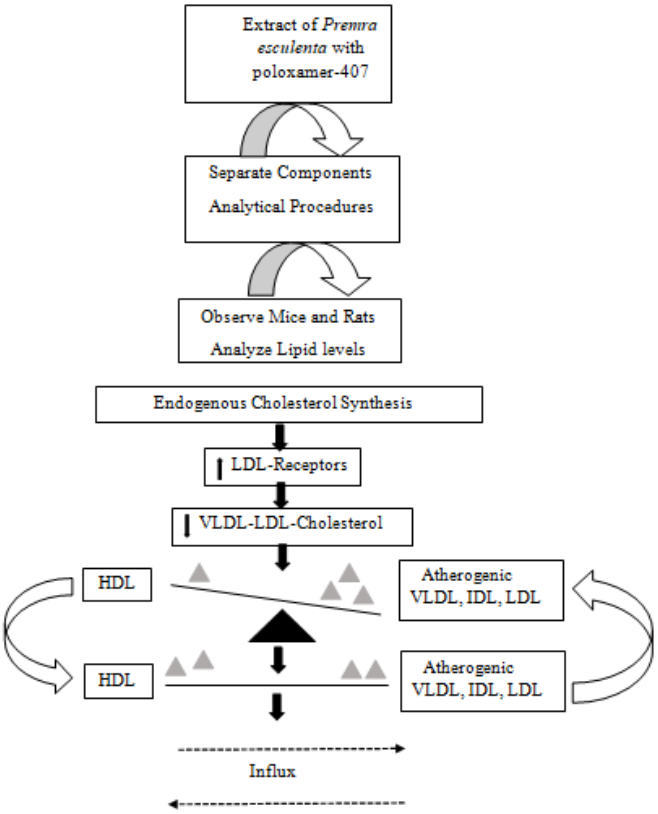

Figure 4: *Premna esculenta* in Poloxamer-407 induced hyperlipidemic mice and rats

5. Conclusion

A review of the literature revealed that *P. esculenta* contains a broad variety of pharmacological qualities that enable that to successfully cure several illnesses. *P. esculenta* is a significant herb with numerous beneficial medicinal qualities. The use of plant extracts for various therapeutic purposes, such as anti-nociceptive and anti-inflammatory, had been successfully identified, as having sedative activity, analgesic, antioxidant, thrombolytic, hepatoprotective, and antihyperlipidemic action. A proper assessment of the plant's use in medicine may be encouraged by the study's phytochemistry and various biological properties of the extracts and constituents.

Author Contributions: The authors confirm contribution to the paper as follows: study conception and design: PRD. data collection: JFS; analysis and interpretation of results: JFS, MAMB, MSR and TB. Draft manuscript preparation: JFH and PRD. All authors reviewed the results and approved the final version of the manuscript. All authors have read and agreed to the published version of the manuscript.

Conflict of interest statement

Authors declare no conflict of interest

Funding

This research did not receive any specific grant from any funding agency in the public, commercial, or not-for-profit sectors.

Ethical approval

This article does not contain any studies with human participants or animals performed by any of the authors.

.

References

1. Umer, S., Asres, K., Veeresham, C. Hepatoprotective activities of two Ethiopian medicinal plants. *Pharm. Biol.* 2010; 48:461–468.
2. Mitra, S.K., Seshadri, S.J., Venkataranganna, M.V., Gopumadhavan, S., Udupa, V.U., Sarma, D.N. Effect of HD-03-a herbal formulation in galactosamine-induced hepatopathy in rats. *Indian J. Physiol. Pharmacol.* 2000; 44:82–86.
3. Uddin, S.N. Traditional uses of ethnomedicinal plants of the Chittagong Hill Tracts. 1st ed. Dhaka: Bangladesh National Herbarium; 2006.
4. Yusuf, M., Begum, J., Hoque, N., Chowdhury, J.U. Medicinal Plants of Bangladesh. 2nd ed. Chittagong: BCSIR Laboratories Chittagong; 2009.
5. Kabra, A., Kabra, R., Baghel, U.S. Premna Species: A Review, *J. Biol. Chem. Chron*. 2015, 1(1); 55-59.
6. Ghani, A., Medicinal plants of Bangladesh with chemical constituents and uses, 2nd ed, Asiatic Society of Bangladesh, Dhaka, 2003, 331-332.
7. Trease, G.E., Evans, W.C., A text book of pharmacognosy, 11th ed, Brailliar Tindall Ltd., London, 1989; 176-180.
8. Shaily, J.F. Investigations of chemical and biological activities of ethanolic extract of *Premna esculenta*. B. Pharma Project, Deptartment of Pharmacy, Primeasia University, 2023
9. Koster, R., Anderson, M., De Beer, E.J. Acetic acid for analgesic screening, *Fed. Proc.*, 1959; 18: 412-417.

10. Altun, M.L., Citoglu, G.S., Yılmaz, B.S., Ozbek, H. Antinociceptive and anti-inflammatory activities of *Viburnum opulus*. *Pharmaceut. Biol.* 2009; 47:653–658.
11. Winter, C.A., Risley, E.A., Nuss, G.W. Carrageenan-induced edema in the hind paw of the rat as an assay for anti-inflammatory drugs. *Proc. Soc. Exp. Biol. Med.* 1962; 111:544–547.
12. Yesilada, E., Kupeli, E. *Berberis crataegina* DC. root exhibits potent anti-inflammatory, analgesic, and febrifuge effects in mice and rats. *J. Ethnopharmacol.* 2002; 79:237–248.
13. Gupta, B.D., Dandiya, P.C., Gupta, M.L., A psychopharmacological analysis of behavior in rat. *J. Pharmacol.* 1971; 21: 293-298.
14. Takagi, K., Watanabe, M., Saito, H., Studies on the spontaneous movement of animals by the hole cross test: Effect of 2-dimethylaminoethanol and its acyl esters on the central nervous system. *Jpn. J. Pharmacol.* 1971; 21 (6): 797-810.
15. Prasad, S., Rajpal, S.K., Jayant, Y.D., Hemant, J.P., Girdhar, M.T., Hatim, F.D. Development of an *in vitro* model to study clot lysis activity of thrombolytic drugs. *Thrombosis J.* 2006; 4:14.
16. Ratnasooriya, W.D., Fernando, T.S., Madubashini, P.P. *In vitro* thrombolytic activity of Sri Lankan black tea, *Camellia sinensis* (L.) O. Kuntze. *J. Nat. Sci. Found. Sri Lanka* 2008; 36:179–181.
17. Ahmed, B., Alam, T., Khan, S.A. Hepatoprotective activity of *Luffa echinata* fruits. *J. Ethnopharmacol*. 2001; 76:187–189.
18. Brand-Williams, W., Cuvelier, M.E., Berset, C. Use of a free radical method to evaluate antioxidant activity. *LWT Food Sci. Technol.* 1995; 28:25–30.
19. Yogendrasinh, B.S., Sunita, M.J. Antihyperlipidemic activity of *Clitoria ternatea* and *Vigna mungo* in rats. *Pharm. Biol.* 2010; 48:915–923.

JBEP

Journal of Biosciences and Experimental Pharmacology
ISSN-2960-284X

Original Article

In vitro Screening of *Litsea monopetala* (Roxb.) Pers. (*Lauraceae*) Extract: Potential Antioxidant, Cytotoxic, Thrombolytic, and Anti-Inflammatory Properties

Mir Shahriar Kamal[1], Sania Ashrafi[1], Sara Sultana[2], Mohammad Rashedul Haque[1,*]

[1]*Department of Pharmaceutical Chemistry, Faculty of Pharmacy, University of Dhaka, Dhaka 1000, Bangladesh; shahriark678@gmail.com, sania.ashrafi@du.ac.bd, haquemr@du.ac.bd.*

[2]*Department of Pharmacy, Faculty of Pharmacy, University of Dhaka, Dhaka 1000, Bangladesh; sara-2017714152@pharmacy.du.ac.bd.)*

Correspondence *E-mail: haquemr@du.ac.bd

Abstract: *Litsea monopetala* (Roxb.) Pers. is a plant of significant ethnobotanical importance, and in this study, we conducted a comprehensive investigation into its potential bioactive properties. Different fractions of the ethyl acetate (EtOAc) crude extract of the plant leaves were evaluated for antioxidant, cytotoxicity, thrombolytic, and anti-inflammatory activities, *in vitro*. The hexane-soluble fraction (LMH) exhibited notable antioxidant activity with IC_{50} value of 5.44 µg/ml and cytotoxicity with LC_{50} value of 1.10 µg/ml in DPPH radical scavenging assay and Brine shrimp lethality bioassay, respectively. Moreover, Dichloromethane soluble fraction (LMD) exhibited the highest thrombolytic activity, achieving an impressive rate of 31 %, compared to the standard Streptokinase (45 %). Additionally, LMD demonstrated a significant inhibition of 36 % of hemolysis, while LMH exhibited a slightly lower inhibition rate of 33 %, while the standard drug acetyl salicylic acid achieved a 47 % inhibition of hemolysis, suggesting their relevance in the context of inflammation-related disorders. These results underscore the multifaceted pharmacological properties of *Litsea monopetala* and provide a solid foundation for further research, including the isolation and characterization of bioactive compounds, elucidation of underlying mechanisms, and potential applications in drug development and healthcare.

Keywords: *Litsea monopetala*; Cytotoxicity; DPPH; Antioxidant; Thrombolytic; Anti-inflammatory;

Citation: Kamal, S. M.; Ashrafi, S.; Sultana, S.; Haque, M. R.; *In vitro* screening of *Litsea monopetala* (Roxb.) Pers. (*Lauraceae*) extract: potential antioxidant, cytotoxic, thrombolytic, and anti-inflammatory properties. *J. Bio. Exp. Pharm* 2023, 1:25-38.

Received: November 16, 2023
Accepted: December 2, 2023
Published: December 15, 2023

Publisher's Note: JBEP stays neutral with regard to jurisdictional claims in published maps and institutional affiliations.

1. Introduction

Oxidative stress arises when there is an imbalance between the protective functions provided by the body's antioxidant system and the generation of reactive

oxygen species (ROS). Reactive oxygen species are produced as a natural part of cellular processes. However, when their production surpasses the body's ability to effectively counteract them through antioxidants, they can lead to the oxidative damage of various components, including blood vessel walls, carbohydrates, DNA, lipids, and other molecules [1]. The utilization of synthetic antioxidants for medical treatments has been restricted due to their significant adverse reactions. As a result, contemporary scientists have shifted their focus to natural antioxidants, with a particular emphasis on phenolic compounds, which have garnered substantial attention. These natural antioxidants exhibit promise in the advancement of therapeutic approaches that do not produce harmful side effects [2,3].

Cancer represents a significant global public health challenge, with an approximate 18.1 million new cases and 9.6 million cancer-related deaths reported in the year 2018 [4]. According to a World Health Organization (WHO) report, there are presently 14 million individuals worldwide who have been diagnosed with cancer, and the number of fatal cases totals 8 million [5]. Many cancer patients begin exploring alternative approaches, such as herbal remedies, due to the elevated mortality rates associated with cancer and the potentially harmful side effects of conventional anticancer treatments [6].

The development of blood clots (thrombi) in arteries, stemming from disruptions in the body's natural equilibrium, can lead to blockages in coronary arteries, resulting in severe consequences like acute heart attacks and strokes. Thrombolytic drugs are employed to dissolve these blood clots, a process known as thrombolysis [7]. There is a growing need for natural sources of thrombolytic agents because they hold the potential to offer safer, more cost-effective alternatives to synthetic drugs, potentially with fewer side effects. Additionally, natural sources can provide a sustainable and renewable supply of therapeutic agents.

Inflammation is the complex biological response of body tissues, often involving a cascade of events that includes the activation of various cellular enzymes, subsequent membrane damage, and overall tissue dysfunction. Consequently, focusing on the stabilization of cell membranes may be a vital strategy in addressing inflammation and its related consequences [8]. Numerous drugs, including steroids, nonsteroidal anti-inflammatory drugs, and immunosuppressants, are available to manage and reduce inflammatory crises. However, these medications often come with adverse effects. Our objective is to use the lowest effective dose that provides maximum efficacy with minimal side effects. To achieve this, incorporating natural anti-inflammatory agents into treatment can enhance the drug's effectiveness while minimizing unwanted side effects [9].

Presently, approximately 88 % of the world's population, roughly 3.5 billion people, are utilizing herbal remedies from medicinal plants. This extensive utilization underscores the importance of finding new compounds with potent healing attributes and few side effects. These compounds could have a significant impact on addressing diverse health issues like oxidative stress, cancer, thrombosis, and inflammation. Consequently, the exploration of novel bioactive substances from medicinal plants remains essential, expanding treatment possibilities and enhancing global healthcare outcomes [10].

Litsea monopetala (Roxb.) Pers., a member of the *Lauraceae* family, is a small tree that can reach heights of up to 18 meters. It is primarily found in Nepal but can also be located in other Asian countries, including India and Bangladesh. In Bangladesh, it is known as "khara jora," while in Malaysia, it goes by "medang busok" and "bangang." Indonesians refer to it as "huru koneng," Thais as "kathang," and in Myanmar, it's called "ondon laukya." In northeast India, it's referred to as "sualu," and in Tamil, it's known as "maidalagadil." It holds significance in Ayurvedic medicine, where in Sanskrit, it's named "maidaa-lakdi." In Ayurveda, the bark is recognized for its stimulant, astringent, spasmolytic, and antidiarrheal properties, while the roots are applied externally to alleviate pains, bruises, and contusions [11].

In Nawalparasi District, Nepal, the seeds are employed to alleviate stomach aches [12]. In Bangladesh, the Naik clan of the Rajbongshi tribe uses the bark to address constipation [13], while the Bongshi tribe utilizes both leaves and bark to combat chronic severe fever [14]. Folk medicinal practitioners in Dinajpur District, Bangladesh, turn to the plant's leaves for treating bone fractures in cattle [15]. Additionally, in Sreemangal, Maulvibazar District, Bangladesh, tribal tea workers rely on the leaves to manage jaundice accompanied by fever [16]. These diverse applications of the plant highlight its significance in folk medicine across different cultures.

In the present investigation, a comprehensive assessment was conducted to elucidate the potential bioactive properties of the plant extract. Specifically, the study encompassed an evaluation of antioxidant, anticancer, thrombolytic, and anti-inflammatory activities. The primary objective was to discern whether the plant harboured latent bioactivity beyond its established traditional usage and previously documented research findings.

2. Materials and Methods

2.1 Sample Collection and Preparation

Whole plant of *L. monopetala* were collected in Gazipur, Bangladesh, and a voucher specimen was preserved. Authentication was conducted by an expert at the Bangladesh National Herbarium (BNH). Leaves were meticulously harvested, cleaned to remove impurities, and then subjected to two weeks of shaded drying with proper ventilation, followed by additional sun drying. Subsequently, a high-capacity grinding machine was used to finely grind the leaves into approximately 1000 grams of coarse powder.

2.2 Drugs and Chemicals

All the chemicals and solvents were sourced from reputable suppliers, including Active Fine Chemicals Ltd. in Bangladesh, Merck in Germany, and DaeJung in Korea. Specific compounds, such as Tert-butyl-1-hydroxytoluene (BHT), vincristine sulfate (VS), streptokinase (SK), and acetylsalicylic acid (AcSA), were acquired from Opsonin Pharma Ltd., a pharmaceutical company located in Bangladesh.

2.3 Experimental Design

2.3.1 Extraction of Plant Material

The coarse plant powder was placed in clean, 3-liter amber bottles. EtOAc was added to fully immerse the powder, and this mixture was soaked for 18 days with regular agitation. Afterward, the mixture underwent filtration through a cotton plug and Whatman No.1 filter paper. The resulting crude extract was then concentrated using low-temperature evaporation, keeping the temperature below 40°C and maintaining proper pressure. The final concentrated crude extract was precisely weighed for measurement.

2.3.2 Preparation of Different Partitions for Biological Tests

The partitioning of the crude EtOAc extract followed a method initially devised by Kupchan and later modified by Van Wagenen et al [17]. It involved fractionation using hexane, dichloromethane (DCM), and ethyl acetate solvents, resulting in three distinct fractions: hexane-soluble (LMH), DCM-soluble (LMD), and ethyl acetate-soluble (LME). Each fraction was separately evaporated using a rotary evaporator.

2.4 Antioxidant Assay

2.4.1 DPPH free radical scavenging assay

To assess the free radical scavenging activity of plant extracts, we prepared a mixture by combining 3.0 ml of a 20 g/ml DPPH methanol solution with 2.0 ml of a plant extract solution at various concentrations, ranging from 500 g/mL to 0.977 g/mL. This experiment aimed to gauge the plant extracts' capacity to counteract 1,1-diphenyl-2-picrylhydrazyl (DPPH) free radicals. We compared the fading of the purple DPPH methanol solution induced by the plant extract with the fading caused by BHT, which served as a reference compound [18].

$$\%\ Inhibition\ of\ free\ radical\ DPPH = \left(1 - \frac{Absorbance\ of sample}{Absorbance\ of the\ control\ reaction}\right) x\ 100$$

2.4.2 Total phenolic content

To determine the total phenolic content, we employed the Folin-Ciocalteu Reagent (FCR) as an oxidizing agent and used gallic acid as the reference standard, following the protocol outlined by Harbertson et al. Specifically, 2.5 ml of FCR was mixed with 2 ml of Na_2CO_3 with 0.5 ml of an extract solution (2 mg/ml). After a 20-minute incubation at room temperature, absorbance values were recorded at 760 nm using a UV spectrophotometer. By analyzing a standard curve generated with gallic acid at various concentrations, we calculated the total phenol content, expressed in milligrams of gallic acid equivalent (GAE) per gram of extract [19].

2.5 Cytotoxicity Assay

2.5.1 Brine Shrimp Lethality Bioassay

To assess potential cytotoxicity, we conducted a brine shrimp lethality test. An artificial saltwater solution was prepared by dissolving 38 g of NaCl in 1000 mL of distilled water, with the pH adjusted to 8.0 using NaOH. Brine shrimp eggs were incubated in this solution to hatch into nauplii. Test samples and the reference standard (vincristine sulfate) were prepared in diluted dimethylsulphoxide (DMSO) at various concentrations (ranging from 400 µg/mL to 0.78125 µg/mL). After visually counting the nauplii, each vial received 5 ml of simulated saltwater, exposing the nauplii to the test compounds. Cytotoxic effects were assessed based on their impact on the brine shrimp nauplii [20].

2.6 In vitro Thrombolytic Assay

The study followed the methodology outlined by Bhowmick et al [21]. 10 ml of venous blood was collected from healthy volunteers and distributed it into

pre-weighed, sterile Eppendorf tubes (0.5 ml per tube). These tubes were incubated at 37°C for 45 minutes, allowing the blood to clot. Following incubation, all the serum was meticulously removed that had separated from the clots, leaving only the clots in each tube. Subsequently, we re-weighed the tubes to determine the clot weights.

$$Clot\ weight = weight\ of\ clot\ containing\ tube - weight\ of\ the\ tube\ alone$$

In the tubes containing the clots, 100 µl of the extract solutions were added. As a positive control, a separate tube received 100 µl of streptokinase, while each individual tube received 100 µl of distilled water. Subsequently, all the tubes, including both control and test samples, were incubated at 37°C for 90 minutes. The difference in weight before and after clot lysis was calculated, expressing this difference as a percentage of clot lysis. This percentage indicated the extent to which the clots were dissolved or lysed by the respective samples.

2.7 In vitro Anti-inflammatory Assay (Membrane Stabilizing Activity)

2.7.1 Heat-induced Haemolysis

Two groups of centrifuge tubes were prepared, each containing 5 ml of isotonic buffer with a plant extract concentration of 2.0 mg/ml. In a separate tube, an equal volume of a vehicle was added as a control. To each tube, 30 µl of erythrocyte suspension was added and gently mixed by inverting the tubes. One group of tubes was incubated at 54°C for 20 minutes in a water bath, while the other group was maintained at a temperature between 0 and 5°C using an ice bath. After the incubation period, the reaction mixture was centrifuged at 1300 g for 3 minutes. The resulting supernatant was then analyzed by measuring its absorbance at 540 nm using a UV spectrometer. The equation provided was utilized to determine the percentage inhibition of hemolysis or membrane stabilization [22].

$$\%\ inhibition\ of\ hemolysis\ = (1 - \frac{OD2 - OD1}{OD3 - OD1}) \times 100$$

Where, OD1 = test sample unheated; OD2 = test sample heated; and OD3 = control sample heated

3. Results

3.1 Effect of L. monopetala extracts on DPPH Free Radical Scavenging Activity

The study aimed to evaluate the antioxidant potential of various extracts from *L. monopetala* in neutralizing free radicals. The results indicated that the extracts demonstrated increased free radical scavenging ability with rising concentrations, displaying a dose-dependent trend. Notably, at a concentration of 500 µg/mL, LMH exhibited the highest scavenging activity (93.85 %) with IC_{50} value of 5.44 µg/mL, followed by LMD (92.92 %) with IC_{50} value of 12.69 µg/mL.

The percentage inhibition of the standard was calculated at 92.96 %. The determination of IC_{50} values for both BHT and the fractions utilized linear regression equations, as depicted in Figure **1**.

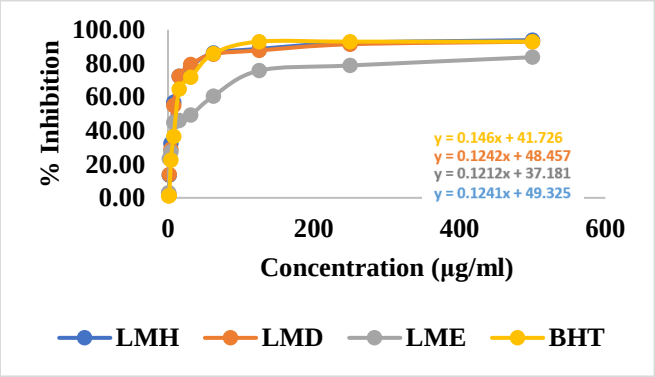

Figure 1: Percentage inhibition and the regression line prediction of BHT and various extracts of *L. monopetala*.

3.2 Total Phenolic Content

To determine the total phenolic content of different fractions of *L. monopetala*, we conducted a test using Folin-Ciocalteu reagent. The absorbance values of the various fraction solutions were utilized for colorimetric analysis, comparing them to the standard curve of gallic acid equivalents. The total phenolic content of each sample was expressed in milligrams of gallic acid equivalent (GAE) per gram of extract, as presented in **Table 1**. Among all the extracts, LMH displayed the highest phenolic content (13.45 mg of GAE/g of extract), followed by LME (3.5 mg of GAE/g of extract). LMD exhibited the lowest phenolic content (0.16 mg of GAE/g of extract).

Table 1: Total Phenolic Content (mg of GAE/gm Extract) of Different Fractions of *Litsea Monopetala*

Plant Part	Sample Code	Absorbance	Total phenolic content (mg of GAE/ gm of extract)
Leaves	LMH	1.03	13.45
	LMD	0.375	0.16
	LME	0.5175	3.05

3.3 Effect of L. monopetala extracts on Brine Shrimp Lethality Bioassay

In the brine shrimp lethality test, it was noted that different extracts of *L. monopetala* displayed a dose-dependent escalation in mortality rates compared to the standard substance. Notably, the LMD extract showed the highest mortality percentage, with an IC_{50} value of 1.10 compared to that of standard (0.88) **(Figure 2)**

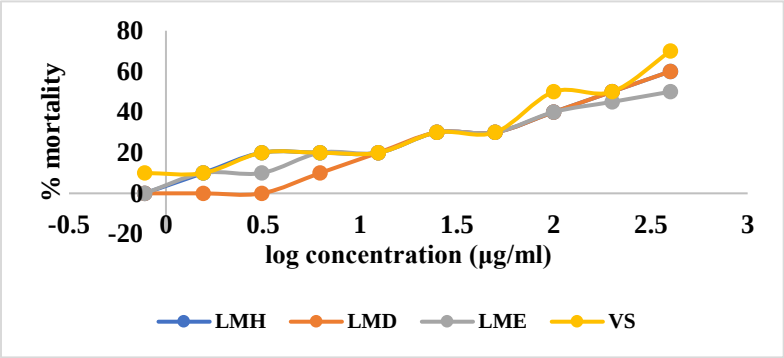

Figure 2: % Mortality and predicted regression line of vincristine sulphate and different extracts of *L. monopetala.*

3.4 Effect of L. monopetala extracts on Thrombolytic Assay

The study aimed to explore the potential cardio-protective properties of extracts obtained from *L. monopetala* by assessing their thrombolytic activity. The findings, as detailed in **Table 2**, revealed that among the tested extracts, LMD derived from the methanolic extract of the plant demonstrated the highest thrombolytic activity, achieving a rate of 31 %. In contrast, LMH exhibited the lowest thrombolytic activity, with a rate of 17 %. **Figure 3** provides a visual comparison of the thrombolytic activities of these various extracts.

Table 2: Effects of different fractions of *L. monopetala* crude extract on thrombolytic and membrane stabilizing assay.

Sample	% clot lysis	% inhibition of heat-induced hemolysis
LMH	17 %	33 %
LMD	31 %	36 %
LME	27 %	7 %
SK	45 %	-
AcSA	-	47 %

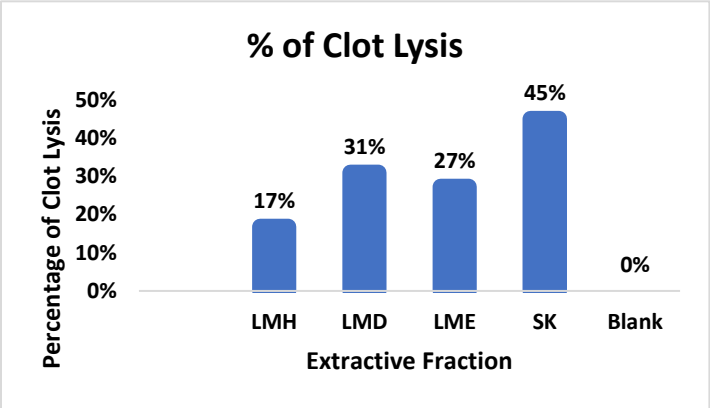

Figure 3: Percentage clot lysis of different fractions of methanolic crude extract of *L. monopetala*.

3.5 Effect of L. monopetala extracts on Membrane Stabilizing Assay

The methanolic extract and its various fractions from *L. monopetala* were found to possess effective membrane-stabilizing activity, preventing the lysis of erythrocytes induced by heat. Among these fractions, LMD inhibited 36 % of hemolysis, and LMH inhibited 33 % inhibition **(Table 2)**. As a point of reference, Acetyl Salicylic Acid, used as the standard drug for assessing membrane stabilizing activity, displayed a 47 % inhibition of hemolysis under normal conditions.

4. Discussion

Synthetic drugs frequently come with a higher likelihood of side effects, making them intolerable at elevated doses for certain individuals. In contrast, traditional medicinal plants have played a vital role in treating numerous ailments, even though the precise mechanisms behind their effectiveness remain elusive. Throughout history, plant extracts have been employed to address various infections, and herbal remedies continue to enjoy popularity due to their cost-effectiveness and milder nature in comparison to synthetic medications [23].

Our study was conducted to investigate the antioxidant, cytotoxic, thrombolytic, and anti-inflammatory properties of different fractions of the EtOAc crude extract of the plant through *in vitro* experiments. Our quantitative phytochemical analysis revealed that LMH has a total phenolic content (TPC) of 13.45 milligrams of gallic acid equivalents per gram (mg GAE/g). Additionally, various fractions of the plant exhibited varying degrees of potential in terms of antioxidant, cytotoxic, thrombolytic, and anti-inflammatory activities.

Phenolic compounds have been directly linked to antioxidant, and anti-inflammatory activities. These compounds have been demonstrated to possess a wide range of beneficial properties, including analgesic, antibacterial, antioxidant, anticancer, anti-inflammatory, and antimicrobial effects [24,25]. The *Litsea* genus

is known for being a rich source of biologically-active compounds, including butanolides found in the leaves of *Litsea acutivena* [26], flavonoids present in the leaves of *Litsea coreana* and *Litsea japonica* [27], sesquiterpenes found in the leaves and twigs of *Litsea verticillate* [28], and essential oils extracted from the leaves of *Litsea cubeba*, as well as from the fruits, flowers, and bark of *Litsea monopetala*, and the fruits of *Litsea glutinosa* [29]. This suggests that *L. monopetala* might possess a significant reducing capacity and the capability to interrupt free radical chain reactions due to presence of the flavonoids.

Medicinal plants are valuable resources for discovering new chemotherapeutic agents. The brine shrimp lethality assay is a method used to assess the lethality of compounds, making it a quick, straightforward, and readily accessible bioassay technique. It is particularly useful for evaluating the potential anticancer and cytotoxic properties of compounds and can serve as a reference for assessing the toxicity of pesticides and substances with antiviral, antibacterial, antimalarial, and antitumor properties [30]. We observed notable toxicity for our plant extract when compared to the standard drug vincristine sulfate. These toxic effects may be attributed to the secondary metabolites generated by the bioactive compounds within our plant extract, some of which have previously been linked to cytotoxicity [31].

Ischemic stroke, which is often the leading cause of death in individuals over 60 worldwide, is typically the result of a cerebral artery blockage caused by an embolus or local thrombus. Streptokinase was the first thrombolytic agent introduced for clinical use and has demonstrated significant effectiveness. However, it also comes with limitations, notably an increased risk of hemorrhagic complications due to the degradation of circulating fibrinogen and factors V and VII.

Thrombolytic agents function by activating the plasminogen enzyme, which in turn breaks down cross-linked fibrin networks, leading to the formation of soluble clots. Additionally, these agents initiate various proteolysis activities involving several enzymes, ultimately aiming to restore blood flow that has been obstructed by occlusions [32]. Different fractions of the extract demonstrated a moderate level of thrombolytic activity when compared to the positive control, streptokinase. This observation could be attributed to the presence of bioactive secondary metabolites within the extract.

Medications like corticosteroids (steroids) and non-steroidal anti-inflammatory drugs (NSAIDs) exert their anti-inflammatory effects by stabilizing cell membranes. It's crucial to recognize, though, that these drugs can come with significant side effects [33]. Given the context, investigating natural products that possess the capacity to stabilize cell membranes may be a more

attractive option when seeking anti-inflammatory treatments. LMD and LMH fractions of the plant studied in this research exhibited remarkable membrane-stabilizing abilities against both heat-induced hemolysis. This makes the plant a highly promising candidate for further exploration and investigation as a potential source of anti-inflammatory compounds.

5. Conclusion

In summary, our bioactivity analysis of *Litsea monopetala* has led to the demonstration of remarkable antioxidant, cytotoxic, thrombolytic, and anti-inflammatory properties. These findings underscore the significant potential of the plant as a valuable source of bioactive terpenoids with diverse pharmacological activities. This study paves the way for exciting future research endeavors. Firstly, further investigations are needed to uncover the phytochemicals along with their precise molecular mechanisms responsible for the observed bioactivities.

Author Contributions: Conceptualization- MSK., and M.H.; methodology- MSK, and SA; software- MSK., and SA; validation- MSK and MRH; formal analysis- MSK and SA; investigation- MSK and SA; resources- MRH; data curation- MSK and MRH; writing—original draft preparation- MSK, SA and SS; writing—review and editing- MSK, SA and SS; visualization- MRH; supervision- MRH; project administration- MRH. All authors have read and agreed to the published version of the manuscript.

Funding: This research received no external funding.

Informed Consent Statement: Not applicable

Data Availability Statement: Data is available in the manuscript.

Acknowledgments: Authors are grateful to all the folkloric practitioners of the country to provide valuable evidences for the scientific experiment.

Conflicts of Interest: There are no known financial or research-based conflicts of interest among the authors.

References

1. Hayes, J.D., Dinkova-Kostova, A.T., Tew, K.D. Oxidative stress in cancer. *Cancer Cell* 2020; 38: 167–197.
2. Chang, X., Zhang, T., Zhang, W., Zhao, Z., Sun, J. Natural drugs as a treatment strategy for cardiovascular disease through the regulation of oxidative stress. *Oxid. Med. Cell. Longev.* 2020; 5430407.
3. Forman, H.J., Zhang, H. Targeting oxidative stress in disease: promise and limitations of antioxidant therapy. *Nat. Rev. Drug Discov.* 2021; *20:* 689–709.
4. Luo, H., Vong, C.T., Chen, H., Gao, Y., Lyu, P., Qiu, L., Zhao, M., Liu, Q., Cheng, Z., Zou, J. Naturally occurring anti-cancer compounds: shining from chinese herbal medicine. *Chin. Med.* 2019; 14: 48.
5. Kooti, W., Servatyari, K., Behzadifar, M., Asadi-Samani, M., Sadeghi, F., Nouri, B., Zare

Marzouni, H. Effective medicinal plant in cancer treatment, Part 2: Review Study. *J. Evid. Based. Complementary Altern. Med.* 2017; *22*: 982–995.

6. Samouh, Y., Lemrani, A., Mimouni, H., Mohamad, J., Said, A.A.H. Ethnopharmacological study of herbal medicines used to treat cancer in Morocco. *J. Phytopharm.* 2019; 8: 135–141.
7. Leite, P.M., Martins, M.A.P., das Graças Carvalho, M., Castilho, R.O. Mechanisms and interactions in concomitant use of herbs and warfarin therapy: an updated review. *Biomed. Pharmacother.* 2021; 143: 112103.
8. Greten, F.R., Grivennikov, S.I. Inflammation and cancer: triggers, mechanisms, and consequences. *Immunity* 2019; 51: 27–41.
9. Ghasemian, M., Owlia, S., Owlia, M.B. Review of anti-inflammatory herbal medicines. *Adv. Pharmacol. Pharm. Sci.* 2016; 2016: 9130979.
10. Shahidullah, A.K.M., Haque, C.E. Linking medicinal plant production with livelihood enhancement in Bangladesh: implications of a vertically integrated value chain. *J. Transdiscipl. Environ. Stud.* 2010; 9: 1-18.
11. Hanif Hasan, M., Islam, M.Z., Rahman, S.M., Islam, M.R., Rahman, S., Rahmatullah, M. Antihyperglycemic activity of methanolic extract of *litsea monopetala* (roxb.) pers. leaves. *Adv. Nat. Appl. Sci.* 2014; 8: 51–55.
12. Bhattarai, S., Chaudhary, R.P., Taylor, R.S.L. Ethno-medicinal plants used by the people of Nawalparasi district, central Nepal. *Our Nat.* 2009; 7: 82–99.
13. Mou, S.M., Mahal, M.J., Bhuiyan, P., Zakaria, A.S.M., Datta, B., Rana, M., Islam, A., Khatun, Z., Rahmatullah, M. Medicinal plants and formulations of small tribes of Bangladesh: a case study of the naik clan of the Rajbongshi tribe. *Am-Eur J Sustain Agr* 2012; *6*: 248–253.
14. Rahmatullah, M., Ferdausi, D., Mollik, A., Jahan, R., Chowdhury, M.H., Haque, W.M. A survey of medicinal plants used by Kavirajes of Chalna area, Khulna district, Bangladesh. *African J. Tradit. Complement. Altern. Med.* 2010; 7(2): 91–97.
15. Islam, M.A., Yeasmin, M., Rahmatullah, M. Ethnoveterinary practices among folk medicinal practitioners of three randomly selected villages of Dinajpur district, Bangladesh. *Am. J. Sustain. Agric.* 2013; 7: 75–84.
16. Kabir, M.H., Hasan, N., Rahman, M.M., Rahman, M.A., Khan, J.A., Hoque, N.T., Bhuiyan, M.R.Q., Mou, S.M., Rahmatullah, M. Tribal medicine in tribes who have lost their identities: medicinal plants of tea garden workers in Sreemangal, Maulvibazar district, Bangladesh. *Am-Eur. J. Sustain. Agr.* 2013; 7: 251–258.
17. VanWagenen, B.C., Larsen, R., Cardellina, J.H., Randazzo, D., Lidert, Z.C., Swithenbank, C. Ulosantoin, a potent insecticide from the sponge ulosa ruetzleri. *J. Org. Chem.* 1993; 58: 335–337.
18. Singh, T.P., Singh, O.M. Recent progress in biological activities of indole and indole alkaloids. *Mini Rev. Med. Chem.* 2018; 18: 9–25.
19. Harbertson, J., Viticulture, Spayd S Measuring phenolics in the winery. *Am. J. Enol. Vitic.* 2006; 57: 280–288.
20. Jasiewicz, B., Kozanecka-Okupnik, W., Przygodzki, M., Warżajtis, B., Rychlewska, U.,

Pospieszny, T., Mrówczyńska, L. Synthesis, antioxidant and cytoprotective activity evaluation of c-3 substituted indole derivatives. *Sci. Reports* 2021; 11: 1–14.

21. Bhowmick, R., Sarwar, M.S., RahmanDewan, S.M., Das, A., Das, B., Nasir Uddin, M.M., Islam, M.S., Islam, M.S. *In vivo* analgesic, antipyretic, and anti-inflammatory potential in swiss albino mice and *in vitro* thrombolytic activity of hydroalcoholic extract from *litsea glutinosa* leaves. *Biol. Res.* 2014; 47: 1–8.
22. Islam, T., Das, A., Shill, K.B., Karmakar, P., Islam, S., Sattar, M.M. Evaluation of membrane stabilizing, anthelmintic, antioxidant activity with phytochemical screening of methanolic extract of *Neolamarckia cadamba* fruits. *J. Med. Plants Res.* 2015; 9: 151–158.
23. Shovo, M.A.R.B., Tona, M.R., Mouah, J., Islam, F., Chowdhury, M.H.U., Das, T., Paul, A., Ağagündüz, D., Rahman, M.M., Emran, T. Bin computational and pharmacological studies on the antioxidant, thrombolytic, anti-inflammatory, and analgesic activity of *Molineria capitulata*. *Curr. Issues Mol. Biol.* 2021; 43: 434–456.
24. Liang, Y.-C., Huang, Y.-T., Tsai, S.-H., Lin-Shiau, S.-Y., Chen, C.-F., Lin, J.-K. Suppression of inducible cyclooxygenase and inducible nitric oxide synthase by apigenin and related flavonoids in mouse macrophages. *Carcinogenesis* 1999; 20: 1945–1952.
25. Uddin, M.M.N., Ahmed, S., Kabir, M.S.H., Rahman, M.S., Sultan, R.A., Emran, T. B. *In vivo* analgesic, anti-inflammatory potential in swiss albino mice and *in vitro* thrombolytic activity of hydroalcoholic fruits extract from *Daemonorops Robusta* Warb. *J. Appl. Pharm. Sci.* 2017; 7: 104–113.
26. Aimaiti, S., Saito, Y., Fukuyoshi, S., Goto, M., Miyake, K., Newman, D.J., O'Keefe, B.R., Lee, K.-H., Nakagawa-Goto, K. Isolation, structure elucidation, and antiproliferative activity of butanolides and lignan glycosides from the fruit of *Hernandia Nymphaeifolia*. *Molecules* 2019; 24: 4005.
27. Ji, S.Y., Bang, E., Hwangbo, H., Kim, M.Y., Kim, D.H., Koo, Y.T., Kim, J.S., Lee, K.W., Park, S.Y., Kwon, C.-Y. Improvement of immune and hematopoietic functions by *Litsea japonica* fruit extract in cyclophosphamide-treated BALB/c mice. *Appl. Sci.* 2022; 13: 145.
28. Hossen, M.F., Hossain, S., Ahamed, M.I., Patwary, M.S., Imtiaz, O., Hasan, M., Al Mahmud, A. Evaluation of *in vivo* analgesic, antiemetic and anxiolytic effect of methanolic extract of *Litsea monopetala* in animal model. *Discov. Phytomedicine* 2019; 6: 126–129.
29. Tripathi, P., Yami, H., Shukla, A.K. Determination of antifungal activity against phytopathogenic fungi by essential oils extracted from some medicinal plants. *Biopestic. Int.* 2021; 17(2): 163-171.
30. Yesmin, S., Paul, A., Naz, T., Rahman, A.B.M., Akhter, S.F., Wahed, M.I.I., Emran, T. Bin, Siddiqui, S.A. Membrane stabilization as a mechanism of the anti-inflammatory activity of ethanolic root extract of choi (*Piper chaba). Clin. Phytoscience* 2020; 6: 1–10.
31. Khanal, S., Bhatt, B.D. Study on biological activity of *Litsea monopetala* from Panchthar district of Nepal. *J. Inst. Sci. Technol.* 2020; 25: 113–118.
32. Emran, T. Bin, Rahman, M.A., Uddin, M.M.N., Rahman, M.M., Uddin, M.Z., Dash, R., Layzu, C. Effects of organic extracts and their different fractions of five bangladeshi plants on *in vitro*

thrombolysis. *BMC Complement. Altern. Med.* 2015; 15: 1–8.

33. Poetker, D.M., Reh, D.D. A comprehensive review of the adverse effects of systemic corticosteroids. *Otolaryngol. Clin. North Am.* 2010; 43: 753–768.

JBEP

Journal of Biosciences and Experimental Pharmacology
ISSN-2960-284X

Review Article

Recent Advances in Nanocarriers as Targeted Drug Delivery Systems

Mahira Islam Asfie[1], Junayet Hossain Khan[1], Sultan Alshehri[2], Mohsin Kazi[3], Mohammad Hossain Shariare[1]*

[1] *Department of Pharmaceutical Sciences, North South University, Dhaka, Bangladesh*

[2] *Department of Pharmaceutical Sciences, College of Pharmacy, Al Maarefa University, Ad Diriyah 13713, KSA*

[3] *Department of Pharmaceutics, College of Pharmacy, POBOX-2457, King Saud University, Riyadh, KSA*

***Correspondence *E-mail*:** mohammad.shariare@northsouth.edu

Abstract: Targeted drug delivery and the use of nanocarriers in drug delivery systems have shown significant impacts in mitigating various diseases. The limitation lies in designing nanocarriers for an effective therapeutic outcome. The concept of targeted drug delivery is drawn from the 'magic bullet' concept, which reduces toxicity, enhances effectiveness, and helps control the drug release rate. Targeted drug delivery strategies can be performed in various ways but mainly depend on ligand–receptor binding and the enhanced permeability and retention method (EPR). Different nanocarriers have been developed over the years, including liposomes, solid lipid nanoparticles, lipid-polymer hybrid nanoparticles, niosomes, ethosomes, dendrimers, polymeric micelles, carbon nanotubes, and metallic nanoparticles. Drug loading in nanocarriers occurs by covalent bonding, electrostatic interactions, or encapsulation. Nanocarriers have been developed over the years, and novel nanocarriers have been designed to enhance their effectiveness, reduce side effects, increase circulation time, and accumulate at the target site. This article discusses the different strategies of drug delivery systems, different types of nanocarriers, and their advantages as targeted drug delivery systems. This article also discusses the recent advances of novel designed nanocarriers as targeted drug delivery systems.

Keywords: Nanocarriers 1; targeted drug delivery 2; drug loading 3; receptor binding 4; novel design 5; therapeutic efficacy 6.

Citation: Asfie, M. I.; Khan J. H.; Kazi M.; Shariare M. H.; Recent advances in nanocarriers as targeted drug delivery systems. *J. Bio. Exp. Pharm.* 2023, 1:39–69.

Received: November 19, 2023
Accepted: December 11, 2023
Published: December 15, 2023

Publisher's Note: JBEP stays neutral with regard to jurisdictional claims in published maps and institutional affiliations.

1. Introduction

Nanotechnology has been in use for a long time, but its use has recently emerged in drug delivery. There have been many advances in this field to make effective site-specific medications. Nanotechnology is now widely used to make

drug delivery more effective at the target site, reducing side effects. Targeted drug delivery is required to obtain the maximum efficacy at a lesser amount and enhanced therapeutic effect without side effects resulting from accumulation at the nontarget site. Various nanocarriers have been developed, each with unique properties for targeted drug delivery. Target drug delivery can also reduce multidrug resistance, for which the use of nanocarriers has become a topic of interest for delivering lifesaving drugs. Recent advances in nanocarriers as a means of targeted drug delivery systems have paved the way for mitigating various diseases, such as cancer, acne, Alzheimer's disease, and infections. It is also used for vaccines and the delivery of insulin. Recently, nanocarriers were used to produce the COVID-19 vaccine, which has been an issue worldwide. Nanocarriers that help in the drug delivery system are less than 200 nm in size, and the weight is more than 40 kDa. This specification allows nanocarriers to cross the microcapillaries of the body very easily and reach the desired target site. On the other hand, higher weight does not allow it to be eliminated easily by the kidney. They remain in the circulation system for a long time, which helps them accumulate in the target site, resulting in a maximum therapeutic effect [1, 2].

Nanocarriers are loaded with drugs through three main strategies: covalent bonding, encapsulation, and electrostatic interaction. Moreover, functionalizing nanocarriers with the help of polymers, ligands, surfactants, and biomolecules has made drug delivery more efficient. This has helped in the reduction of toxic effects along with better therapeutic outcomes [3]. Liposomes, solid lipid nanocarriers, carbon nanotubes, polymeric micelles, virosomes, transferosomes, niosomes, dendrimers, carbon nanotubes, and mesoporous silica are some of the most used nanocarriers in drug delivery systems. They are not only used for the delivery of drugs but also have effects in diagnosis, treatment, immunization, biosensing, etc. Functionalization of these nanocarriers by using various ligands, polymers, and biomolecules to make novel-designed nanocarriers that overcome the drawbacks of conventionally used nanocarriers. Some novel-designed nanocarriers are cubosomes, lipid drug conjugates, nanostructured lipid carriers, quantum dots, etc. These novel-designed nanocarriers are more specific and pose little to no threat of toxicity, as they have a specific affinity for the target site [4, 5, 6].

This paper mainly focuses on the advances of nanocarriers in targeted drug delivery, strategies for targeted drug delivery, ways of loading drugs on nanocarriers,

functionalization of nanocarriers, and some of the novel designed nanocarriers that are better than conventionally used nanocarriers.

2. Targeted Drug Delivery

Drug delivery, in general, describes the processes, methods, technologies, and formulations used to carry the drug substance in the body to achieve the required therapeutic effect. The drug delivery system's primary focus is administering the drug appropriately with the proper dosage and target. Targeted drug delivery is the system by which the drug is administered to a specific target in a specific location. Targeted drug delivery systems have made remarkable advances because they are responsible for increased safety due to target specificity, which also increases efficacy [7]. On the other hand, a conventional drug delivery system does not focus on drug delivery at a specific site, minimization of toxicity, or enhancement of effectiveness and, as a whole, has low therapeutic indices [8]. In a targeted drug delivery system, the drug is not released at any other nontarget site.

The concept of targeted drug delivery came from the “magic bullet” vision of Paul Ehrlich to selectively target by drugs and have affinity only for that target without harming other sites [9, 10]. The term magic bullet was postulated, as the drug would pose a lethal effect on the pathogen without harming the human body. This magic bullet acts as a gunman's bullet that exclusively hits the target and nothing else in the surroundings [11].

The concept of a magic bullet mainly included identifying toxic drugs and then modifying those drugs to pose less toxicity by increasing the specificity [12]. The components that help in the effective delivery of the drug to the target site include the selection of the target moiety, selecting a target to effectively bind with the target, and the drug that will provide therapeutic action [13]. Carriers deliver the intact drug to the exclusively selected site of action, and there can be various types of carriers to entrap the drug moiety [14].

2.1 Advantages of Targeted Drug Delivery

Target drug delivery focuses on delivering a specific quantity of drug to a particular site on the organ or tissue. The concept depends on the accumulation of the drug, specifically at the target site. This process helps find solutions to problems faced with conventional medications. Thus, there are various advantages of the target drug delivery system. The drug concentration at the target site due to nanocarrier integrated drug is high, whereas the concentration at the nontarget site is low. At the

same time, side effects and toxic reactions are less as the drug accumulates at high concentrations only at the desired site of action. For this reason, the amount of drug required to obtain a therapeutic effect is lower, reducing the cost of treatment. The toxicity can be reduced which is usually the result of high doses for showing therapeutic effects and drugs with small therapeutic indices. The protocols required for the administration of the drug are also simple. The absorption of the drug from the target site is higher and improved and it helps improve the drug's pharmacodynamic, pharmacokinetic, and other therapeutic effects as desired. After the administration, the drug passes through various pathways, but the biodistribution is controlled before reaching the target site. At the same time, the drug's half-life can also be modified so that the drug is not eliminated before showing therapeutic efficacy. It improves patient compliance as dosing and size of dose can be reduced. Thus, the efficacy of the drug is enhanced [13, 15, 16].

2.2 New Strategies of Targeted Drug Delivery

Target drug delivery strategies are classified into two major methods. They are passive targeting and active targeting. Apart from these three, there are other targeting strategies as well. Although the targeting strategies might differ, the main reason for the release of the drug at the target site is the change in temperature, pH, or both. The target drug delivery strategies for the drugs via nanocarriers are as follows:

2.2.1 *Passive targeting:* Passive targeting is the process that is based on the enhanced permeability and retention (EPR) effect, which is the accumulation of the drug at the target site [17]. In this process, nanocarriers carrying the drug are drained into the leaky vasculature of the target tumor cells. The tumor vasculatures are incomplete and are of size ranging from 100nm to 780nm depending on the type of the tumor whereas, normal vessels have tight endothelial junctions [18]. Accumulation in the blood occurs over time, as they are not small enough to be excreted by the kidney or large enough to be captured by the reticuloendothelial system [19]. The molecular weight of the nanosized drug is more than 40 kDa, which does not allow it to enter through the capillary beds. At the same time, the vasculature of tumors consists of leaky vessels, so it is easier for high molecular weight drugs to specifically enter the target tumor. Apart from leaky vessels, tumor microenvironment lacks a well-defined drainage

system. This results in the enhanced drug entry and retention in the target site, which results in increased efficacy and reduced side effects as the drugs accumulate only at the diseased site [1, 20]. Nanocarriers with hydrophilic surfaces and 200 nm size or less have a greater EPR effect as they circulate in the blood for a longer time [2]. Conversely, if the molecular weight is low, the drug will diffuse away from the target and re-enter the blood circulation [21]. Doxil (doxorubicin in PEGylated liposomes) is a clinically approved drug that follows passive targeting [22].

2.2.2 *Active Targeting:* Active targeting is a type of ligand–receptor binding technique. In this strategy, nanocarriers are bound with a ligand on their surface, and this ligand binds actively to specific receptors [23]. The ligand chosen in this case needs to determine the overexpressed receptors on the diseased cells. Ligands can be peptides, lectins, antibodies, polysaccharides, nucleic acids, etc. [24]. Active targeting proves more specificity than passive targeting, as it binds to the target site with a high affinity. This avoids unexpected bonding of the drug and reduces side effects and multidrug resistance [25]. Receptors that are only expressed in cancer cells are targeted, for example, folate receptors in lung cancer cells and epidermal growth factor receptors in ovarian cancer. [26]. Active targeting can be classified into four orders of targeting. Targeting is different in these four orders. For instance, first-order targeting targets the capillary bed of the desired target site, second-order targeting targets tumor cells, third-order targeting targets intracellular sites, and fourth-order targeting targets macromolecules such as DNA and proteins. The advantage of active targeting is that it does not have to depend on the leaky vasculature of the diseased cell and the EPR effect [27]

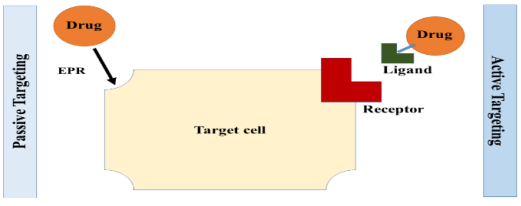

Figure 1: Passive targeting occurs as drug accumulate at the target site due to enhanced permeability and retention effect and active targeting takes place as the nanocarrier is bound with a ligand that can specifically detect the overexpressed receptor on the diseased cell.

2.2.3 *Inverse Targeting:* Inverse drug targeting is the process in which a blank nanocarrier inhibits the activity of the reticuloendothelial system. In the reticuloendothelial system, some cells are responsible for the phagocytosis of foreign materials. The use of inverse targeting results in the accumulation of cells with blank nanocarriers, which will, in turn, suppress the defense mechanism [28].

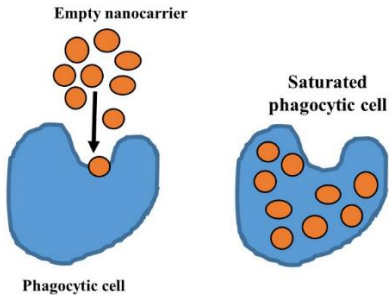

Figure 2: Inverse Targeting.

2.2.4 *Dual Targeting:* Dual targeting is the strategy in which the nanocarrier has the drug's therapeutic activity. It provides synergistic activity, enhancing the effect of the drug. [29].

2.2.5 *Double Targeting:* The double targeting strategy combines the theory of spatial and temporal controls. Spatial control delivers the drug to the specific target site, and temporal control delivers the drug to the target site at a controlled rate [7].

2.2.6 *Combination Targeting:* Various elements with a particular affinity for the target site are used in combination, for which this targeting system is called combination targeting. In combination targeting, the most commonly used molecules are polymers, homing devices, and carriers of molecular specificity. Triple targeting is the most effective and selective form of combination targeting. This helps provide direct interaction with the target site [29].

2.2.7 *Biological Targeting:* Biological targeting involves the delivery of the drug to the target area by using antibodies, peptides, or other biomolecules that have an affinity for the target cell receptor [31].

2.2.8 *Physical Targeting:* Physical targeting is the process that takes specific characteristics such as size, shape, rigidity property, light intensity, electric

field, and composition into account. These characteristics are responsible for the accumulation of the drug in the target site, increased uptake rate, increased drug circulation time in the blood, and tissue retention [32].

2.2.9 *Chemical Targeting:* Chemical targeting occurs when nanocarriers are responsive to pH, temperature, enzymes, and site-specific prodrugs. This responsiveness allows the drug to localize in the target area and leads to controlled drug release [7, 31].

2.2.10 *Local Targeting and Systemic Targeting:* The drug is delivered to the local site in local targeting. It is a noninvasive process. On the other hand, systemic targeting focuses on delivering the drug to the systemic circulation by intravenous administration. It is an invasive process. The major disadvantage of these techniques is that they are not target specific, which affects nontarget cells and may cause adverse effects [33].

2.2.11 *Location-Based Targeting and Disease-Based Targeting:* Location-based targeting is the process by which the drug is delivered to organelles, organs, cells, or intracellular targets in the gastrointestinal tract, brain, etc. On the other hand, disease-based targeting is based on targeted delivery to the disease site. These advanced targeting processes can now be used as an alternative to antibiotic therapy, and nanovaccines can also be produced. This can be done by functionalizing the nanoparticles with antimicrobial agents [7].

3. Nanotechnology and Nanocarriers

Nanotechnology is the science and technology that manipulates matter on a nanoscale, *i.e.*, 1 to 100 nanometers [34]. It helps make new structures and materials on the atomic scale. It has advanced in many areas, including medicine. Nanomaterials have distinct physical and chemical properties [35]. They help enhance the pharmacological properties of medications. The therapeutic effect of drugs made by nanotechnology can be achieved by different routes of administration, such as oral nasal, transdermal, intravenous, intramuscular, intrathecal, and intra-articular routes. [36].

Nanocarriers are nanometer-range colloidal nanosystems. They are loaded with therapeutic agents that help the therapeutic agent reach the desired target site. They selectively accumulate in the target site and show the desired therapeutic effect [37, 38]. Nanocarriers must be biodegradable, nontoxic, nonimmunogenic,

cost-effective, stable, have a high surface area, and release the therapeutic agent at the target site [39, 40].

3.1 Nanocarriers in Drug Delivery

Nanocarriers in drug delivery systems have been rapidly developing since their emergence. It can be used as an effective drug delivery system for almost all routes of administration with some specific modification in shape, size, structure, and surfactant properties. Nanocarriers are used not only in drug delivery systems but also for diagnostic purposes and immunization. It is being used to mitigate various diseases, from COVID-19 vaccines to Alzheimer's. It is also used for acne and infection treatment by loading antibiotics in nanocarriers and as a chemotherapeutic agent delivery system in different cancers [4, 5, 41, 42].

Apart from using nanocarriers for the delivery of drugs in different diseased cells, they have various other advantages. They enable long-term circulation in the blood, resulting in increased accumulation, overcome the reticuloendothelial system, have high stability, have increased biodistribution and are made of biocompatible materials for which they are biodegradable. They also show an increased pharmacokinetic profile, reduced toxicity due to enhanced specificity, controlled release rate, enhanced solubility, and increased accumulation at the target site that decreases secondary effects [43].

3.2 Development and Manufacturing of Nanocarriers

In manufacturing nanocarriers, the vital points that need to be focused on are size, shape, dimension, and structure, as they play a prominent role in the release and stability of the compound. Manufacturing of nanocarriers can be performed by two approaches, *i.e.*, bottom-up or top-down techniques. The top-down method involves the breakdown of the bulk into several nanosized particles. This process produces the desired structure by removing or breaking the bulk material. Breaking down a bulk material might not always be perfect for which the desired shape and size are not achieved. This process creates more waste. This method involves milling, laser ablation, electro-expulsion, etching, etc. The bottom-up method involves the building up of a nanoparticle from the bottom. The atoms, molecules, or clusters are accumulated and made into the desired shape, size, and structure with minimum waste. It is more economical. External stimuli under specific conditions are applied to make the components form a complex structure of the desired type. This process involves spinning, chemical vapor deposition, precipitation, molecular condensation,

etc. Since it poses more accuracy in shape, size, and structure, this is a more widely used method of nanoparticle development by scientists [6, 44, 45].

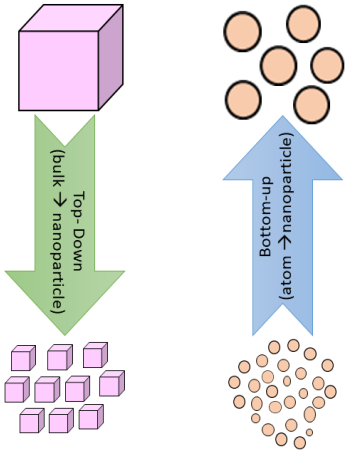

Figure 3: Top-down method involves the breakdown of a bulk material into several nanosized particles and bottom-up method involves the building up of a nanosized particle from atoms and molecules. [6]

3.3 Drug Loading and Release Strategy in Nanocarriers

Drug loading in the nanocarrier is required to deliver the drug to the target site for the desired therapeutic effect. To load nanocarriers with drugs, there are three main strategies, such as, covalent binding, encapsulation and electrostatic interaction.

Covalent bonding: Covalent bonding occurs between the drug and the nanocarrier due to the presence of appropriate functional groups (hydroxyl group, carboxylic group, etc.) on the surface of the nanocarrier and the drug. This forms a nanocarrier-drug conjugate. Sometimes linkers such as succinic acid or succinic anhydride can be used to facilitate the conjugation process [46]. These conjugates diffuse through the cell membrane of the target site, and then enzymes and chemicals break through the covalent bond that releases the drug at the desired site. [47].

Encapsulation: The drug is loaded in the hollow cavity of the nanocarriers where the hydrophobic region encapsulates the hydrophobic drugs, and the hydrophilic region encapsulates the hydrophilic drug. Drug release occurs via hydrolysis, thiolysis, pH change, or temperature change [48].

Electrostatic Interaction: Different high-density functional groups, such as carboxylic or amine groups on the nanocarriers, interact electrostatically with the drug material. This helps the drug to be incorporated into the nanocarriers effectively [49].

3.4 Functionalization of Nanocarriers

The functionalization of nanocarriers is performed by the attachment of functional groups, ligands, polymers, surfactants, or biomolecules by covalent or noncovalent conjugation. It increases selectivity, biocompatibility, and controlled release of the drug in the target site [3, 50].

Polymers such as polyethylene glycol can be used to functionalize nanocarriers, increasing the permeability and retention effect, making it target specific, and helping in the controlled release of the drug [51].

Nanocarriers are also functionalized by ligands that specifically bind to the receptors of the target site. It is also known as an active targeting strategy [52]. It helps reduce the side effects and unwanted binding to other nontarget sites. It also helps increase drug accumulation at the target site, as it does not interact with other sites. It increases treatment accuracy [53].

Surfactants (sodium cholate, polysorbate, span 80, tween 80, etc.) are used in functionalizing nanocarriers, as the nanocarriers may show bursting effects, instability, premature degradation, and poor accumulation in the target site. Using surfactants with nanocarriers can overcome these drawbacks, resulting in better drug delivery and enhanced accumulation at the target site without unwanted drug degradation [54].

Biomolecules can be used to functionalize nanocarriers to reduce cytotoxic effects and enable site-specific drug delivery. Biomolecules have cell-mimicking properties that make them biocompatible and enable them to remain in blood circulation for a long time. This allows them to have time to accumulate at the target site. They also overcome the reticuloendothelial system. This is why they do not pose any immunological disturbance or allergic reaction in the individual. The biomolecules used in functionalizing nanocarriers can be antibodies, oligonucleotides, nucleic acids, peptides, folate, etc. [55, 56, 57].

3.5 Different Types of Nanocarriers

3.5.1 Liposome

Liposomes are spherical lipid bilayer structures. They have a hydrophilic core and a hydrophobic space that encloses the hydrophilic core. The hydrophobic region encapsulates lipophilic drugs, and the hydrophilic core encapsulates hydrophilic drugs. They are made from physiological lipids, cholesterol, or naturally occurring phospholipids. Liposomes can be uni-lamellar or multilamellar. They are

available in cream, gel, suspension, and solid dosage forms and can be administered via the parenteral route. The accumulation of liposomes in the target site is due to their small size and prolonged circulation. Drugs loaded in liposomes are used to deliver drugs such as doxorubicin and daunorubicin for the treatment of mammary gland tumors and AIDS-linked Kaposi's melanoma. [58] Liposomes are metastable, which results in an uncontrolled release of the drug. The phospholipids undergo hydrolysis or oxidation, resulting in a short half-life, leakage, and fusion of the encapsulated drug. Since liposomes are unstable, they need special storage conditions and preparation techniques [59, 60].

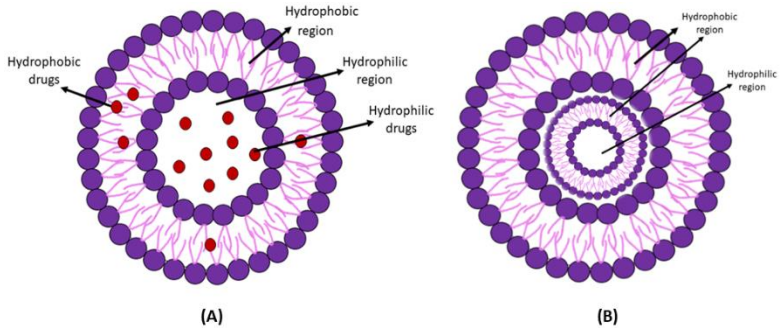

Figure 4: (A) Unilamellar liposome, (B) Multilamellar liposome

3.5.2 Solid lipid Nanocarriers (SLN)

Solid lipid nanocarriers consist of a solid lipid core that is surrounded by surfactants. The lipid core helps to solubilize lipophilic drugs. The surfactant surrounding the solid lipid core works as an emulsifier to keep the lipid nanoparticles stable. The amount and type of emulsifier depends on the route of administration [61]. The solid lipid core is made up of lipids that are solid at room temperature, for example, free fatty acids, steroids, waxes, triglycerides, lecithin, etc. Solid lipid nanocarriers are used to deliver chemotherapeutic agents and ophthalmic drugs and can also be used to deliver genes [62, 63]. Solid lipid nanoparticles for drug delivery have proven safer due to biodegradable lipids that do not pose any toxicity threat. The stability, drug payload, and drug release rate control are better than those of other carriers, such as polymeric carriers [64]. In contrast, burst release can occur if the drug is not homogenously distributed in the drug. This hampers the controlled release effect. It can also have other problems, such as forming a lipid crystal matrix and changing the physical state of the solid lipid. For this reason, novel forms of solid lipid nanocarriers have recently been developed [65].

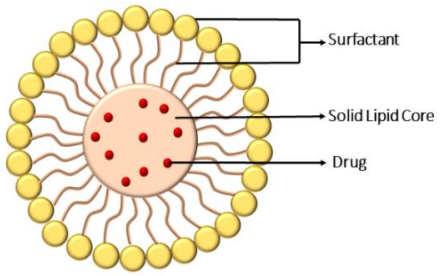

Figure 5: Solid Lipid Nanocarrier.

3.5.3 Polymeric micelles

Polymeric micelles are amphiphilic polymers that contain both hydrophilic and hydrophobic regions. They consist of a hydrophobic core and a hydrophilic shell that can self-assemble and form a unique core-shell structure. There can also be reverse micelle formation with the hydrophilic head toward the core and the hydrophobic tail on the outer surface [66]. In a polymeric micelle, the drugs remain encapsulated at the core, and the outer hydrophilic shell helps keep it stable in the aqueous region. This is also why polymeric micelles are effectively administered through the intravenous route [67]. On the other hand, the opposite occurs in a reverse micelle where the hydrophilic core encapsulates the hydrophilic drug, and the hydrophobic region is integrated within the membrane. This helps transport both hydrophobic and hydrophilic drugs [68]. Drug loading in polymeric micelles increases the therapeutic window of lipophilic drugs, reduces rapid clearance, prolongs circulation, and enhances the accumulation of the drug at the target site. Paclitaxel has been loaded in polymeric micelles to deliver it to the target site. It is known as Genexol-PM [69].

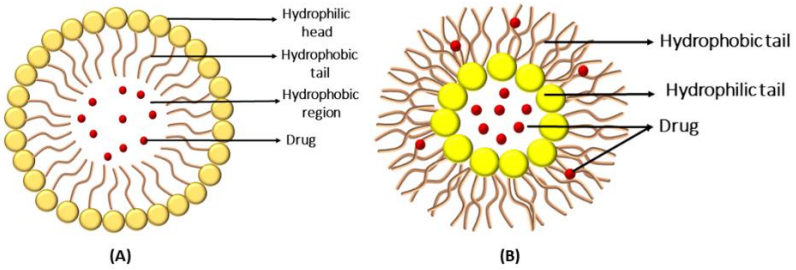

Figure 6: (A) Polymeric micelle, (B) Reverse micelle

3.5.4 Metallic Nanoparticles

Metallic nanocarriers are made of a metallic core. This core can be made of nickel, cobalt, iron, manganese, silver, titanium, platinum, or noble metal gold. These nanocarriers have magnetic and optical properties [70]. They obtain their biocompatibility from the core metal, size, and coating on the nanocarrier. Most metals pose a toxicity profile. Despite this, iron oxide is widely used in biomedicine due to its lower toxicity.

The metallic core has magnetic attraction, resulting in the formation of agglomerates. These agglomerates are identified by the reticuloendothelial system and eliminated [71, 72]. To stop this process, metallic nanoparticles are coated with liposomes, polymers, biological molecules, or surfactants. The nanoparticle can also be functionalized by ligands, nucleotides, antibodies, enzymes, etc. [73]**.** This enhances the stability of the drug, makes it more hydrophilic, enhances biocompatibility, increases drug delivery at the target site, and reduces toxicity [74]. The most commonly used metallic nanoparticles for medicine are gold and iron oxide nanocarriers. An example of iron oxide as a nanocarrier along with conjugation with a ligand is IGF1-IONPDOX (recombinant human insulin-like growth factor 1 as a targeting ligand with iron oxide nanoparticles containing doxorubicin) to inhibit human pancreatic tumors [75, 76, 77].

Recent studies have also shown that metallic nanoparticles have an antimicrobial effect. The shape and charge play the most critical role in antimicrobial activity [78]. This effect arises as the positive charge on the metallic nanoparticle interacts with the negative charge on the bacterial surface. This enhances the binding efficiency targeted to the bacteria and results in a bactericidal effect. This plays a vital role in overcoming antibiotic resistance, which is currently the major reason for death [79, 80].

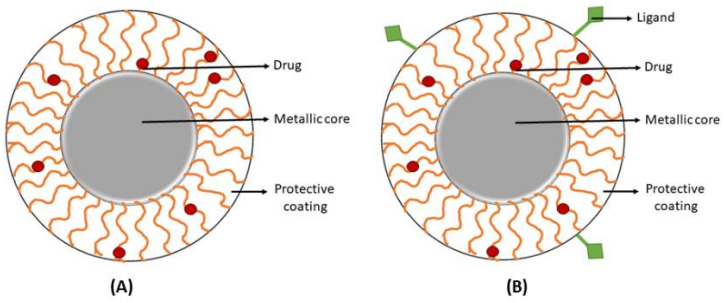

Figure 7: (A) Metallic nanocarrier, (B) Metallic Nanoparticles with ligands

3.5.5 Carbon nanotubes

Carbon nanotubes are hollow tubes with graphene sheets wrapped around them at a specific angle. These are needle-like tubes of carbon. The needle structure makes them better than spherical nanocarriers. This structure helps them to cross the cell membrane very easily by endocytosis. They have a high surface area, enhanced specificity, increased efficacy, fewer side effects, and enhanced cellular uptake [81, 82]. These tubes are formed by carbon atom hexagons in a helical structure. The carbon nanotube diameter is 0.4-100 nm, and the length is a thousand times greater than the diameter [83]. They have been used for diagnosis and drug delivery to the target site [84]. It delivers peptides, APIs, and nucleic acids and can also be attached with fluorescence to help diagnose [85]. These nanocarriers are usually toxic and water insoluble. This can result in the accumulation of nanotubes in different tissues, which can result in toxic effects [86]. To overcome this problem, functionalization of carbon nanotubes can make them water soluble, increase efficacy, and increase circulation time. Functional groups (carboxylic groups or amine groups), polymers (PEG), or ligands enhance biocompatibility [87, 88]. Carbon nanotubes can carry drugs by loading the nanotube with drugs, attaching the drug by surface functionalization, or linking the drug to it by a chemical. They can be made of single- or multilayer graphene, also known as single-walled carbon nanotubes or multiwalled carbon nanotubes [89]. An example of carbon nanotubes for disease mitigation is the use of single-walled carbon nanotubes conjugated with epidermal growth factor (EGF) and cisplatin. It showed higher affinity for entering and killing the targeted cancer cell. [90]

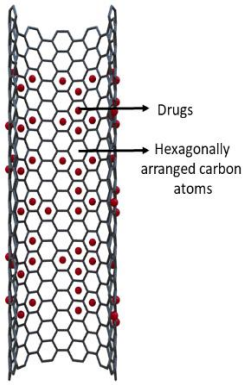

Figure 8: Carbon Nanotube

3.5.6 Dendrimers

Dendrimers are spherical, multivalent, hyperbranched macromolecules [91]. They are radially symmetrical and act as a nonviral vector. They have a central core, branches like a tree, and terminal functional groups. The branches are joined by a junction that makes the dendrimer structure resemble a sphere. These junctions are called generations. As the generation increases, the drug loading capacity and cationic amine group at the periphery also increase. They are made from nucleotides, sugar, or amino acids. The most used dendrimers are PPI (polypropylene imines), PAMAM (polyamidoamines), and PLL (poly-L-lysine). Dendrimers have a unique molecular weight that differentiates them from other types of nanocarriers. There are cavities within the branches where drugs can be encapsulated. This helps in the sustained release of the drug at the target site. The use of dendrimers is immense in gene delivery, antiviral drugs, and vaccine delivery. They can easily cross the blood–brain barrier and are used as an effective treatment for drug delivery in cases of brain tumors. For this reason, a doxorubicin-loaded dendrimer (PLL) functionalized with tumor necrosis factor (TNF) is used to effectively target and treat glioma. [92] In addition, it can also be used in breast cancer, cervical cancer, and colorectal cancer treatment. The release of the drug in the target site occurs due to a change in pH that causes protonation or deprotonation of the tertiary amine group depending on the acidic or basic nature of the microenvironment of the target site [93, 94].

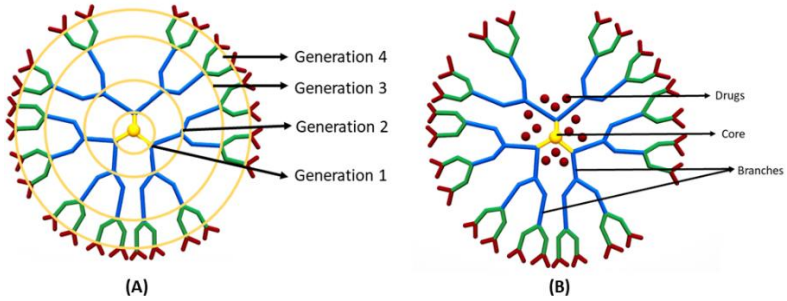

Figure 9: (A) Dendrimer generations, (B) Dendrimer

3.5.7 Mesoporous silicon

Mesoporous silicon is a porous structure that enables drugs to be incorporated more effectively. The pores resemble a honeycomb structure. It can be used to encapsulate both hydrophobic and hydrophilic drugs. For better targeted delivery, it can also be conjugated with ligands. Since they possess a large surface area and are porous, they enable higher drug loading, biocompatibility, and enhanced stability. By using mesoporous silica for the delivery of therapeutic agents, many resistance

mechanisms can be overcome. Methotrexate can be effectively delivered via mesoporous silica nanocarriers [95, 96].

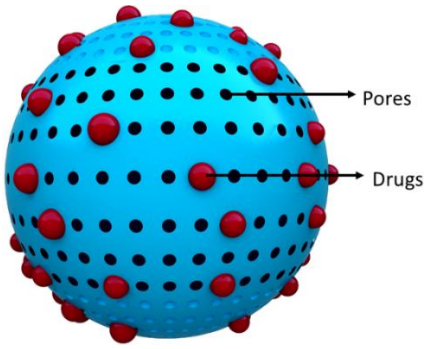

Figure 10: Mesoporous Silica

3.6 Novel Designed Nanocarriers

3.6.1 Hybrid Nanocarriers

A hybrid nanocarrier is a combination of both organic and inorganic nanocarriers. The two types of nanocarriers are combined to eliminate the problems and enhance the benefits as the delivery system's effectiveness and accumulation in the target site become more specific. This combination can also help in biosensing and imaging of the tumor alongside therapeutic effects. One such hybrid nanocarrier is the hybrid of dendrimer and gold nanocarrier. The dendrimer is loaded with the desired drug for therapeutic effect, and the gold nanoparticle helps in computed tomography imaging of the diseased site. The dual nature enhances the properties in many ways [97]. Better encapsulation of drugs, sustained release of drugs, high stability, and high cellular uptake are some of the properties that are observed by this combination. The hybrid of mesoporous silica and lipid polymer showed better intracellular delivery, high retention rate, and controlled release of zoledronic acid in breast cancer therapy. Novel albumin hybrid peptides (for delivery and even distribution of hydrophilic peptides), lipid-polymer hybrid nanocarriers, ceramic-polymer hybrid nanocarriers (ceramic nanocarriers consist of oxides of silica, alumina, etc.) are some examples of hybrid nanocarrier systems. The criteria for the selection of a suitable nanocarrier are its ability to increase bioavailability and decrease side effects compared to the conventional method [98]. Among the hybrid nanocarriers, lipid-polymer hybrid nanocarriers are discussed below:

Lipid-polymer hybrid nanocarriers: Lipid-polymer hybrid nanocarriers comprise a solid polymeric core encapsulated by a lipid shell. The polymeric core acts as a

cytoskeleton, providing a larger surface area, narrow size distribution, and better stability. On the other hand, the lipid shell increases biocompatibility, as it resembles the cell membrane and protects the inner polymer layer. This lipid layer is also responsible for preventing leakage of drugs from the core. The dual nature of the lipid and the polymer helps encapsulate both hydrophilic and hydrophobic drugs, which allows the codelivery of both forms of drugs. In this way, epigenetic (DAC) and chemotherapeutic drugs (Doxorubicin) were able to be code-livered [99].

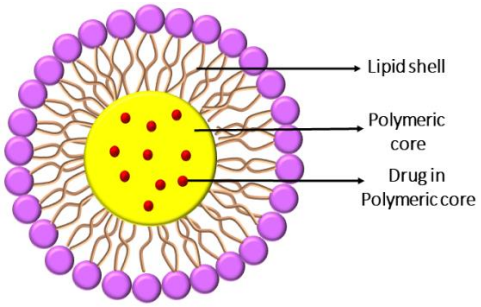

Figure 11: Lipid-polymer hybrid nanocarrier

3.6.2 Novel-Designed Polymeric Micelle

Polymeric micelles have been modified to have better effects, for which some new approaches are taken that make the nanocarrier a novel-designed drug delivery system. Some of the most recently used novel designs of a polymeric micelle include, urosolic acid-loaded polymeric micelle and smart multifunctional polymeric micelle.

Ursolic Acid-Loaded Polymeric Micelle: Ursolic acid is hydrophobic and has been proven to have a therapeutic effect against cancer. Since ursolic acid is hydrophobic, its clinical application is complex. With the help of micelles, ursolic acid can be encapsulated in the hydrophobic core, making it a novel drug delivery system. The hydrophilic shell of the micelle will make it easy to transport in aqueous media [100].

Smart Multifunctional Polymeric Micelle: Target-specific accumulation can be achieved by adding various ligands and specific moieties to a polymeric micelle. The ligands help in binding to specific receptors. Some contrast agents and stimuli-sensitive groups show better drug-release properties when incorporated in the polymeric micelle. All these properties are combined in one type of micelle that gives rise to a smart multifunctional polymeric micelle. This type of polymeric micelle can have target-specific accumulation, circulation, enhanced drug release at the target site, active or passive drug targeting, and improved efficiency. This nanocarrier can

efficiently deliver small interfering RNA (siRNA), hydrophobic drugs, and other therapeutic agents. Small interfering RNA helps in silencing the gene expression of specifically targeted tumor cells. The combination of siRNA and drug in a polymeric micelle helps in targeted delivery. At the same time, it also shows reduced growth of the tumor cell and toxic effects toward the tumor cell by the drug. Therefore, two major functions are being carried out effectively for cancer therapy by smart multifunctional polymeric micelles [101].

3.6.3 Novel Designed Dendrimers

Dendrimers are considered a novel delivery system because of their unique structure. The shape of the dendrimer allows it to have a large surface area. This allows efficient encapsulation of drugs [102]. Dendrimers can be functionalized by adding covalently bonded drugs, encapsulating the dendrimer with micelles, or forming complexes with nucleic acids. These are some novel approaches that makes it more suitable for drug delivery with more precision.

Dendrimers with drugs conjugated to dendrimers: Drugs are conjugated to dendrimers by covalent bonding as shown in **figure: 12 (B).** This conjugation is usually performed at the peripheral region of the dendrimer, where there are multiple sites for the drugs to be conjugated to the dendrimer. This results in one dendrimer being conjugated with multiple drug molecules. Since many drugs are conjugated simultaneously, more drugs will be delivered to the target site, resulting in better therapeutic efficacy and selective accumulation at the target site. This also increased water solubility and slowed drug release to attain the therapeutic index. Drug release occurs through the degradation of chemical bonds. Drugs conjugated with dendrimers showed better properties than free drugs in treating a disease [103].

Encapsulation of the dendrimer: Dendrimers can be encapsulated by liposomes or polymeric micelles so that the drug can be carried effectively to the target site despite being hydrophobic or hydrophilic as shown in **figure: 12 (C).** This enhances the toxicity and solubility of the drug against diseased cells. This encapsulation method also overcomes the stability issues of the drugs and improves drug loading into the dendrimer to many folds at a time [104]. These carriers usually follow a passive targeting strategy, enhancing accumulation and reducing toxicity against nontarget cells [105].

Dendrimers with nucleic acids complexed: Dendrimers can be conjugated to nucleic acids such as plasmid DNA or siRNA as shown in **figure: 12 (C).** The nucleic

acids are negatively charged, and dendrimers contain a cationic amine group at their periphery, for which they can form a bond [106]. The oligonucleotide attached to the dendrimer consists of genetic information for apoptosis, delayed growth of tumor cells, code for TNF-α, etc. These results in obtaining the desired effect on the diseased cell. Dendrimers complexed with siRNA were used in prostate tumors that showed gene silencing in the tumor, which resulted in an anticancer effect against the tumor. The dendrimer branches help bind to the siRNA and effectively deliver it to the target site [107]. Dendrimers can be conjugated with nucleic acids and the drug required for treating the disease to obtain a synergistic effect. They can also be conjugated with PEG or peptides to enhance cellular uptake and accumulation at the target site [108].

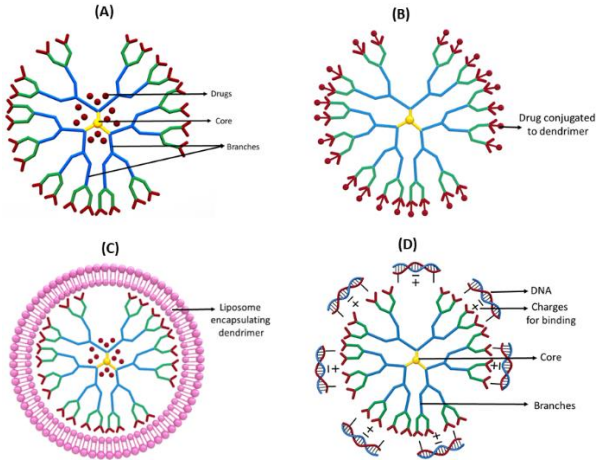

Figure 12: (A) Dendrimer, (B) Dendrimer with drug conjugated, (C) Dendrimer within liposomes, (D) Dendrimer with nucleic acid.

3.6.4 Quantum Dot

Quantum dots are nanosized semiconductor materials used widely for biosensing, diagnosis, drug delivery, therapy, and treatment of diseases. It consists of a core and a shell [109]. It efficiently helps release drugs from the vesicles by transforming the near-infrared light into heat. It is mostly used in the case of cancer diagnosis. The surface of the quantum dots is modified to make it biocompatible and water soluble to reduce toxicity and improve targeting [110]. Quantum dots contain noble metals, semiconductors, and magnetic transition metals in mixed conditions. The noble optical characteristics of the quantum dot are present with quantum dots that contain cadmium. Cadmium poses a toxic threat to humans. To reduce toxicity, ZnS is used to enclose these quantum dots [111].

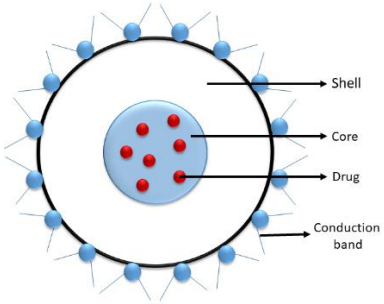

Figure 13: Quantum dot

Carbon can be used in quantum dots with a low toxicity profile and increased biocompatibility. Quantum dots can also be graphene-based, encapsulated in lipid-based micelles, and used as a cap on mesoporous silica, enhancing the encapsulation efficiency of drugs in mesoporous silica. A study showed that the co-loading of quantum dots and drugs in a solid lipid nanocarrier increases the drug loading capacity along with higher therapeutic efficacy [112, 113]. It is a noble-designed drug delivery system, as it can be conjugated with oligonucleotides, peptides, folates, and antibodies for high accuracy. It can help provide multiple attachment sites for drugs that help cross the membrane easily and deliver the drug to the target site [114, 115].

3.6.5 Nanostructured Lipid Carriers (NLCs) and Lipid Drug Conjugates (LDCs)

Solid lipid nanoparticles (SLNs) are stable, have better efficacy, are cost-effective, and can be produced on a large scale. However, it still poses some drawbacks, for which novel-designed carriers are composed of a mixture of lipids. They are nanostructured lipid carriers (NLCs) and lipid drug conjugates (LDCs). These are known to overcome the drawbacks of conventional solid lipid nanocarriers. A nanostructured lipid carrier (NLC) is a mixture of solid and liquid lipids. It has a solid lipid core at room temperature. The lipid mixture and less ordered lipid matrix help in high drug encapsulation, drug loading, controlled drug release, and better storage without a bursting effect, such as in SLN (solid lipid nanoparticle) [116]. Lipid drug conjugates (LDCs) are carriers modified to have better hydrophilic drug loading capacity. These are made to overcome the drawback of conventional solid lipid nanoparticles, which is the low capacity of hydrophilic drug loading. LDC is made by salt formation or covalent linking processed in an aqueous surfactant solution. It can be used as an effective carrier to deliver the drug to the brain in the case of infectious diseases [117, 118].

3.6.6 Cubosomes

Cubosomes are bicontinuous lipids generated by self-assembling amphiphilic molecules in the presence of a stabilizer [119]. Cubosomes have a solid crystalline cubic-like structure similar to a honeycomb structure. This structure helps entrap hydrophobic, hydrophilic, and amphiphilic drugs. They have more bioavailability and at the same time more drug loading capacity. Cubosomes are biodegradable and nontoxic and have high solubility in aqueous and lipid media [120]. They have narrow pore sizes, which allow them to release the drug at a controlled rate. This also helps maintain the stability and efficacy of the drug [121]. The release of the drug occurs depending on the difference in molecular weight and polarity [122].

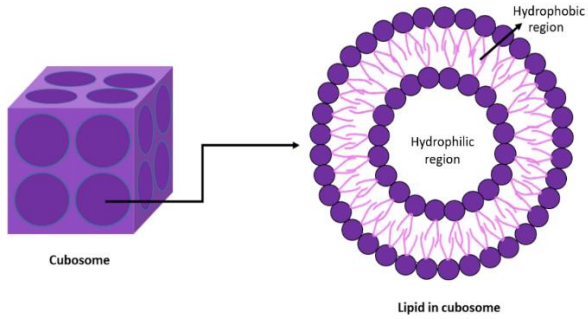

Figure 14: Cubosome

It is considered a novel lipid delivery system because it is nonirritant, has more residence time, has better bioavailability, increased absorption, has fewer side effects, has higher drug loading capacity, etc. It can be used in ocular drug delivery and transdermal administration and has been proven to show a hypoglycemic effect in rats after the oral administration of insulin-loaded cubosomes [123, 124].

3.6.7 Novel-Designed Liposomes

Liposomes used as nanocarriers for drug delivery have various drawbacks, such as uncontrolled release, low drug loading, inability to penetrate the skin and effective delivery of drugs to the blood circulation, and they also show limitations in orally delivered drugs due to the lack of stability of the vesicles. To overcome these drawbacks, liposomes are modified into ethosomes, transferosomes, niosomes, and virosomes for effective delivery of the drug to the target site.

Ethosome and Transferosome: Ethosomes and transferosomes are also vesicular systems that are more flexible and softer. The flexibility comes from the addition of surfactant (sodium cholate, polysorbate, span 80, tween 80, sodium deoxycholate, etc.) and ethanol in it. Transferosomes can transfer high- or low-molecular-weight

drugs through the skin. Ethosomes and transferosomes are both widely used for the transdermal administration of drugs, as ethanol is a known permeability enhancer. They also deliver nonsteroidal anti-inflammatory medications on the skin surface for pain relief. In addition, they can also be used for transdermal delivery of insulin, treatment of fungal infection (e.g., ketoconazole), delivery of vaccines, and treatment of herpes virus. They have a better penetration rate and retention in the circulatory system in comparison with liposome drug delivery, making them a novel designed nanocarrier [125, 126, 127].

Niosomes: Niosomes are nanometric delivery systems in which the drug material is encapsulated in the bilayer of a nonionic surfactant. These contain cholesterol and charge-inducing substances. They can carry both lipophilic and amphiphilic drugs. They are stable and do not require any special storage or preparation technique compared to liposomes. Niosomes are mostly used for drug delivery to the skin (e.g., treatment of herpes virus, transdermal delivery of insulin) [127].

Virosomes: Virosomes are a type of liposome that contains viral protein. It is used for immunization. It can be administered through nasal, vaginal, and intramuscular routes. Virosomes can also be incorporated with other molecules that can uptake dendritic cells. The receptor-mediated pathway performs this process. They can be used for the delivery of vaccines, antitoxins, etc. A study was conducted where plasmid DNA was loaded in liposomes decorated with viral protein. This helps in gene transfer to the targeted cell. Cell targeting is efficient with this process, as some viral proteins target specific types of cells, and as a result, they efficiently deliver the content to the targeted site [128, 129, 130].

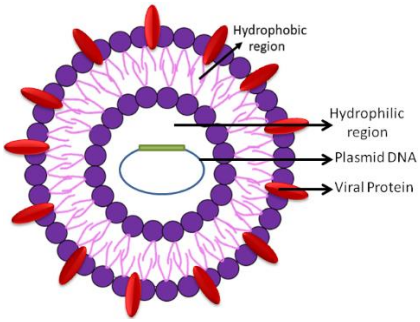

Figure 15: Plasmid DNA-loaded virosome

4. Conclusion

Nanocarriers have shown immense development in targeted drug delivery systems that have helped gain many benefits over the conventional use of free drugs. Target drug delivery has various advantages that are mastered by using nanocarriers. A targeted drug delivery system can exhibit better efficacy by minimizing the toxicity and side effects of the lifesaving drug. Nanocarriers can be used in diagnosis, treatment, and drug delivery. Nanotechnology has shown promising advantages in disease mitigation via targeted drug delivery. Although this technology has advanced considerably and many new carriers have emerged with their novel properties, some challenges remain in developing these nanocarriers. A slight change in the nanocarrier's shape, size, or structure can result in toxicity or altered pharmacokinetic properties of the drug. A desirable size for the nanocarrier is required to pass through the capillaries for therapeutic effect without being eliminated quickly. If these challenges can be overcome in the near future, nanocarriers can be used as targeted drug delivery systems for curing deadly diseases.

Author Contributions: Conceptualization, MIA, MHS; resources, MIA; writing—original draft preparation, MIA, MHS; writing—review and editing, JHK, SA, MK. All authors have read and agreed to the published version of the manuscript.

Funding: This research work received no dedicated funding from agencies in public, private or non-profit sectors.

Institutional Review Board Statement: This manuscript is a review paper. No human subjects or animals were used in any experiment.

Data Availability Statement: All data are availed in the result section of this manuscript.

Acknowledgments: Department of Pharmaceutical Sciences, North South University

Conflicts of Interest: There is no conflict of interest.

References

1. Wu, J. The enhanced permeability and retention (EPR) effect: the significance of the concept and methods to enhance its application. *J. Pers. Med.* 2021; 11: 771.
2. Fang, J., Nakamura, H., Maeda, H. The EPR effect: unique features of tumor blood vessels for drug delivery, factors involved, and limitations and augmentation of the effect. *Adv. Drug Deliv. Rev.* 2011; 63: 136–151.
3. Chou, L.Y.T., Ming, K., Chan, W.C.W. Strategies for the intracellular delivery of nanoparticles. *Chem. Soc. Rev.* 2011; 40: 233–245.
4. Guerrini, G., Magrì, D., Gioria, S., Medaglini, D., Calzolai, L. Characterization of nanoparticles-based vaccines for COVID-19. *Nat. Nanotechnol.* 2022; 17: 570–576.
5. Yeh, Y.-C., Huang, T.-H., Yang, S.-C., Chen, C.-C., Fang, J.-Y. Nano-based drug delivery or targeting to eradicate bacteria for infection mitigation: a review of recent advances. *Front. Chem.* 2020; 8: 286.

6. Beer, P., & Singh, P. Top-down and bottom-up approaches for synthesis of nanomaterials. 145: 92-130. Available Online: 2023 https://ccsuniversity.ac.in/bridge-library/pdf/L-3%20Synthesis%20of%20Nanostructured%20Materials%20Prof%20BPS.pdf
7. Tewabe, A., Abate, A., Tamrie, M., Seyfu, A., Siraj, E.A. Targeted drug delivery — from magic bullet to nanomedicine: principles, challenges, and future perspectives. *J. Multidiscip. Healthc.* 2021; 14: 1711–1724.
8. Edgar, J.Y.C., Wang, H. Introduction for design of nanoparticle-based drug delivery systems. *Curr. Pharm. Des.* 2017; 23(14): 2108–2112.
9. Fahmy, T.M., Fong, P.M., Goyal, A., Saltzman, W.M. Targeted for drug delivery. *Mater. Today*, 2005; 8: 18–26.
10. Benyettou, F., Motte, L. Nanomedicine: toward the "Magic Bullet" science. *J. Bioanal. Biomed.* 2016; 08.
11. Gradmann, C. Magic bullets and moving targets: antibiotic resistance and experimental chemotherapy, 1900-1940. *Dynamis* 2011; 31: 305–321.
12. Valent, P., Groner, B., Schumacher, U., Superti-Furga, G., Busslinger, M., Kralovics, R., Zielinski, C., Penninger, J.M., Kerjaschki, D., Stingl, G. Smolen, J.S. Paul Ehrlich (1854-1915) and his contributions to the foundation and birth of translational medicine. *J. Innate Immun.* 2016; 8: 111–120.
13. Torchilin, V.P. Drug targeting. *Eur. J. Pharm. Sci.* 2000; 11: S81–S91.
14. Prabahar, K., Alanazi, Z., Qushawy, M. Targeted drug delivery system: advantages, carriers and strategies. *Indian J. Pharm. Educ. Res.* 2021; 55: 346–353.
15. Rani K., Paliwal S. A. Review on targeted drug delivery: its entire focus on advanced therapeutics and diagnostics. *Sch. J. App. Med. Sci.* 2014; 2(1C): 328–331.
16. Dunuweera, S.P., Rajapakse, R.M.S.I., Rajapakshe, R.B.S.D., Wijekoon, S.H.D.P., Nirodha Thilakarathna, M.G.G.S., Rajapakse, R.M.G. Review on targeted drug delivery carriers used in nanobiomedical applications. *Curr. Nanosci.* 2019; 15: 382–397.
17. Maeda, H., Sawa, T., Konno, T. Mechanism of tumor-targeted delivery of macromolecular drugs, including the EPR effect in solid tumor and clinical overview of the prototype polymeric drug SMANCS. *J. Control. Release* 2001; 74: 47–61.
18. Nakamura, Y., Mochida, A., Choyke, P.L., Kobayashi, H. Nanodrug delivery: is the enhanced permeability and retention effect sufficient for curing cancer? *Bioconjug. Chem.* 2016; 27: 2225–2238.
19. KOBAYASHI, H., BRECHBIEL, M. Nano-sized MRI contrast agents with dendrimer cores. *Adv. Drug Deliv. Rev.* 2005, 57: 2271–2286.
20. Stirland, D.L., Nichols, J.W., Denison, T.A., Bae, Y.H. Targeted drug delivery for cancer therapy. *Biomaterials for Cancer Therapeutics* Woodhead Publishing: 2013; 31–56.
21. Matsumura, Y., Maeda, H. A new concept for macromolecular therapeutics in cancer chemotherapy: mechanism of tumoritropic accumulation of proteins and the antitumor agent SMANCS. *Cancer Res.* 1986; 46: 6387–6392.
22. Shi, J., Kantoff, P.W., Wooster, R., Farokhzad, O.C. Cancer nanomedicine: progress, challenges and opportunities. *Nat. Rev. Cancer* 2016; 17: 20–37.
23. Nacev, A., Beni, C., Bruno, O., Shapiro, B. Magnetic nanoparticle transport within flowing blood and into surrounding tissue. *Nanomed.* 2010; 5: 1459–1466.

24. Danhier, F., Feron, O., Préat, V. To exploit the tumor microenvironment: passive and active tumor targeting of nanocarriers for anti-cancer drug delivery. *J. Control. Release.* 2010; 148: 135–146.
25. Sun, T., Zhang, Y.S., Pang, B., Hyun, D.C., Yang, M., Xia, Y. Engineered nanoparticles for drug delivery in cancer therapy. *Angew. Chem. Int. Ed.* 2014; 53(46): 12320-12364.
26. Pirollo, K.F., Rait, A., Zhou, Q., Zhang, X., Zhou, J., Kim, C.-S., Benedict, W.F., Chang, E.H. tumor-targeting nanocomplex delivery of novel tumor suppressor rb94 chemosensitizes bladder carcinoma cells *in vitro* and *in vivo*. *Clin. Cancer Res.* 2008; 14: 2190–2198.
27. Kannagi, R., Izawa, M., Koike, T., Miyazaki, K., Kimura, N. Carbohydrate-mediated cell adhesion in cancer metastasis and angiogenesis. *Cancer Sci.* 2004; 95: 377–384.
28. Baas, J., Senninger, N., Elser, H. The reticuloendothelial system. an overview of function, pathology and recent methods of measurement. *Z. fur Gastroenterol.* 1994; 32: 117–123.
29. Vyas, S.P., Sihorkar, V., Mishra, V. Controlled and targeted drug delivery strategies toward intraperiodontal pocket diseases. *J. Clin. Pharm. Ther.* 2000; 25: 21–42.
30. Papademetriou, I., Tsinas, Z., Hsu, J., Muro, S. Combination-targeting to multiple endothelial cell adhesion molecules modulates binding, endocytosis, and *in vivo* biodistribution of drug nanocarriers and their therapeutic cargoes. *J. Control Release* 2014; 188: 87–98.
31. Mills, J.K., Needham, D. Targeted drug delivery. *Expert Opin. Ther. Pat.* 1999; 9: 1499–1513.
32. Morachis, J.M., Mahmoud, E.A., Almutairi, A. Physical and chemical strategies for therapeutic delivery by using polymeric nanoparticles. *Pharmacol. Rev.* 2012; 64: 505–519.
33. Devarajan, P.V., Jain, S., Eds. *Targeted Drug Delivery: Concepts and Design*, Springer International Publishing: Springer Cham Heidelberg New York Dordrecht London, 2015; (No. 11558).
34. National Nanotechnology Initiative. *About Nanotechnology | National Nanotechnology Initiative*. www.nano.gov. Available Online: 2023 https://www.nano.gov/about-nanotechnology
35. *CDC - Nanotechnology - NIOSH Workplace Safety and Health Topic*. (2019). Available Online: 2023 https://www.cdc.gov/niosh/topics/nanotech/
36. Fang, X., Cao, J., Shen, A. Advances in anti-breast cancer drugs and the application of nano-drug delivery systems in breast cancer therapy. *J. Drug Deliv. Sci. Technol.* 2020; 57: 101662.
37. Meng, H., Leong, W., Leong, K.W., Chen, C., Zhao, Y. Walking the line: the fate of nanomaterials at biological barriers. *Biomaterials* 2018; 174: 41–53.
38. Lôbo, G.C.N.B., Paiva, K.L.R., Silva, A.L.G., Simões, M.M., Radicchi, M.A., Báo, S.N. Nanocarriers used in drug delivery to enhance immune system in cancer therapy. *Pharmaceutics* 2021; 13: 1167.
39. Poste, G., Kirsh, R. Site–specific (targeted) drug delivery in cancer therapy. *Biotechnol.* 1983; 1: 869–878.
40. Ochekpe, N., Olorunfemi, P., Ngwuluka, N. Nanotechnology and drug delivery part 1: background and applications. *Trop. J. Pharm. Res.* 2009; 8(3).
41. Khan, N.H., Mir, M., Ngowi, E.E., Zafar, U., Khakwani, M.M.A.K., Khattak, S., Zhai, Y.K., Jiang, E.S., Zheng, M., Duan, S.F. Wei, J.S. Nanomedicine: a promising way to manage alzheimer's disease. *Front. Bioeng. Biotechnol.* 2021; 9: 630055.

42. Singh, V., Redhu, R., Verma, R., Mittal, V., Kaushik, D. Anti-acne treatment using nanotechnology based on novel drug delivery system and patents on acne formulations: a review. *Recent Pat. Nanotechnol*. 2020; 15(4): 331-350.
43. Chamundeeswari, M., Jeslin, J., Verma, M.L. Nanocarriers for drug delivery applications. *Environ. Chem. Lett.* 2018; 17: 849–865.
44. Liu, Y., Mai, S., Li, N., Yiu, C.K.Y., Mao, J., Pashley, D.H., Tay, F.R. Differences between top-down and bottom-up approaches in mineralizing thick, partially demineralized collagen scaffolds. *Acta Biomater.* 2011; 7: 1742–1751.
45. Pal Singh, J., Kumar, M., Sharma, A., Pandey, G., Chae, K., Lee, S. Bottom-up and top-down approaches for MgO. *Sonochemical Reactions* Intech Open: London, United Kingdom, 2020; 15-32.
46. Eras, A., Castillo, D., Suárez, M., Vispo, N.S., Albericio, F., Rodriguez, H. Chemical conjugation in drug delivery systems. *Front. Chem.* 2022; 10: 889083.
47. Liu, J.-M., Zhang, D.-D., Fang, G.-Z., Wang, S. Erythrocyte membrane bioinspired near-infrared persistent luminescence nanocarriers for *in vivo* long-circulating bioimaging and drug delivery. *Biomaterials* 2018; 165: 39–47.
48. Recent studies on the delivery of hydrophilic drugs in nanoparticulate systems. *J. Drug Deliv. Sci. Technol.* 2016; 32: 298–312.
49. Kumari, A., Singla, R., Guliani, A., Yadav, S.K. Nanoencapsulation for drug delivery. *EXCLI J.* 2014; 13: 265–286.
50. Moyano, D.F., Rana, S., Bunz, U.H.F., Rotello, V.M. Gold nanoparticle-polymer/biopolymer complexes for protein sensing. *Faraday Discuss.* 2011; 152: 33.
51. Petros, R.A., DeSimone, J.M. Strategies in the design of nanoparticles for therapeutic applications. *Nat. Rev. Drug Discov.* 2010; 9: 615–627.
52. Onzi, G., Guterres, S.S., Pohlmann, A.R., Frank, L.A. Active targeting of nanocarriers. *The ADME Encyclopedia* Springer Cham: 2021; 1–13.
53. Khan, N., Ruchika, Dhritlahre, R.K., Saneja, A. Recent advances in dual-ligand targeted nanocarriers for cancer therapy. *Drug Discov. Today*, 2022; 27(8): 2288-2299.
54. Miyazawa, T., Itaya, M., Burdeos, G.C., Nakagawa, K., Miyazawa, T. A critical review of the use of surfactant-coated nanoparticles in nanomedicine and food nanotechnology. *Int. J. Nanomed.* 2021; 16: 3937–3999.
55. Male, D., Gromnicova, R. Nanocarriers for delivery of oligonucleotides to the CNS. *Int. J. Mol. Sci.* 2022; 23: 760.
56. Julien, D.C., Behnke, S., Wang, G., Murdoch, G.K., Hill, R.A. Utilization of monoclonal antibody-targeted nanomaterials in the treatment of cancer. *mAbs* 2011; 3: 467–478.
57. Li, X., Jian, M., Sun, Y., Zhu, Q., Wang, Z. The peptide functionalized inorganic nanoparticles for cancer-related bioanalytical and biomedical applications. *Molecules* 2021; 26: 3228.
58. Markman, M. Pegylated liposomal doxorubicin in the treatment of cancers of the breast and ovary. *Expert Opin. Pharmacother.* 2006; 7: 1469–1474.

59. Akbarzadeh, A., Rezaei-Sadabady, R., Davaran, S., Joo, S.W., Zarghami, N., Hanifehpour, Y., Samiei, M., Kouhi, M., Nejati-Koshki, K. Liposome: classification, preparation, and applications. *Nanoscale Res. Lett.* 2013; 8: 1-9.
60. Laouini, A., Jaafar-Maalej, C., Limayem-Blouza, I., Sfar, S., Charcosset, C., Fessi, H. Preparation, characterization and applications of liposomes: state of the art. *J. Colloid Sci. Biotechnol.* 2012; 1: 147–168.
61. Severino, P., Andreani, T., Macedo, A.S., Fangueiro, J.F., Santana, M.H.A., Silva, A.M., Souto, E.B. Current state-of-art and new trends on lipid nanoparticles (SLN and NLC) for oral drug delivery. *J. Drug Deliv.* 2012; 750891.
62. Fricker, G., Kromp, T., Wendel, A., Blume, A., Zirkel, J., Rebmann, H., Setzer, C., Quinkert, R.-O., Martin, F., Müller-Goymann, C. Phospholipids and lipid-based formulations in oral drug delivery. *Pharm. Res.* 2010; 27: 1469–1486.
63. Uner, M., Yener, G. Importance of solid lipid nanoparticles (SLN) in various administration routes and future perspectives. *International J. Nanomed.* 2007; 2: 289–300.
64. Attama, A.A., Momoh, M.A., Builders, P.F. Lipid nanoparticulate drug delivery systems: a revolution in dosage form design and development. *Recent Adv. Novel Drug Carrier Syst.* 2012; 5: 107-140.
65. Wissing, S.A., Kayser, O., Müller, R.H. Solid lipid nanoparticles for parenteral drug delivery. *Adv. Drug Deliv. Rev.* 2004; 56: 1257–1272.
66. Wennerström, H. Micelles. Physical chemistry of surfactant association. *Phys. Rep.* 1979; 52: 1–86.
67. Adams, M.L., Lavasanifar, A., Kwon, G.S. Amphiphilic block copolymers for drug delivery. *J. Pharm. Sci.* 2003; 92: 1343–1355.
68. Lu, H., Wang, J., Wang, T., Zhong, J., Bao, Y., Hao, H. Recent progress on nanostructures for drug delivery applications. *J. Nanomat.* 2016; 2016: 1–12.
69. Ali, Y., Alqudah, A., Ahmad, S., Abd Hamid, S., Farooq, U. Macromolecules as targeted drugs delivery vehicles: an overview. *Des. Monomers Polym.* 2019; 22: 91–97.
70. Koo, H., Huh, M.S., Sun, I.-C., Yuk, S.H., Choi, K., Kim, K., Kwon, I.C. *In vivo* targeted delivery of nanoparticles for theranosis. *Acc. Chem. Res.* 2011; 44: 1018–1028.
71. Xia, T., Wang, J., Wu, C., Meng, F., Shi, Z., Lian, J., Feng, J., Meng, J. Novel complex-coprecipitation route to form high quality triethanolamine-coated Fe3O4 nanocrystals: their high saturation magnetizations and excellent water treatment properties. *Cryst. Eng. Comm.* 2012; 14: 5741.
72. Neuberger, T., Schöpf, B., Hofmann, H., Hofmann, M., von Rechenberg, B. Superparamagnetic nanoparticles for biomedical applications: possibilities and limitations of a new drug delivery system. *J. Magn. Magn. Mater.* 2005; 293: 483–496.
73. Gupta, A.K., Gupta, M. Synthesis and surface engineering of iron oxide nanoparticles for biomedical applications. *Biomaterials* 2005; 26: 3995–4021.
74. Ling, D., Hyeon, T. Chemical design of biocompatible iron oxide nanoparticles for medical applications. *Small* 2012; 9: 1450–1466.
75. Siddique, S., Chow, J.C.L. Gold nanoparticles for drug delivery and cancer therapy. *Appl. Sci.* 2020; 10: 3824.
76. Ali, A., Zafar, H., Zia, M., ul Haq, I., Phull, A.R., Ali, J.S., Hussain, A. Synthesis, characterization, applications, and challenges of iron oxide nanoparticles. *Nanotechnol. Sci. Appl.* 2016; 9: 49–67.

77. Lee, G.Y., Qian, W.P., Wang, L., Wang, Y.A., Staley, C.A., Satpathy, M., Nie, S., Mao, H., Yang, L. Theranostic nanoparticles with controlled release of gemcitabine for targeted therapy and mri of pancreatic cancer. *ACS Nano* 2013; 7: 2078–2089.
78. Bera, R.K., Mandal, S.M., Raj, C.R. Antimicrobial activity of fluorescent Ag nanoparticles. *Lett. Appl. Microbiol.* 2014; 58: 520–526.
79. Besinis, A., De Peralta, T., Handy, R.D. The antibacterial effects of silver, titanium dioxide and silica dioxide nanoparticles compared to the dental disinfectant chlorhexidine on *Streptococcus mutans* using a suite of bioassays. *Nanotoxicol.* 2012; 8: 1–16.
80. Yaqoob, A.A., Ahmad, H., Parveen, T., Ahmad, A., Oves, M., Ismail, I.M.I., Qari, H.A., Umar, K., Mohamad Ibrahim, M.N. Recent advances in metal decorated nanomaterials and their various biological applications: A Review. *Front. Chem.* 2020; 8: 341.
81. Wong, B.S., Yoong, S.L., Jagusiak, A., Panczyk, T., Ho, H.K., Ang, W.H., Pastorin, G. Carbon nanotubes for delivery of small molecule drugs. *Adv. Drug Deliv. Rev.* 2013; 65: 1964–2015.
82. Ng, C.M., Loh, H.-S., Muthoosamy, K., Sridewi, N., Manickam, S. Conjugation of insulin onto the sidewalls of single-walled carbon nanotubes through functionalization and diimide-activated amidation. *Int. J. Nanomed.* 2016; 11: 1607–1614.
83. Iijima, S. Helical microtubules of graphitic carbon. *Nature* 1991; 354: 56–58.
84. Eatemadi, A., Daraee, H., Karimkhanloo, H., Kouhi, M., Zarghami, N., Akbarzadeh, A., Abasi, M., Hanifehpour, Y., Joo, S. Carbon nanotubes: properties, synthesis, purification, and medical applications. *Nanoscale Res. Lett.* 2014; 9: 393.
85. Minelli, C., Lowe, S.B., Stevens, M.M. Engineering nanocomposite materials for cancer therapy. *Small* 2010; 6: 2336–2357.
86. Li, J., Yap, S.Q., Yoong, S.L., Nayak, T.R., Chandra, G.W., Ang, W.H., Panczyk, T., Ramaprabhu, S., Vashist, S.K., Sheu, F.S. Tan, A. Carbon nanotube bottles for incorporation, release and enhanced cytotoxic effect of cisplatin. *Carbon* 2012; 50: 1625–1634.
87. Lay, C.L., Liu, H.Q., Tan, H.R., Liu, Y. Delivery of paclitaxel by physically loading onto poly (ethylene glycol) (PEG)-graft carbon nanotubes for potent cancer therapeutics. *Nanotechnol.* 2010; 21: 065101.
88. Shao, W., Paul, A., Rodes, L., Prakash, S. A new carbon nanotube-based breast cancer drug delivery system: preparation and *in vitro* analysis using paclitaxel. *Cell Biochem. Biophys.* 2015, 71, 1405–1414.
89. Matsumura, S., Ajima, K., Yudasaka, M., Iijima, S., Shiba, K. Dispersion of cisplatin-loaded carbon nanohorns with a conjugate comprised of an artificial peptide aptamer and polyethylene glycol. *Mol. Pharm.* 2007; 4; 723–729.
90. Bhirde, A.A., Patel, V., Gavard, J., Zhang, G., Sousa, A.A., Masedunskas, A., Leapman, R.D., Weigert, R., Gutkind, J.S., Rusling, J.F. Targeted killing of cancer cells *in vivo* and *in vitro* with EGF-directed carbon nanotube-based drug delivery. *ACS Nano* 2009; 3: 307–316.
91. Abbasi, E., Aval, S., Akbarzadeh, A., Milani, M., Nasrabadi, H., Joo, S., Hanifehpour, Y., Nejati-Koshki, K., Pashaei-Asl, R. Dendrimers: synthesis, applications, and properties. *Nanoscale Res. Lett.* 2014; 9: 247.
92. Liu, S., Guo, Y., Huang, R., Li, J., Huang, S., Kuang, Y., Han, L., Jiang, C. Gene and doxorubicin co-delivery system for targeting therapy of glioma. *Biomaterials* 2012; 33: 4907–4916.

93. Kaga, S., Arslan, M., Sanyal, R., Sanyal, A. Dendrimers and dendrons as versatile building blocks for the fabrication of functional hydrogels. *Molecules* 2016; 21: 497.
94. Dwivedi, N., Shah, J., Mishra, V., Mohd Amin, M.C.I., Iyer, A.K., Tekade, R.K., Kesharwani, P. Dendrimer-mediated approaches for the treatment of brain tumor. *J. Biomater. Sci. Polym. Ed.* 2016; 27: 557–580.
95. Wang, Y., Zhao, Q., Han, N., Bai, L., Li, J., Liu, J., Che, E., Hu, L., Zhang, Q., Jiang, T. and Wang, S. Mesoporous silica nanoparticles in drug delivery and biomedical applications. *Nanomed.: Nanotechnol. Biol. Med.* 2015; 11: 313–327.
96. Frickenstein, A.N., Hagood, J.M., Britten, C.N., Abbott, B.S., McNally, M.W., Vopat, C.A., Patterson, E.G., MacCuaig, W.M., Jain, A., Walters, K.B. McNally, L.R. Mesoporous silica nanoparticles: properties and strategies for enhancing clinical effect. *Pharmaceutics* 2021; 13: 570.
97. Wang, S., Sun, Zhu, Du, Liu, Qian, W.-Y. PH-sensitive strontium carbonate nanoparticles as new anticancer vehicles for controlled etoposide release. *Int. J. Nanomed.* 2012; 5781.
98. Khoshnejad, M., Parhiz, H., Shuvaev, V.V., Dmochowski, I.J., Muzykantov, V.R. Ferritin-based drug delivery systems: hybrid nanocarriers for vascular immunotargeting. *J. Control. Release* 2018; 282: 13–24.
99. Garg, N.K., Tandel, N., Jadon, R.S., Tyagi, R.K., Katare, O.P. Lipid–polymer hybrid nanocarrier-mediated cancer therapeutics: current status and future directions. *Drug Discov. Today* 2018; 23: 1610–1621.
100. Zhou, M., Yi, Y., Liu, L., Lin, Y., Li, J., Ruan, J., Zhong, Z. Polymeric micelles loading with ursolic acid enhancing anti-tumor effect on hepatocellular carcinoma. *J. Cancer* 2019; 10: 5820–5831.
101. Jhaveri, A.M., Torchilin, V.P. Multifunctional polymeric micelles for delivery of drugs and SiRNA. *Front. Pharmacol.* 2014, 5: 77.
102. Yu, X., Trase, I., Ren, M., Duval, K., Guo, X., Chen, Z. Design of nanoparticle-based carriers for targeted drug delivery. *J. Nanomat.* 2016; 2016: 1–15.
103. Malik, N., Evagorou, E.G., Duncan, R. Dendrimer-platinate: a novel approach to cancer chemotherapy. *Anti-Cancer Drugs* 1999; 10; 767–776.
104. WOLINSKY, J., GRINSTAFF, M. Therapeutic and diagnostic applications of dendrimers for cancer treatment☆. *Adv. Drug Deliv. Rev.* 2008; 60: 1037–1055.
105. Somani, S., Dufès, C. Applications of dendrimers for brain delivery and cancer therapy. *Nanomedicine* 2014; 9: 2403–2414.
106. Sato, N., Kobayashi, H., Saga, T., Nakamoto, Y., Ishimori, T., Togashi, K., Fujibayashi, Y., Konishi, J., Brechbiel, M.W. Tumor targeting and imaging of intraperitoneal tumors by use of antisense oligo-DNA complexed with dendrimers and/or avidin in mice. *Clin. Cancer Res.* 2001; 7: 3606–3612.
107. Liu, X., Liu, C., Laurini, E., Posocco, P., Pricl, S., Qu, F., Rocchi, P., Peng, L. Efficient delivery of sticky SiRNA and potent gene silencing in a prostate cancer model using a generation 5 triethanolamine-core PAMAM dendrimer. *Mol. Pharm.* 2012; 9: 470–481.
108. Han, L., Huang, R., Li, J., Liu, S., Huang, S., Jiang, C. Plasmid PORF-HTRAIL and doxorubicin co-delivery targeting to tumor using peptide-conjugated polyamidoamine dendrimer. *Biomaterials* 2011; 32: 1242–1252.
109. Abbasi, E., Kafshdooz, T., Bakhtiary, M., Nikzamir, N., Nikzamir, N., Nikzamir, M., Mohammadian, M., Akbarzadeh, A. Biomedical and biological applications of quantum dots. *Artif. Cells Nanomed. Biotechnol.* 2015; 44(3): 1–7.

110. Cai, W., Shin, D.-W., Chen, K., Gheysens, O., Cao, Q., Wang, S.X., Gambhir, S.S., Chen, X. Peptide-labeled near-infrared quantum dots for imaging tumor vasculature in living subjects. *Nano Lett.* 2006; 6: 669–676.
111. Hardman, R. A toxicologic review of quantum dots: toxicity depends on physicochemical and environmental factors. *Environ. Health Perspect.* 2006; 114; 165–172.
112. Dubertret, B. *In vivo* imaging of quantum dots encapsulated in phospholipid micelles. *Science* 2002; 298: 1759–1762.
113. Olerile, L.D., Liu, Y., Zhang, B., Wang, T., Mu, S., Zhang, J., Selotlegeng, L., Zhang, N. Near-infrared mediated quantum dots and paclitaxel co-loaded nanostructured lipid carriers for cancer theragnostic. *Colloids Surf. B.* 2017; 150: 121–130.
114. Jamieson, T., Bakhshi, R., Petrova, D., Pocock, R., Imani, M., Seifalian, A.M. Biological applications of quantum dots. *Biomaterials* 2007; 28: 4717–4732.
115. Liu, X., Shou, D., Chen, C., Mao, H., Kong, Y., Tao, Y. Core-shell structured polypyrrole/mesoporous SiO_2 nanocomposite capped with graphene quantum dots as gatekeeper for irradiation-controlled release of methotrexate. *Mater. Sci. Eng.* 2017; 81: 206–212.
116. Vyas, A., Kumar Sonker, A., Gidwani, B. Carrier-based drug delivery system for treatment of acne. *Sci. World J.* 2014; *2014*: 1–14.
117. Irby, D., Du, C., Li, F. Lipid–drug conjugate for enhancing drug delivery. *Mol. Pharm.* 2017; 14: 1325–1338.
118. Olbrich, C., Gessner, A., Kayser, O., Müller, R.H. Lipid-drug-conjugate (LDC) nanoparticles as novel carrier system for the hydrophilic antitrypanosomal drug diminazenediaceturate. *J. Drug Target* 2002; 10: 387–396.
119. Chaudhary, K., Sharma, D. Cubosomes: a potential drug delivery system. *Asian j. pharm. res. dev.* 2021; 9: 93–101.
120. Caboi, F., Amico, G.S., Pitzalis, P., Monduzzi, M., Nylander, T., Larsson, K. Addition of hydrophilic and lipophilic compounds of biological relevance to the monoolein/water system. I. phase behavior. *Chem. Phys. Lipids* 2001; 109: 47–62.
121. Landau, E.M., Rosenbusch, J.P. Lipidic cubic phases: a novel concept for the crystallization of membrane proteins. *Proc. Natl. Acad. Sci.* 1996; 93: 14532–14535.
122. Higuchi, W.I. Diffusional models useful in biopharmaceutics. *J. Pharm. Sci.* 1967; 56: 315–324.
123. Chung, H., Kim, J., Um, J.Y., Kwon, I.C., Jeong, S.Y. Self-assembled "Nanocubicle" as a carrier for peroral insulin delivery. *Diabetologia* 2002; 45: 448–451.
124. Umar, H., Wahab, H.A., Gazzali, A.M., Tahir, H., Ahmad, W. Cubosomes: design, development, and tumor-targeted drug delivery applications. *Polymers* 2022; 14: 3118.
125. Elsayed, M.M.A., Abdallah, O.Y., Naggar, V.F., Khalafallah, N.M. Lipid vesicles for skin delivery of drugs: reviewing three decades of research. *Int. J. Pharm.* 2007; 332: 1–16.
126. Jadhav, S., Morey, P., Karpe, M., Kadam, V. Novel vesicular system: an overview. *J. Appl. Pharm. Sci. 2012*; 193–202.
127. Karande, P., Mitragotri, S. Enhancement of transdermal drug delivery via synergistic action of chemicals. *Biochim. Biophys. Acta - Biomembr.* 2009; 1788: 2362–2373.
128. Cusi, M.G. Applications of influenza virosomes as a delivery system. *Human Vaccines* 2006; 2: 1–7.

129. Chen, Y.-Z., Yao, X.-L., Tabata, Y., Nakagawa, S., Gao, J.-Q. Gene carriers and transfection systems used in the recombination of dendritic cells for effective cancer immunotherapy. *Clin. Dev. Immunol.* 2010; 2010: 1–12.
130. Kaneda, Y. Virosomes: evolution of the liposome as a targeted drug delivery system. *Adv. Drug Deliv. Rev.* 2000; 43: 197–205.

JBEP

Journal of Biosciences and Experimental Pharmacology
ISSN-2960-284X

Original Article

Effect of Polymer Concentration on the Release of Naproxen from Enteric Coated Sustained Release Tablets

Syed Abdul Kuddus[1], Afsana Alam[1], Abdullah Md. Sifat[1], Tasmi Tamanna[1], Shaiful Alam[1], Farjana Abedin[1], Reatul Karim[1], Md. Zakir Sultan[2], Ferdous Khan[1*]

[1]*Department of Pharmaceutical Sciences, North South University, Dhaka-1229, Bangladesh*
[2]*Centre for Advanced Research in Sciences (CARS), University of Dhaka, Dhaka-1000, Bangladesh*

***Correspondence *E-mail*:** khan.ferdous@northsouth.edu; Tel.: 880-2-55668200 Extn-6270

Abstract: Five different formulations of naproxen sodium core tablets were prepared using different amounts of Methocel K15M CR by direct compression method. From a particular formulation, 50 % of tablets were kept uncoated and enteric coating was applied to the remaining 50 % using cellulose acetate phthalate (6 % w/w). Dissolution, swelling and erosion tests of uncoated tablets were conducted 8 hours in phosphate buffer (pH 7.4). For enteric coated tablets, dissolution test was performed for first 2 hours in acidic medium (pH 1.2) then 8 hours in phosphate buffer (pH 7.4). Enteric coating was able to prevent the disintegration of the matrix tablets and dissolution of naproxen in the acidic medium. In the buffer medium, irrespective of the presence or absence of enteric coating, higher percentage of Methocel K15 MCR increased swelling of the tablets in first few hours which was followed by erosion of the tablet matrix. Dissolution studies revealed that high percentage of Methocel K15M CR retarded the release of naproxen for a longer period of time. Taking the swelling and erosion pattern and dissolution data together we concluded that with the increase of hydrophilic polymer content, the release mechanism of naproxen shifted towards swelling and erosion dependent processes.

Keywords: Methocel K15M CR; Enteric coating; Naproxen sodium; Swelling; Release mechanism

Citation: Kuddus, SA.; Alam A.; Sifat AM; Tamanna T; Alam S; Abedin F; Karim R; Sultan MZ; Khan F. Effect of polymer concentration on the release of naproxen from enteric coated sustained release tablets. *J. Bio. Exp. Pharm* 2023, 1:70–90

Received: November 14, 2023
Accepted: December 11, 2023
Published: December 15, 2023

Publisher's Note: JBEP stays neutral with regard to jurisdictional claims in published maps and institutional affiliations.

1. Introduction

Conventional immediate release oral formulations offer faster and clinically effective therapy for many drugs. But by the same token, they have some limitations that include high dosing frequency and fluctuations of drug plasma concentrations [1]. For all drugs, to get an optimum therapeutic response without any toxic effect, it is important to maintain the plasma levels within the therapeutic window with minimal variations. Sustained release formulations help to overcome the drawbacks of conventional immediate release dosage forms. Especially for the oral

administration of many drugs, sustained-release matrix tablets have become dosage form of choice because they give more consistent plasma concentrations and reduce the frequency of dosing [2]. Hydroxypropyl methylcellulose (HPMC) is a hydrophilic semi-synthetic ether-based polymer which has been widely used in the sustained or controlled release formulations to control the release rate by forming a matrix system. It works well in the direct compression process because of its good compressibility [3].

Enteric coating prevents the disintegration and dissolution of solid oral dosage forms in the stomach and thus helps to bypass the stomach. For this reason, the enteric coating has become increasingly popular for drugs which cause gastric irritation and drugs which are degraded by the acidic environment of the stomach. Enteric coating polymers work by forming a layer which is stable at the acidic environment of the stomach but breaks down rapidly at relatively alkaline pH of the small intestine [4].

Naproxen, a propionic acid derivative, a non-steroidal anti-inflammatory drug, is readily absorbed in the gastrointestinal tract and has a bioavailability of 95 %. Naproxen can be administered either in acid form or in sodium salt form; both produce the same effects but differ in the rate and extent of absorption due to different solubility [5]. Though the drug is highly effective against diseases like rheumatoid arthritis osteoarthritis, ankylosing spondylitis, etc., it may cause an ulcer, kidney failure, and elevate bleeding after surgery [6]. Naproxen is a poorly water-soluble drug with high permeability and hence considered as a class II drug according to the Biopharmaceutics classification system [7]. Nevertheless, many pharmaceutical manufacturers are now formulating the drug in sustained release matrix tablets for prolonged relief of pain. On the other hand, it is a reversible inhibitor of cyclooxygenases and thus inhibits the biosynthesis of prostaglandins which play important role in the protection of gastric mucosa from the acidic condition [8]. Like other inhibitors of cyclooxygenases, naproxen is conventionally formulated in enteric coated dosage form [9]. By taking the necessity of prolonged drug release and its adverse effect on gastric mucosa in consideration, we hypothesized that preparing enteric coated sustained release matrix tablet of naproxen would be a safe and effective therapeutic strategy.

The main objective of this study was to compare sustained-release uncoated and enteric coated tablets of naproxen sodium. For doing this, sustained-release core tablets of naproxen sodium were prepared using different amounts of Methocel K15M CR. Then enteric coating was applied on half of the tablets of each formulation using cellulose acetate phthalate (CAP). Finally, physicochemical parameters, swelling, erosion, release rate, extent, and mechanisms were investigated in the aim of making comments about the impact of the varying amount of Methocel

K15M CR on swelling, erosion and drug release in the presence and in the absence of the enteric coating.

2. Materials and Methods

2.1 Materials

Naproxen Sodium, Methocel K15M CR and cellulose acetate phthalate (CAP) were generous gifts of IBN Sina Pharmaceuticals, Bangladesh. Ludipress was collected from BASF, Bangladesh. Aerosil and magnesium stearate were purchased from Merck, Germany. All other reagents and chemicals used in this experiment were analytical grade.

2.2 Micromeritic properties of the powder blend

2.2.1 Carr's index and Hausner ratio

Carr's index is the measurement of the powder consolidation tendency. It helps to measure the inter-particulate interactions among the powder particles. It was calculated by the following equation.

$CI\ (\%) = (V_0-V_f)/V_0 \times 100$

Where, CI = Carr's index, V_0 = Untapped volume, V_f = Tapped volume

Hausner ratio has a close relation with Carr's index and it was calculated by the following equation [10].

$\text{Hausner ratio} = V_0/V_f$

In this equation, V_0 = Volume before tapping, V_f = Volume after tapping

2.2.2 Angle of repose

In this experiment angle of repose of the powdered materials was determined by funnel method. The powder was taken in a funnel and was permitted to flow via the funnel on a paper freely. The funnel height was adjusted in a way so that the funnel tip touched the apex of the powder mass. The diameter of the powder cone and the height of the powder cone from the surface were measured and the angle of repose was calculated by the following equation [11].

$\text{Angle of repose, } \theta = \tan^{-1}(h/r)$

Here, h = Height of the powder cone; r = Radius of the powder cone

2.3 Study of drug excipient compatibility by Fourier Transmitted Infrared Spectroscopy (FTIR) and Differential Scanning Calorimetry (DSC)

The infrared spectra of naproxen sodium, Methocel K15M CR, and physical mixture of the formulation (F-5) were recorded in the wavelength region of 2000 to 600 cm^{-1} using FTIR spectrometer (IR Affinity-1, Shimadzu, Japan). Samples IR spectra were acquired by potassium bromide (KBr) disk method [12]. DSC was performed for naproxen sodium, Methocel K15M CR and the optimized formulation (F-5) using Differential Scanning Calorimeter (DSC 60, Shimadzu, Japan). The measuring temperature was between 30°C to 400°C with a heating rate of 10°C/min [13].

2.4 Preparation of matrix tablets

All the tablets were prepared by using 500 mg naproxen for each tablet by direct compression method. This dose was determined by considering the recommended dosing regimen, which is generally 500 mg 2 to 3 times per day with a total daily highest dose of 1500 mg [14]. Formulations were prepared by different amount of polymer but keeping the amount of all other ingredients constant. In brief, naproxen sodium, Methocel K15M CR powder and other excipients except Mg-stearate was sieved through 60 mesh size and mixed thoroughly. Then Mg-stearate was added to the mixture to increase lubrication and was compressed to prepare the uncoated tablets of 600, 620, 640, 660, and 680 mg weight by a 3 stationed tablet compression machine using 13 mm die according to the compositions mentioned in **Table 1**.

Table 1: *Formula of naproxen sodium uncoated matrix tablets containing varying amounts of Methocel K15M CR and other excipients.*

Formulation code	Naproxen Sodium (mg	Methocel K15M CR (mg)	Ludipress (mg)	Aerosil (mg)	Mg-stearate (mg)	Total (mg)
F-1	500	40	50	5	5	600
F-2	500	60	50	5	5	620
F-3	500	80	50	5	5	640
F-4	500	100	50	5	5	660
F-5	500	120	50	5	5	680

F-6 was prepared by enteric coating of F-1 and F-7 was prepared by enteric coating of F-2 and so on.

2.5 Preparation of enteric coated tablets

The enteric coating was prepared in solution method using cellulose acetate phthalate (6 % w/w) as enteric coating polymer, PEG (1.5 % w/w) as plasticizer and acetone (60 % w/w) as a solvent. After adjustment of rest of the volume by diethyl phthalate, the mixture was constantly stirred by a mechanical stirrer (1000 rpm) for 1 hour and the solution was finally filtered through muslin cloth according to the previously described method [15]. Coating of tablets was done by using a perforated pan coating apparatus by maintaining the weight gain percentage within a specified range. Half of the tablets from each formulation were used for preparing the enteric coated tablets; for example, F-6 was prepared by enteric coating of F-1 and F-7 was prepared by enteric coating of F-2 and so on.

2.6 Physical properties of the uncoated and coated tablet

2.6.1 Weight variation and weight gain

Twenty uncoated tablets from each formulation were weighed individually using an electronic balance (Electronic Balance, Adam, UK). Average weight, the standard deviation of the weight of each tablet was calculated according to a previously described method [16]. On the other hand, percent weight gain due to enteric was calculated for enteric coated tablets according to the following equation [17]:

$$\% \text{ Weight gain} = (Wta - Wtb)/ Wtb \times 100$$

Here, Wta is the weight of tablet after coating and Wtb is the weight before coating.

2.6.2. Tablet hardness, thickness, and diameter

In the present study, tablet hardness was determined by using a dial type hardness tester and was measured in kg/cm^2. Tablet thickness and diameter were measured by using digital Vernier calipers. The tablets were positioned between the arms of the calipers to measure the thickness and diameter according to the procedure followed by Ahmed and co-workers [18].

2.6.3 Tablet friability

Friability test was done to confirm the physical strength of the tablet. For this, ten tablets from each formula both uncoated and enteric coated were weighed before putting them into the rotating disk of a tablet friability tester (Veego Friability tester, Model: VFT-2D). Then the disk was allowed to rotate at a speed of 25 rpm for four minutes, in order to complete 100 revolutions. After that, the tablets were taken out

of the drum and weight loss percentage was calculated by the following equation [19, 20].

Friability= $(W_0 - W)/W_0 \times 100$

Here, W_0 = initial weight; W = final weight

2.7 In vitro dissolution studies

Dissolution studies of the formulated tablets were performed by using USP type II apparatus (Logan Instruments, USA) with 900 ml medium at 37±0.5°C and in 100 rpm [18]. For uncoated tablets, the total duration of the dissolution was 8 hours and phosphate buffer at pH 7.4 was used as a dissolution medium. 5 ml of samples were withdrawn, from each dissolution vessel, at the interval of 1, 2, 3, 4, 5, 6, 7 and 8 h. After every withdrawal, 5 ml of fresh buffer solution was added to each vessel to readjust the volume of the medium. After filtration and dilution absorbance values were measured at 249 nm for naproxen sodium by using a UV visible spectrophotometer (UV-1800, Shimadzu Corp). On the other hand, dissolution study of enteric coated tablets was performed in same test conditions except for the fact that first two hours dissolution was done using 900 ml 0.1 N HCl solution as medium followed by 8 hours in phosphate buffer (pH 7.4).

2.8 Release kinetics studies

Release kinetics study was done by data obtained from the *in vitro* drug release and plotting it in various release kinetic models like zero-order, first-order, Higuchi, Hixson-Crowell, and Korsmeyer-Peppas [21, 22].

Zero-order equation: $Q_t = Q_0 + K_0t$

Where, Q_t = dissolved drug amount at time t, Q_0 = initial drug amount, K_0 = release constant of zero order expressed in units of concentration/time.

First-order equation: $\log C = \log C_0 - Kt/2.303$

In the above equation, the initial concentration of the drug is C_0, first-order rate constant is K and time is t.

Higuchi equation: $Q = KHt^{1/2}$

Where, Q = drug release amount at time t; KH= Higuchi diffusion rate constant.

Korsmeyer–Peppas equation: $Q = M_t / M_\infty = Kt^n$

Where Q is the amount of drug release, Mt is the amount of drug release at time t and M∞ is the drug release amount at an infinite time, K is the constant of release rate and n is the exponent of release. In order to characterize the release of cylindrically shaped matrices, n is used.

Hixson-Crowell equation:

The cube root equation of Hixson and Crowell is a frequently used model for explaining the effect of change in diameter and surface area of tablets or particles due to swelling and erosion [23]. In the present study, the release data were fitted with Hixson-Crowell equation in the aim of investigating the impact of tablet matrix swelling and erosion upon the release of naproxen.

$$Q_0^{1/3} - Q_t^{1/3} = K_{HC} \times t$$

Where Q0 is the initial amount of drug, Qt is the remaining amount of drug at time t, and KHC is the Hixson-Crowell constant.

2.9 Determination of mean dissolution time (MDT)

Mean dissolution time (MDT) was calculated with the help of dissolution data. It helps in the drug release rate characterization from the dosage form polymer retarding efficiency [24].

$$MDT = (n/n+1)K^{-1/n}$$

Where, n = release exponent and K = release rate constant obtained from Korsmeyer–Peppas equation.

2.10 Swelling index studies

Swelling index of the uncoated matrix tablets from each formula was evaluated by using phosphate buffer at pH 7.4. Initial weights (w_1) of the tablets were taken and then tablets were immersed in a Petri dish containing phosphate buffer at 370C temperature. For enteric coated tablets, this was done in two phases: first two hours in acid medium (pH 1.2) and then 8 hours in buffer medium (pH 7.4). The tablets were taken out of the buffer 1, 2, 3, 4, 5, 6, 7, and 8 hours and then final weight (w_2) was taken using the balance. In case of enteric coated matrix tablets first two hours swelling was evaluated by using 0.1 N HCl solution and then for 8 hours in phosphate buffer and final weights were calculated in each hour as was done in case of uncoated tablets. The swelling index was calculated using the following formula [25].

Swelling index = 100 $(w_2-w_1)/w_1$

Where, w_1 = initial weight, w_2 = final weight

2.11 Erosion studies

Erosion study of the core and coated tablets was carried out according to the method of Ravi et al. [26]. Briefly, the uncoated tablets (F-1 to F-5) were immersed in the buffer medium (pH 7.4) which was maintained under the same conditions as specified in the dissolution study. For the enteric coated tablets, it was performed in a combination of two phases as it was done in case of swelling study. After each hour matrix tablet was taken away from the dissolution vessel using a small basket and was dried at a temperature of 45°C until a constant weight was obtained. Erosion of the formulated matrix tablets after each hour was calculated by using a previously reported equation of Sriamornsak and co-workers [27]:

Erosion = 100 $(W_0-W_2)/W_0$

Where, W_0 = initial weight, W_2 = final weight after drying

2.12 Statistical evaluation

All the experiments related to average percent release with time, mean dissolution time (MDT) percent erosion and swelling index were done in triplicate. Statistical significance was calculated by the student's t-test, and the difference was considered as significant when the value of p was less than 0.05.

A model-independent approach like the similarity (f2) and dissimilarity (f1) factor were used to compare the dissolution profiles of the uncoated and coated formulation. In this instance equation proposed by Moore and Flanner was used which are given below [28].

$$\mathbf{f_1 = \{[\sum_{t=1}^{n}(R_t - T_t)]/\ \sum_{t=1}^{n} R_t]\} * 100}$$

$$\mathbf{f_2 = 50\ log\ \{[1+ (1/n) \sum_{t=1}^{n}(R_t - T_t)^2]^{-0.5} * 100}$$

Where f_1= dissimilarity factor

f_2 = similarity factor

n = number of observations

R_t = % drug dissolved from reference formulation

T_t = % drug dissolved from test formulation

3. Results and Discussion

3.1 Physical properties of powder blends

For proper tableting, measurement of powder flow is a key requirement as it is directly related to tablet weight, integrity and content uniformity [11]. For the evaluation of flow-ability and compressibility, Carr's index (CI) and Hausner ratio (HR) of different powder blends were investigated. Carr's index (CI) and Hausner ratio (HR) of all formulations were found to be within passable range (CI, 21-25 and HR, 1.26-1.34) according to the specification of United States Pharmacopoeia. Additionally, the measured angle of repose of F-1, F-2, F-3 was within passable range (41◦-45◦), F-4 and F-5 were found within fair range (36◦-40◦) [18] **(Table-2).**

Table 2: *Pre-compression physical properties of powder blends of different formulations.*

Formulation code	Carr's index (%)	Hausner ratio	Angle of repose (θ^0)
F-1	22.0 ± 0.352	1.30 ± 0.03	43.0 ± 1.22
F-2	21.6 ± 0.241	1.27 ± 0.04	44.2 ± 1.15
F-3	21.8 ± 0.326	1.28 ± 0.05	43.0 ± 1.31
F-4	22.3 ± 0.561	1.31 ± 0.02	38.7 ± 0.84
F-5	23.2 ± 0.785	1.33 ± 0.03	38.2 ± 0.91

3.2 Drug-excipient compatibility studies

Formulation-5 (F-5) which contained the highest amount of K15M CR and found to control the release for the longest period of time with minimum fluctuation was selected for compatibility study by Fourier-transform infrared spectroscopy (FTIR) and differential scanning calorimetry (DSC). Pure naproxen sodium, Methocel K15M CR, and the physical mixture of F-5 were characterized by FTIR **(Figure 1A).** Naproxen sodium gives several strong and weak absorption bands in between 1450 and 1600 cm^{-1} due to C-C stretching vibration modes of the aromatic rings [29]; visible strong peaks at 1363 and 1388 cm^{-1} resemble -CH3 bending vibration group [30]; it shows a weak absorption band due to C=O stretching at 1558 cm^{-1} [31] **(Figure 1A).** Methocel K15M CR shows weak intensity peak at 1732 cm^{-1} that confirms C=O stretching vibration [32]; weak absorption peak at 1633 cm^{-1} because of the presence CO six-member cyclic rings [33]; weak absorption bands at 570 and 507 cm^{-1} are due to C-C stretching [31] **(Figure 1B).** Formulation F-5 gives a weak peak at 1631 cm^{-1} due to C=C stretching vibration; strong to medium intensity peaks at 856 and 688 cm^{-1} are observed due to the presence of =C-H bending vibration group [32]; medium to weak intensity peaks at 688 and 522 cm^{-1} are because of C-C stretching [31] **(Figure 1C).**

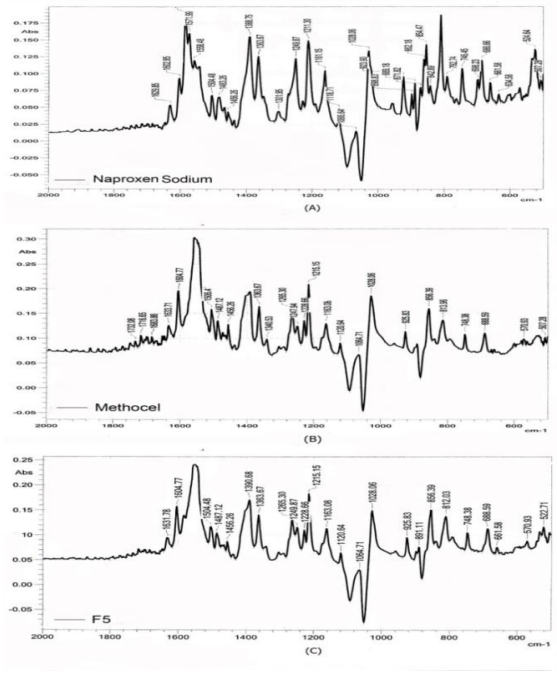

Figure 1: FTIR spectrum of (A) Naproxen Sodium (B) Methocel K15M CR and (C) Formulation F-5

Study shows that all characteristic peaks of pure naproxen and Methocel K15M CR were easily detectable before mixing and there was no sharp change in the absorption peaks in the physical mixture of our selected formulation (F-5) indicating that there was no major incompatibility between the drug and the excipients.

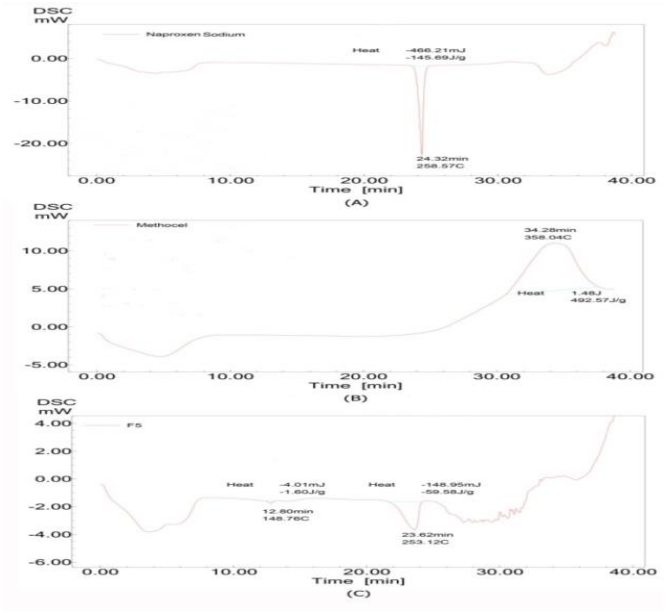

Figure 2: DSC thermogram of (A) Naproxen Sodium (B) Methocel K15M CR and (C) Formulation F-5

This finding was further confirmed by DSC analysis **(Figure 2).** The DSC thermogram of pure naproxen sodium showed a sharp melting endotherm at 2580C with normalized energy of -145.69 J/g **(Figure 2A),** which is consistent to its actual melting point [30]. The thermograms of solid admixtures of naproxen with various excipients showed a similar peak at 2530C with same normalized energy, indicating that naproxen is unaffected in the presence of various excipients used in the preparation of sustained release matrix tablet. Methocel K15M CR showed a sharp exothermic peak at 358°C (492.57 J/g) followed by a broad endothermic peak which might be due to the re-crystallization of the polymer [34] **(Figure 2B).** However, minor changes of peaks observed in formulation F-5 are due to the mixture of the drug and the excipients which don't indicate the incompatibility of the drug with excipients **(Figure 2C).**

3.3 Physical characteristics of the uncoated and enteric coated tablets

Naproxen sodium sustained release uncoated and enteric coated tablets were prepared by using different amounts of Methocel K15M CR and fixed the amount of ludipress, aerosol, and magnesium stearate as mentioned in the previous section (Table-1). Results of the hardness, thickness, diameter, weight variations, and friability for uncoated tablets are presented in **Table-3** and enteric coated tablets in **Table-4**.

Table 3: *Physical properties of core tablets of different formulations.*

Formulation code	Average hardness (kg/cm^2)	Average Friability (%)	Average thickness (mm)	Average diameter (mm)	Average Weight (mg)
F-1	6.7 ± 0.11	0.61 ± 0.00(	7.30 ± 0.08	11.51 ± 0.1(	601 ± 4.3(
F-2	6.4 ± 0.20	0.27 ± 0.00	7.34 ± 0.11	11.52 ± 0.12	619 ± 3.75
F-3	6.5 ± 0.12	0.31 ± 0.00	7.40 ± 0.10	11.50 ± 0.11	642 ± 3.74
F-4	6.6 ± 0.20	0.47 ± 0.00	7.44 ± 0.09	11.50 ± 0.0	661 ± 4.2(
F-5	6.3 ± 0.12	0.45 ± 0.00	7.50 ± 0.08	11.52 ± 0.0	682 ± 4.5

Physical evaluation of the tablets revealed that the tablets average thickness, diameter, weight of core tablets and weight gain due to enteric coating was uniform. Friability values of the tablets were less than 1 % and the hardness of the tablets was between 6.3 to 6.7 kg/cm^2 indicating that the results were within specification [18] and tablet surfaces were strong enough to withstand the mechanical shock or attrition during storage and transportation.

Table 4: *Physical properties of naproxen sodium tablets after enteric coating.*

Formulation code	Average thickness (mm	Average diameter (mm)	Weight gain due to coatin (%)	Average Weight (mg)
F-6	7.55 ± 0.071	12.48 ± 0.107	6.67 ± 0.119	640 ± 4.31
F-7	7.62 ± 0.121	12.51 ± 0.112	6.13 ± 0.213	658 ± 3.60
F-8	7.70 ± 0.122	12.50 ± 0.102	6.09 ± 0.109	679 ± 5.10
F-9	7.82 ± 0.092	12.52 ± 0.092	6.21 ± 0.182	701 ± 4.22
F-10	7.85 ± 0.088	12.53 ± 0.101	6.03 ± 0.154	721 ± 4.40

3.4 Dissolution study of uncoated and coated tablets

The dissolution test of uncoated tablets was performed in the buffer medium (pH 7.4). On the other hand, the dissolution test of enteric coated tablets was conducted in two phases: 2 hours in acid medium, followed by 8 hours in a buffer medium. It was observed from the release profile that the variation in the amount of the polymer Methocel K15M CR had a variable effect on the release rate and extent of the drug. In case of uncoated tablets, the initial drug release was rapid and inconsistent for the formulations having lower amount (F-1, F-2, and F-3) of polymer; as the amount (F-4 and F-5) of the polymer was increased the release patterns became slower and steady **(Figure 3A).**

On the other hand, the enteric coating effectively prevented the release of naproxen from the matrix tablets in acid medium. But, in the buffer medium, the enteric coating dissolved immediately and matrix tablets released the drug almost in the same pattern as it did in case uncoated tablet **(Figure 3B).**

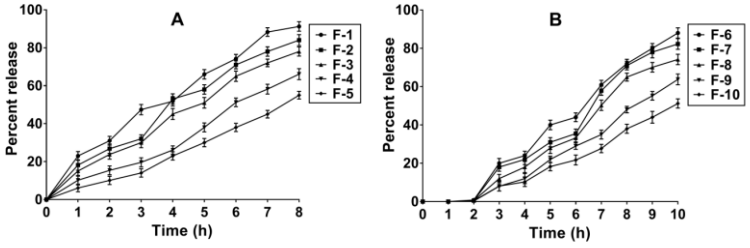

Figure 3: Average percent release of naproxen sodium calculated from dissolution data for different formulations of uncoated (A) and enteric coated (B) matrix tablets. The dissolution test of uncoated tablet was conducted in buffer medium (pH 7.4) for 8 hours. On the other hand, dissolution study of enteric coated tablets was performed in 0.1 N HCl solution for first 2 hours which was followed by 8 hours in phosphate buffer (pH 7.4).

It is clear from the data that there was no initial burst release of naproxen in the buffer medium, which is also consistent with the previous finding, where Manjula and co-workers demonstrated that initial rapid release from hydrophilic matrix is associated with highly soluble drugs [35]. Both in case of uncoated and enteric coated tablets after 8 hours of dissolution test in the buffer medium (pH 7.4) the total percent release was approximately 90 % for the matrix tablets which were prepared by using lowest amount (40 mg) of Methocel K15M CR. Conversely, for the tablets prepared by the highest amount of polymer (120) the average percent release at the end of 8 hours dissolution in the buffer medium was close to 55 %. In the present study, the amount of polymer in each formulation has been increased from the previous one by 20 mg (Table-1). Comparison between F-1 and F-2 revealed that due to this 20 mg change of polymer content, the average percent release at the end of 8 hours was not changed significantly. But the comparison between F-1 and F-3 revealed that 40 mg increase was able to change the percent release significantly (p<0.05) both in case of coated and uncoated tablets.

Drug release mechanism from the matrix to the dissolution medium involves the participation of different physical and/or chemical phenomena making it difficult to get a perfect mathematical model for describing it [36]. The most frequently used mathematical models for the last few years, in general, are the zero-order model, Higuchi model, first-order model, Korsmeyer-Peppas model and Hixson-Crowell model [37]. From the Korsmeyer and Peppas equation, the values of release exponent (n) were calculated which are 0.831, 0.823, 0.859, 0.911, and 0.942 for F-1 to F-5 for uncoated matrix tablets of naproxen sodium in that order **(Table-5)**. According to the Korsmeyer-Peppas model F-1, F-2, and F-3 followed non-Fickian diffusion and formula F-4 and F-5 followed super case II transport mechanism [38].

Table 5: Release rate constants and R^2 values of different release kinetics and mechanism of naproxen sodium release from uncoated matrix tablets.

Formulation	Zero Order		First Order		Higuchi		Hixson-Crowe		Korsmeyer	
code	K_0	R^2	K_1	R^2	K_h	R^2	K_{hc}	R^2	n	R^2
F-1	12.77	0.981	-0.23	0.805	37.94	0.931	0.744	0.696	0.831	0.961
F-2	12.34	0.979	-0.17	0.907	36.80	0.937	0.728	0.719	0.823	0.972
F-3	11.62	0.976	-0.12	0.942	34.45	0.923	0.718	0.741	0.859	0.955
F-4	6.77	0.983	-0.04	0.964	19.64	0.903	0.695	0.812	0.911	0.977
F-5	6.13	0.964	-0.03	0.944	17.09	0.866	0.669	0.849	0.942	0.975

The values of release exponent were also calculated for enteric coated tablets by using 8 hour's release data in the buffer phase. The values of release exponent (n) obtained for the enteric coated tablets are 0.847, 0.872, 0.892, 0.915 and 0.987 for F-6 to F10 respectively **(Table-6).**

Table 6: Release rate constants and R^2 values of different release kinetics and mechanism of naproxen sodium release from enteric coated matrix tablets.

Formulation	Zero Order		First Order		Higuchi		Hixson-Crowe		Korsmeyer	
code	K_0	R^2	K_1	R^2	K_h	R^2	K_{hc}	R^2	n	R^2
F-6	13.74	0.958	-0.17	0.795	38.85	0.982	0.691	0.723	0.847	0.979
F-7	12.76	0.959	-0.16	0.948	12.76	0.959	0.670	0.771	0.872	0.964
F-8	10.50	0.953	-0.08	0.987	10.50	0.953	0.686	0.833	0.892	0.970
F-9	6.87	0.941	-0.03	0.946	6.87	0.941	0.658	0.853	0.915	0.873
F-10	4.85	0.936	-0.02	0.908	4.85	0.916	0.635	0.884	0.987	0.976

Both for uncoated and coated tablets, the value of release exponent (n) obtained from Korsmeyer's equation, indicates that formulations containing a lower amount of polymer followed anomalous transport mechanisms; whereas formulations having a relatively higher amount of polymer followed case II and super case II transport mechanisms. This suggests that irrespective of the presence of enteric coating the drug release mechanism shifted towards the same direction in the buffer medium. Moreover, the gradual increase of the values of release exponent with an increase of polymer content in the tablet indicated that polymer chain relaxation and consequent swelling and erosion of the tablet matrix play key roles in controlling the release of sparingly water-soluble drug from the hydrophilic matrix [39]. These findings are also reinforced by the poor fitting with the Higuchi model as indicated by the R^2 values **(Table 4 and 5).** Generally, water-soluble drugs are released in diffusion-controlled mechanisms shows better fitting with the Higuchi model [40]. On the other hand, the release mechanism of the poorly soluble drug, like naproxen, from hydrophilic matrix tablet is relatively complex because it is mainly dependent on the erosion of tablet matrix and relaxation of the hydrated polymer chains [41]. Our observations are also in agreement with the findings of several other researchers who have already reported that soluble component of the dosage form is released by Fickian diffusion and the insoluble portion of the dosage form is released due to the erosion of the solid matrix [1, 42, 43].

The dissolution data were also used to make a comparison between uncoated and coated tablet; for example, F-1 was compared with F-6 and F-2 with F-7 and so on for evaluating the similarity and dissimilarity. According to Center for Drug Evaluation and Research (CDER) of the US Food and Drug Administration (FDA), a value of f2 from 50 to 100 indicates that the dissolution profiles of the formulations are similar [28]. Based on that standard it can be considered that F-1 and F-6 are pharmaceutically equivalent; similarly, any formulation from the uncoated group and its corresponding formulation from the coated group are also found to be pharmaceutically equivalent **(Table-7).**

Table 7: Similarity and dissimilarity between uncoated and enteric coated tablets based on dissolution data.

Reference Formulation (R_t)	Test Formulation (T_t)	Similarity Factor (f_2)	Dissimilarity Factor (f_1)
F-1	F-6	70.07 ± 2.39	6.35 ± 0.45
F-2	F-7	67.77 ± 2.54	5.42 ± 1.33
F-3	F-8	60.20 ± 3.09	8.89 ± 0.79
F-4	F-9	78.30 ± 2.14	6.39 ± 1.39
F-5	F-10	82.65 ± 3.31	5.47 ± 0.84

The main benefit of using f1 and f2 is that it is an easy way to compare the dissolution data as well as their equivalence. However, this method lacks the effectiveness of using variability and correlation of the data [44]. For this reason, different model dependent approaches, as mentioned above, were also used in this study to understand the drug release mechanism more comprehensively.

3.5 Polymer content altered the mean dissolution time (MDT)

Sustained release matrix tablets should be able to retard the drug release rate which is necessary for the consistent and prolonged drug delivery for the maintenance of plasma drug concentration in the therapeutic window with minimum fluctuation. This release controlling ability is achieved generally through the judicious use of an optimum amount of polymer with appropriate viscosity grade [45]. Therefore, to evaluate the impact of the different amount of Methocel K15M CR on release, we also calculated mean dissolution time (MDT), by using the value of release exponent (n), according to Mockel-Lippold equation [46]. In case of uncoated core tablets formula F-1, which contained the lowest amount (40 mg) of polymer, has the lowest MDT (3.51 hours) and formula F-5, which contained the highest amount (120 mg) of polymer, has the highest MDT (7.5 hours). Same was the pattern in case of enteric coated tablets (7.62 hours) which were not significantly different from the corresponding formulation of the uncoated tablet. Similar to the percent release in this case 20 mg change of polymer was not able to change the MDT significantly but 40 mg change of polymer content was able to change the MDT value significantly ($p<0.05$) **(Figure 4).** Moreover, these findings were in agreement with the observation of Reza and co-workers, where they demonstrated that release retarding ability of matrix tablets increased due to the increase of HPMC content in diltiazem and theophylline-based matrix tablets [47].

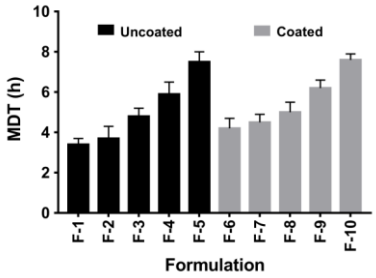

Figure 4: Mean dissolution time (MDT) of naproxen sodium from different formulations of uncoated (F-1 to F-5) and enteric coated (F-6 to F-10) tablets based on the release of drug in buffer medium (pH 7.4) for 8 hours.

3.6 Impact of swelling and erosion on drug release from matrix tablets

This part of our present study was aimed to investigate how the swelling and erosion pattern of hydrophilic matrix tablets influences the release of naproxen. When drug loaded HPMC type hydrophilic matrices are exposed to dissolution fluid, water molecules are absorbed into the polymeric matrix due to the water concentration gradient between the dissolution fluid and the outermost surface of the matrix tablet. Thus, the dissolution medium exerts a plasticizer effect which causes the dramatic lowering of glass transition temperature (Tg) of the polymer [39]. As the Tg approaches the temperature of the system (37°C), the polymer chains continue to relax and eventually disentangle which increases the molecular surface area [48]. The continuous infiltration of water breaks the existing intermolecular hydrogen bonds which were formed during tablet compression and leads to the development of new hydrogen bonds for accommodating incoming water molecules. Therefore, the reduction of Tg, dissociation of old hydrogen bonds between the polymer and other ingredients of tablet and formation of new hydrogen bonds between polymer and water results in the increase of the volume of the tablet matrix [49]. This phenomenon of polymer chain relaxation due to the absorption of solvent and resultant conversion of the polymer from an amorphous glassy state to gel-like rubbery state is termed as ‘swelling’.

The swelling study of uncoated tablets (F-1 to F-5) was performed for 8 hours in a buffer medium and of enteric coated tablets (F-6 to F-10) this was done in two phases: first 2 hours in acidic medium and then 8 hours in buffer medium (pH 7.4). At the end of the first two hours immersion in acidic medium, the enteric coated tablet dimensions remained unchanged with very insignificant swelling (data not shown). As the enteric coated tablets were immersed in the buffer medium (pH 7.4) the enteric coating started to dissolve and tablets started to swell. In both cases, it was observed that formulations containing a lower amount of Methocel K15M CR continued to swell up to the first two hours and then started to lose weight due to the erosion of the matrix. On the other hand, formulations containing a higher amount of

Methocel K15M CR continued to swell up to first 3 hours and then started to lose weight **(Figure 5A and Figure 5B).** Both in case of core and coated tablets release of naproxen sodium from tablet matrix and erosion of the tablet matrix, in the buffer medium, followed the similar trends **(Figure 6A and Figure 6B).** To make the understanding even more quantitative in the pattern, the release data was analysed with Hixson-Crowell's cube root model which is being used to describe the release mechanism by considering the gradual erosion of the surface of the matrix tablets or tablet particles during the dissolution [50]. This erosion dominated release observed in formulations containing the highest amount of polymer (F-5 and F-10) was highly supported by higher correlation co-efficient values of Hixson-Crowell model **(Table 4 and 5).**

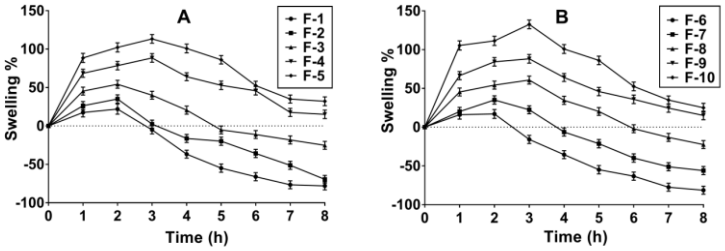

Figure 5: Swelling index for different formulations of naproxen sodium uncoated (A) and enteric coated (B) matrix tablets for 8 hours in buffer (pH 7.4) medium.

The thickness and rheological properties of the gel layer is crucial in describing the release mechanisms of swellable and erodible matrices [27]. When the outer layer becomes completely hydrated, the relaxation of polymer chains reaches to the maximum level and hence can no longer maintain the integrity of the gel layer which results in the erosion of the tablet matrix. Dissolution medium continues to infiltrate towards the center of the matrix until the tablet is completely disintegrated [39]. Hence initial swelling and subsequent erosion can be attributed to control the drug release mechanism from the formulations evaluated in the present study.

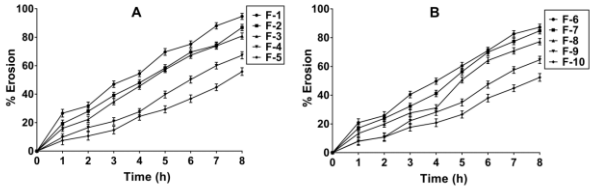

Figure 6: Percent erosion of different formulations of naproxen sodium uncoated (A) and enteric coated (B) matrix tablets for 8 hours in buffer (pH 7.4) medium.

4. Conclusions

Hydroxypropyl methylcellulose containing solid dosage forms are considered as swelling controlled systems in which drug release is mainly affected by the penetration of dissolution medium in the tablet matrix and subsequent relaxation of the polymer chain which culminates in swelling and erosion of the tablet matrix. In the present investigation, tablets prepared by using a higher amount of Methocel K15M CR exhibited higher swelling index at the first few hours which was followed by mechanical erosion of the tablet. Higher MDT values of formulations made from higher amounts of Methocel K15M CR indicates that it has high release retarding efficiency which was also consistently represented in the lower value of average percent release at the end of 8 hours dissolution test. The release of naproxen from all of the 5 uncoated formulations and corresponding 5 enteric-coated formulations were controlled primarily by non-Fickian processes which are dominated by relaxation of the polymer chain followed by swelling and erosion of the matrix tablet. There was no initial burst release of naproxen from the matrix which is generally the pattern of highly soluble drugs and is the characteristic of Higuchi release mechanism. By analyzing all these results, it can be concluded that development of enteric coated sustained release matrix tablets of naproxen sodium using Methocel K15 MCR, or similar grade as a release-controlling polymer, could be a new approach for sustained pain relief with reduced harmful effects on the gastric mucosa.

Author Contributions: Experimental design, Investigation, Writing, Data analysis, SAK; Formulation preparation, Investigation, AA. Formulation preparation, Investigation, AMS; Formulation preparation, Investigation, TT; Investigation, Data analysis, SA; Investigation, Data analysis, FA; Experimental design, Writing and editing, RK; Data analysis, Investigation, MZS. Conceptualization, Experimental design, Data analysis, Writing - original draft, Supervision, FK. All authors have read and agreed to the published version of the manuscript.

Funding: The authors did not receive support from any organization for the submitted work.

Institutional Review Board Statement:

Informed Consent Statement:

Data Availability Statement: The data that support the findings of this study are available on request from the corresponding author

Acknowledgments: The research was conducted in the Department of Pharmaceutical Sciences, North South University, Dhaka, Bangladesh and Centre for Advanced Research in Sciences (CARS), University of Dhaka, Bangladesh. The authors thank the Ibn Sina Pharmaceuticals Ltd, (Gazipur, Bangladesh), for providing gift samples of naproxen sodium, Methocel K15M CR, and cellulose acetate phthalate. Authors also thank BASF, Bangladesh for providing Ludipress.

Conflicts of Interest: The authors whose names are listed in this paper certify that they have NO affiliations with or involvement in any organization or entity with any financial interest.

References

1. Kamboj S., Saroha K., Goel M., Madhu C. Sustained release drug delivery system: An overview. *Pharm. Res*. 2012; 8:169-186.
2. Tamargo J., Le Heuzey J. Y., Mabo P. Narrow therapeutic index drugs: a clinical pharmacological consideration to flecainide. *Eur. J. Clin. Pharmacol*. 2015; 71:549-567.
3. Murtaza G., Ullah H, Khan S. A., Mir S, Khan A. K., Nasir B. Formulation and *in vitro* dissolution characteristics of sustained-release matrix tablets of tizanidine hydrochloride. *Trop. J. Pharm. Res*. 2015; 14(2):219-225.
4. Chen K., Chang H. H. R., Shalviri A., Li J., Lugtu-Pe J. A., Kane A. Investigation of a new pH-responsive nanoparticulate pore former for controlled release enteric coating with improved processability and stability. *Eur. J. Pharm. Biopharm*. 2017; 120:116-125.
5. Leung G. J., Rainsford K., Kean W.F. Osteoarthritis of the hand II: chemistry, pharmacokinetics and pharmacodynamics of naproxen, and clinical outcome studies. *J. Pharm. Pharmacol*. 2014; 66(3):347-357.
6. Todd P. A., Clissold S. P. Naproxen. *Drugs*. 1990; 40(1):91-137.
7. Khadra I., Zhou Z., Dunn C., Wilson C. G., Halbert G. Statistical investigation of simulated intestinal fluid composition on the equilibrium solubility of biopharmaceutics classification system class II drugs. *Eur. J. Pharm. Sci*. 2015; 67:65-75.
8. Ong C., Lirk P., Tan C., Seymour R. An evidence-based update on nonsteroidal anti-inflammatory drugs. *J. Clin. Med. Res*. 2007; 5(1):19-34.
9. Davies N. M. Sustained release and enteric coated NSAIDs: are they really GI safe. *J. Pharm. Sci*. 1999; 2(1):5-14.
10. Amidon G. E., Secreast P. J., Mudie D. Particle, powder, and compact characterization. Developing solid oral dosage forms: Elsevier; 2009. p. 163-186.
11. Shah R. B., Tawakkul M. A., Khan M. A. Comparative evaluation of flow for pharmaceutical powders and granules. *AAPS Pharmscitech*. 2008; 9:250-258.
12. Sharma P., Chawla A., Pawar P. Design, development, and optimization of polymeric based-colonic drug delivery system of naproxen. *Sci. World J*. 2013; 2013: 654829.
13. Hadi M. A., Rao N. R., Rao A. S. Formulation and evaluation of ileo-colonic targeted matrix-mini-tablets of Naproxen for chronotherapeutic treatment of rheumatoid arthritis. *Saudi. Pharm. J*. 2016; 24(1):64-73.
14. Angiolillo D. J., Weisman S. M. Clinical pharmacology and cardiovascular safety of naproxen. *Am. J. Cardiovasc. Drugs*. 2017; 17:97-107.
15. Kamble N. D., Chaudhari P. S., Oswal R. J., Kshirsagar S. S., Antre R. V. Innovations in tablet coating technology: A review. 2011.
16. Fahelelbom K. M., Al-Tabakha M. M., Eissa N. A., Javadi J. Evaluation of certain pharmaceutical quality attributes of lisinopril split tablets. *Sci. Pharm*. 2016; 84(4):646-653.
17. Pan X-m., Li J., Gan R., Hu X-n. Preparation and *in vitro* evaluation of enteric-coated tablets of rosiglitazone sodium. *Saudi. Pharm. J*. 2015; 23(5):581-586.
18. Ahmed A., Ali S. A., Hassan F., Ali S. S., Haque N. Evaluation of acetaminophen tablets by control test. *Pak. J. Pharm. Sci*. 2001; 14(2):47-55.
19. Pharmacopeia U. and National Formulary 25 (2007) US Pharmacopeial Convention. Rockville, MD.621.

20. Uddin M., Mamun A., Rashid M., Asaduzzaman M. In-process and finished products quality control tests for pharmaceutical capsules according to pharmacopoeias. *Br. J. Pharm. Res*. 2016; 9(2):1-9.
21. Hardy I. J, Windberg-Baarup A., Neri C., Byway P. V., Booth S. W, Fitzpatrick S. Modulation of drug release kinetics from hydroxypropyl methyl cellulose matrix tablets using polyvinyl pyrrolidone. *Int. J. Pharm*. 2007; 337(1-2):246-253.
22. Shoaib M. H., Al Sabah Siddiqi S., Yousuf R. I., Zaheer K., Hanif M., Rehana S. Development and evaluation of hydrophilic colloid matrix of famotidine tablets. *AAPS Pharmscitech*. 2010; 11:708-718.
23. Hixson A., Crowell J. Dependence of reaction velocity upon surface and agitation. *J. Ind. Eng. Chem*. 1931; 23(8):923-931.
24. Sutradhar K. B., Ahmed T., Ferdous A., Uddin R. Formulation and comparison of *in vitro* release profile of hydrophilic and hydrophobic polymer based Naproxen matrix tablets. *J. Appl. Pharm. Sci*. 2011; 1:155-159.
25. Shirsand S., Suresh S., Keshavshetti G., Swamy P., Reddy PVP. Formulation and optimization of mucoadhesive bilayer buccal tablets of atenolol using simplex design method. *Int. J. Pharm. Investig*. 2012; 2(1):34.
26. Ravi P. R., Ganga S., Saha R. N. Design and study of lamivudine oral controlled release tablets. *AAPS Pharmscitech*. 2007; 8:167-175.
27. Sriamornsak P., Thirawong N., Korkerd K. Swelling, erosion and release behavior of alginate-based matrix tablets. *Eur. J. Pharm. Biopharm.* 2007; 66(3):435-450.
28. Polli J. E., Rekhi G. S., Augsburger L. L., Shah V. P. Methods to compare dissolution profiles and a rationale for wide dissolution specifications for metoprolol tartrate tablets. *J. Pharm. Sci*. 1997; 86(6):690-700.
29. Carriazo D., del Arco M., Martín C., Ramos C., Rives V. Influence of the inorganic matrix nature on the sustained release of naproxen. *Microporous. Mesoporous. Mater*. 2010; 130(1-3):229-238.
30. Bhise K. S., Dhumal R. S., Paradkar A. R., Kadam S. S. Effect of drying methods on swelling, erosion and drug release from chitosan–naproxen sodium complexes. *AAPS Pharmscitech*. 2008; 9:1-12.
31. Yang H., Yan R., Chen H., Lee D. H., Zheng C. Characteristics of hemicellulose, cellulose and lignin pyrolysis. *Fuel*. 2007; 86(12-13):1781-1788.
32. Pongpiacha S. FTIR spectra of organic functional group compositions in PM2. 5 collected at Chiang-Mai City, Thailand during the haze episode in March 2012. *J. Appl. Sci*. 2014; 14(22):2967-2977.
33. Punitha S., Uvarani R., Panneerselvam A., Nithiyanantham S. Physico-chemical studies on some saccharides in aqueous cellulose solutions at different temperatures–Acoustical and FTIR analysis. *J. Saudi. Chem. Soc*. 2014; 18(5):657-665.
34. Late S., Banga A. Thermal and non-thermal methods to evaluate compatibility of granisetron hydrochloride with tablet excipients. *Die. Pharmazie*. 2008; 63(6):453-458.
35. Manjula B., Srinatha A., Sridhar B. Evaluation of hydrophilic polymers and their combinations in formulation of sustained-release matrix tablets of water-soluble drug. *Ind. J. Pharmaceut. Educ. Res*. 2014; 48:48-59.
36. Manga R. D., Jha P. K. Mathematical models for controlled drug release through pH-responsive polymeric hydrogels. *J. Pharm. Sci*. 2017; 106(2):629-638.
37. Siepmann J., Peppas N. A. Modeling of drug release from delivery systems based on hydroxypropyl methylcellulose (HPMC). *Adv. Drug Deliv. Rev*. 2012; 64:163-174.
38. Kosmidis K., Rinaki E., Argyrakis P., Macheras P. Analysis of Case II drug transport with radial and axial release from cylinders. *Int. J. Pharm*. 2003; 254(2):183-188.

39. Yin X., Li H., Guo Z., Wu L., Chen F., de Matas M. Quantification of swelling and erosion in the controlled release of a poorly water-soluble drug using synchrotron X-ray computed microtomography. *AAPS J*. 2013; 15:1025-1034.
40. Dash S., Murthy P. N., Nath L, Chowdhury P. Kinetic modeling on drug release from controlled drug delivery systems. *Acta Pol. Pharm*. 2010; 67(3):217-223.
41. Shabbir M., Ali S., Raza M., Sharif A., Akhtar F. M., Manan A. Effect of hydrophilic and hydrophobic polymer on *in vitro* dissolution and permeation of bisoprolol fumarate through transdermal patch. *Acta. Pol. Pharm*. 2017; 74(1):187-197.
42. Kuksal A., Tiwary A. K., Jain N. K., Jain S. Formulation and *in vitro*, *in vivo* evaluation of extended-release matrix tablet of zidovudine: influence of combination of hydrophilic and hydrophobic matrix formers. *AAPS Pharmscitech*. 2006; 7: E1-E9.
43. Tiwari S. B., Murthy T. K., Raveendra Pai M., Mehta P. R., Chowdary P. B. Controlled release formulation of tramadol hydrochloride using hydrophilic and hydrophobic matrix system. *AAPS Pharmscitech*. 2003; 4(3):31.
44. Koester LcS., Ortega G. G., Mayorga P., Bassani V. L. Mathematical evaluation of *in vitro* release profiles of hydroxypropylmethylcellulose matrix tablets containing carbamazepine associated to β-cyclodextrin. *Eur. J. Pharm. Biopharm*. 2004; 58(1):177-179.
45. Hattori Y., Ota K., Peerapattana J., Otsuka M. Evaluation of swelling processes of various natural polymer matrix tablets by X-ray computed tomography and controlled drug release. *Biomed. Mater. Eng*. 2018; 29(4):439-450.
46. Möckel J. E., Lippold B. C. Zero-order drug release from hydrocolloid matrices. *Pharm. Res*. 1993; 10:1066-1070.
47. Reza M. S., Quadir M. A., Haider S.S. Comparative evaluation of plastic, hydrophobic and hydrophilic polymers as matrices for controlled-release drug delivery. *J. Pharm. Sci*. 2003; 6(2):282-291.
48. Conti S., Maggi L., Segale L., Machiste E.O., Conte U., Grenier P. Matrices containing Na-CMC and HPMC: 2. swelling and release mechanism study. *Int. J. Pharm*. 2007; 333(1-2):143-151.
49. Li CL., Martini L. G., Ford J. L., Roberts M. The use of hypromellose in oral drug delivery. *J. Pharm. Pharmacol*. 2005; 57(5):533-546.
50. Niebergall P., Milosovich G., Goyan J. Dissolution rate studies II: dissolution of particles under conditions of rapid agitation. *J. Pharm. Sci.* 1963; 52(3):236-241.

JBEP

Journal of Biosciences and Experimental Pharmacology
ISSN-2960-284X

Original Article

Identification of Polyphenols and Evaluation of Antioxidant and α-Amylase Inhibitory Activity of Wheat Bran Extracts

Mirza Alimullah [1], Nishad Anjum [1], Md Junaeid Rahman [1], Khondoker Shahin Ahmed [2], Hemayet Hossain [2], Md Ashraful Alam [1], Nusrat Subhan[1*]

[1]*Department of Pharmaceutical Sciences, North South University, Bangladesh*
[2]*BCSIR Laboratories, Bangladesh Council of Scientific and Industrial Research (BCSIR), Dhaka, Bangladesh*

***Correspondence *E-mail*:** nusrat.subhan@northsouth.edu

Citation: Alimullah, M.; Anjum, N.; Rahman, M. J.; Ahmed, K. S.; Hossain, H.; Alam, M. A.; Subhan, N. Identification of polyphenols and evaluation of antioxidant and α-amylase inhibitory activity of wheat bran extracts. *J. Bio. Exp. Pharm* 2023, 1: 91-114.

Received: October 12, 2023

Accepted: November 25, 2023

Published: December 15, 2023

Publisher's Note: JBEP stays neutral with regard to jurisdictional claims in published maps and institutional affiliations.

Abstract: The aim of this study was to evaluate the bioactive compounds identification and determine the potential antioxidant and alpha(*α*)-amylase inhibitory activities of Wheat Bran (WB) extract. Phytochemical analysis was done by high performance liquid chromatography (HPLC) and gas chromatography (GC) in ethanol and n-hexane extract. Antioxidant potential was determined by nitric oxide scavenging and DPPH free radical scavenging assays. HPLC analysis showed the presence of dihydroxybenzoic acid, catechin hydrate, (-) epicatechin, caffeic acid, rutin hydrate, p-coumaric acid, trans-ferulic acid, rosmarinic acid, quercetin; and kaempferol. GC analysis showed a good number of compounds present in the WB extracts. The extracts showed considerable free radicles scavenging activity in both nitric oxide scavenging and DPPH free radical scavenging assays. IC_{50} of WB ethanol extract in DPPH scavenging assay was found 39.00 µg/mL and 14.57 µg/mL for ascorbic acid. In the *in vitro α*-amaylase inhibitory activity assay, the IC_{50} value of WB ethanol extract was 61.97 µg/mL, whereas the IC_{50} value for standard drug acarbose was 35.80 µg/mL. This investigation revealed that, WB extract is a potential source of bioactive compounds which can be used as alternative supplements for natural antioxidants.

Key words: Wheat Bran; free radicals; *α*-amaylase; nitric oxide; antioxidants.

1. Introduction

Reactive oxygen species (ROS) and reactive nitrogen species (RNS) are generated in biological reactions as by-products of oxygen metabolism, environmental stressors and due to xenobiotic metabolism. They play significant roles in many cellular processes like signal transduction and host defense [1]. However, overproduction of these reactive species causes imbalance, leading to cellular damage and dysfunction, contributing to many immune-pathological conditions such as atherosclerosis, diabetes mellitus, inflammatory diseases, cancer, neurological diseases like Parkinson's disease, Alzheimer's disease, rheumatoid arthritis, etc. Antioxidants play a vital role in suppressing oxidative stress. They

delay or prevent the oxidation of biologically important molecules such as membrane lipids, DNA, proteins, and other molecules by inhibiting the initiation of oxidative chain reactions and subsequently minimizing the risk of many chronic diseases, including cardiovascular disease and cancer [2, 3]. Natural plant products are considered rich sources of antioxidants and flavonoids, considered mainly as polyphenolic compounds. Plant-based natural antioxidants have proven effectiveness in mitigating various degenerative diseases.

Wheat (*Triticum aestivum*) is an abundant source of dietary fiber and one of the leading cereal crops utilized for mainly human consumption and livestock feed [4]. WB (15 % of the grain) is produced during milling and reportedly contains valuable fat-soluble bioactives like tocopherols, sterols, carotenoids and steryl ferulates. These components endow WB with antioxidant properties and represent a source of natural antioxidants for disease prevention [5]. It has been shown in previous clinical trials and epidemiological studies that compounds of WB fraction possess the capability of lowering blood cholesterol and are linked to reduced risk of diseases like colon cancer, diabetes, obesity and cardiovascular disease[4]. One of the minor components of WB oil fraction is steryl ferulate, which is known as oryzanol in rice bran oil has several beneficial health effects, such as anti-diabetic properties [5], reducing serum cholesterol levels [5] and may inhibit tumorigenesis etc. [6]. High-performance liquid chromatography (HPLC) analysis of WB oil extract revealed the presence of multiple natural antioxidants including phytic acid and polyphenolic compounds such as ferulic acids. These constituents demonstrated notable antioxidant potential through several mechanisms of action. Specifically, they were shown to scavenge free radicals, thereby reducing lipid oxidation. Chelation of metal ions and activation of endogenous antioxidant enzymes were additional antioxidant effects observed. The antioxidant profile of WB oil extract and its functional components warrant further investigation into their potential health benefits and applications. [2, 7]. Phytochemicals such as tocopherols, tocoretinols, and γ-oryzanol are reported to have many beneficial health properties. γ-Oryzanol contains cycloartenol, 24-methylene cycloartanyl ferulate, campesteryl ferulate, campestanyl ferulate, β-sitosteryl ferulate and is composed of phytosterols and trans-ferulic acid esters [8]. A previous report suggests that WB contains measurable amounts of γ-oryzanol like components named steryl ferulate [9], having a contribution to reducing cholesterol absorption [10]. Though several studies showed that WB fractions have a serum cholesterol-lowering effect but, there is no previous significant report explaining the mechanism by which it exerts a serum cholesterol-lowering effect [11]. The α- amylase is a digestive enzyme found in both saliva and pancreatic juice, involved in hydrolyzing glycosidic bonds, thus breaking down insoluble starch molecules into smaller absorbable molecules such as glucose, dextrin, maltose, and maltotriose [12]. Alpha-amylase can be a good target and has been given much attention for its anti-diabetic potential for many naturally occurring medicinal plants [13]. Alpha-amylase inhibitors play a significant role in lowering

postprandial blood glucose levels [14]. It has been reported that WB has anti-diabetic potential [15], but there are no studies explaining the mechanism by which it exerts *α*- amylase inhibitory effect. This study aimed to identify the polyphenol content in WB extract through HPLC-DAD and GC-MS. The antioxidant and *α*- amylase inhibitory potential of this WB extract was also evaluated in this study.

2. Materials and Methods

2.1 Chemicals and reagents

Alpha-amylase was procured from *Aspergillus oryzae*, 2,2-diphenyl-1-picrylhydrazyl (DPPH), and Naphthyl ethylenediamine dihydrochloride was obtained from Sigma-Aldrich Chemical Co. (USA). Starch soluble (extra pure) was obtained from J.T. Baker Inc., Phillipsburg, USA. Gallic acid, 3,4-Dihydroxybenzoic acid, Catechin hydrate, Catechol, (-) Epicatechin, Caffeic acid, Vanillic acid, Syringic acid, Rutin hydrate, *p*-Coumaric acid, *trans*-Ferulic acid, Rosmarinic acid, Myricetin, Quercetin, trans-Cinnamic acid, and Kaempferol were purchased from Sigma–Aldrich (St. Louis, MO, USA). Acetonitrile (HPLC), methanol (HPLC), acetic acid (HPLC), and ethanol were obtained from Merck (Darmstadt, Germany). *γ* –Oryzanol (98.5 %), for total sterol analysis and as standard, purchased from Sigma Chemical Company (USA). Other chemicals and reagents used were of analytical grade.

2.2 Plant collection and Preparation of WB oil concentrate

WB (*T. aestivum*) was procured from Diba Flour Mills, Narayanganj, Bangladesh. The collected WB was dried in an oven at 50 ℃ and then ground to obtain a fine powder. 500 gm of powdered bran was macerated with ethanol in a closed glass jar. It was kept in a dark place at room temperature for 5 days with occasional shaking. Then, the mixture was filtered to obtain WB ethanol extract. Finally, ethanol was evaporated with the help of a rotary evaporator operated at 50℃ with 100 rpm to obtain concentrated WB-ethanolic extract. The same process was applied to obtain WB-hexane extract. Two sticky dark-brownish crude extracts were obtained after the evaporation of the solvents. Both obtained extracts were screened for phytochemical analysis using HPLC-DAD and GC-MS methods.

2.3 HPLC-DAD Analysis

HPLC-DAD analysis was conducted using a Shimadzu system (LC-20A, Japan) consisting of a binary pump (LC-20AT), autosampler (SIL-20A HT), column oven (CTO-20A), and photodiode array detector (SPD-M20A), controlled by LC solution software. Separation was achieved on a Luna C18 (5µm) Phenomenex column (4.6 x 250 mm) maintained at 33°C.

2.3.1 Chromatographic conditions

Detection and quantification of selected polyphenolic compounds in WB ethanol extract was determined using high-performance liquid chromatography with

diode array detection (HPLC-DAD) analysis as described by Ahmed et al.[16] with minor modifications. The mobile phase consisted of 1 % acetic acid in acetonitrile (Solvent A) and 1 % acetic acid in water (Solvent B) with the following gradient elution program: 5-25 % A (0.01-20 min), 25-40 % A (20-30 min), 40-60 % A (30-35 min), 60-30 % A (35-40 min), 30–5 % A (40–45 min), and 5 % A (45–50 min).

The sample injection volume was 20µL, and the flow rate was set at 0.5 mL/min. Ultraviolet detection was set at 270 nm and used to validate the method and perform analysis. The mobile phase was filtered through a 0.45 µm nylon 6, 6 membrane filter (India) and degassed under vacuum.

2.3.2 Preparation of working standard solutions HPLC

Standard stock solutions of 16 phenolic compounds were prepared by dissolving in methanol in a 25 mL volumetric flask. The concentrations of stock solutions ranged from 4.0 to 50 µg/mL. Appropriate volumes of each stock solution were mixed and diluted serially with methanol to prepare the working standard solutions. All solutions were stored under refrigeration.

For the preparation of the calibration curve, a standard stock solution was prepared in methanol containing Gallic acid (20 µg/mL); 3,4-Dihydroxybenzoic acid (15 µg/mL); Catechin hydrate (50 µg/mL); Catechol, (-) epicatechin, rosmarinic acid (30 µg/mL each), caffeic acid, vanillic acid, syringic acid, rutin hydrate, *p*-coumaric acid, *trans*-ferulic acid, quercetin (10 µg/mL each); myricetin, kaempferol (8 µg/mL each); trans-cinnamic acid (4 µg/mL). A solution of ethanol extract of WB at a concentration of 10 mg/mL was prepared in ethanol. The samples were stored in the refrigerator.

2.4 Determination of steryl ferulates in WB n-hexan extract

Total *γ*-oryzanol-like steryl ferulate content was estimated following the method described by Kumar et al. [17, 18]. In this study, HPLC-UV (Shimadzu LC 10A system) was used coupled with Shimadzu C18 reversed-phase column (5 µm i.d, 150 mm × 4.6 mm.) and photodiode array detector (SPD-M20A), using isocratic elution with acetonitrile/methanol/ isopropyl alcohol (10:9:1 v/v/v) maintaining flow rate of 1 mL/min. The methanolic solution of the sample was injected (30 µL), and steryl ferulates were monitored at 325 nm, and *γ*-oryzanol was used as a standard for steryl ferulate quantification.

2.5 GC-MS Analysis

Phytochemical analysis of WB ethanol and n-hexane extracts was performed by GC-MS (GC-2010, Shimadzu Corporation, Kyoto, Japan) coupled with a mass spectrometer (GC-MS TQ 8030, Shimadzu Corporation, Kyoto, Japan). The inlet temperature was set at 250 ◦C and the column flow rate was 1 mL/min with Helium gas with a constant pressure of 53.5 kPa. The oven temperature was set at 50 ◦C (1 min), 200 ◦C (2 min), 300 ◦C (7 min). The temperature of the GC to MS interface

was 250 ◦C. The MS was set on a scan mode with a mass range of 50–600 m/z. The total running time for GC–MS was set for 40 min.

2.6 Anti-oxidant Assay

An antioxidant activity study was performed on WB ethanol and n-hexane extracts using nitric oxide radical scavenging assay and DPPH (2,2-diphenyl-1-picryl-hydrazyl-hydrate) free radical Scavenging Assay method.

2.6.1 Nitric Oxide radical ($NO^{\cdot}$) scavenging assay

Nitric oxide scavenging activity of both ethanol and n-hexane extract was measured as described by Alam et al. and Banerjee et al. [19, 20] . In this study, the reaction mixture contains 1mL sodium nitroprusside (10mM) in phosphate buffer saline and either 1 mL extract or ascorbic acid as standard (25 µg to 400 µg/mL). The reaction mixtures were incubated at 25ºC for 90 minutes. Then, after incubation, 0.5mL of Gries-Illosovoy reagent (1 % sulphanilamide and 5 %phosphoric acid) was added and allowed to stand for 7 minutes for diazotization of nitrite ions with sulphanilamide. Then 0.5 mL naphthyl ethylene diamine dihydrochloride (0.1%) was added, resulting in the formation of a pink-colored chromophore. The reaction mixture was allowed to stand at 25ºC for 5 minutes. Finally, the absorbance of the reaction mixtures was measured at 546nm, and the percentage of scavenging activity was calculated following the equation:

$$\textbf{\% Scavenging potential} = [(Abs_{control} - Abs_{extract}) / Abs_{control}] \times 100$$

The IC_{50} was calculated to represent the concentration of the WB extract that scavenged 50 % of nitric oxide radical.

2.6.2 DPPH Free Radical Scavenging Activity

DPPH free radical scavenging potential of WB extracts was determined following the method mentioned by Alam et al. and Ahmed et al. with slight modifications[16, 19]. Serially diluted WB extracts (25µg to 400 µg/mL) were mixed with 0.5 mL methanolic solution of DPPH (0.01 %) and kept in the dark for 30 minutes at room temperature. Finally, the absorbance of the reaction mixtures was measured at 517nm, and the percentage of scavenging activity was calculated following the equation:

$$\textbf{\% Scavenging potential} = [(Abs_{control} - Abs_{extract}) / Abs_{control}] \times 100$$

The IC_{50} was calculated as the plot of inhibition (%) against the concentration of the extract to represent the concentration of the WB extract that scavenged 50 %

of DPPH free radical. This experiment was carried out in triplicate, and ascorbic acid was used as the standard antioxidant.

2.7 Alpha-Amylase Inhibitory Assay

The α-amylase inhibitory assay was performed using a modified method of Kazeem et al. [13]. Serially diluted 250 μL WB extracts (25 µg to 400 µg/mL) were mixed with 250 μL of sodium phosphate buffer containing α-amylase solution (0.5 mg/mL) and incubated for 10 minutes at room temperature. Then 250 μL of sodium phosphate buffer containing 1 % starch solution was added to the reaction mixture and allowed to stand for 10 min at 25ºC. Thereafter, 500 μL dinitrosalicylic acid (DNS) reagent was added, and the reaction mixture was incubated in a hot water bath operated at 50ºC for 5 minutes. After 5 minutes, the test tubes containing reaction mixtures were cooled to room temperature and diluted with 5 mL distilled water. Finally, the absorbance of the reaction mixtures was measured at 540 nm, and the percentage of inhibitory activity was calculated following the equation:

$$\textbf{\% Inhibition} = [(Abs_{control} - Abs_{extract}) / Abs_{control}] \times 100$$

The IC_{50} was calculated the plot of inhibition (%) against the concentration of the extract to represent the concentration of the WB extract that inhibited 50 % of α-amylase. This experiment was carried out in triplicate and Acarbose was used as the standard α-amylase inhibitor.

Statistical Analysis:

Each experiment was performed in triplicate. Statistical analysis was performed using GraphPad Prism version 9 software (GraphPad Software, San Diego, CA, USA).

3. Results

HPLC-DAD analysis of bioactive polyphenols in WB

The chromatographic separation of polyphenolic compounds that are present in the ethanol extract of WB is shown in Figure-1. The chromatogram detects and confirms the presence of 3,4-dihydroxybenzoic acid, catechin hydrate, (-) epicatechin, caffeic acid, rutin hydrate, *p*-coumaric acid, trans-ferulic acid, rosmarinic acid, quercetin and kaempferol in WB ethanol extract. All of the identified phenolic compounds are reported to have strong antioxidant properties. The content of each phenolic compound found in the ethanol extract of WB was calculated from the corresponding calibration curve, as shown in **Table 1**.

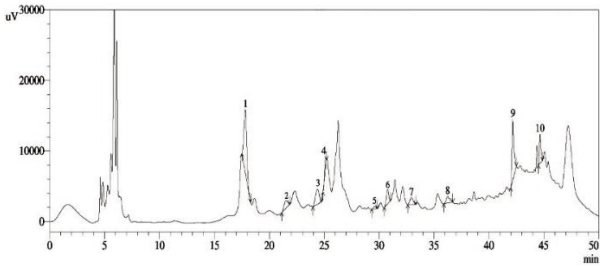

Figure 1. HPLC chromatogram of ethanol extract of WB**.** Peak: 1. 3,4-Dihydroxybenzoic acid; 2. Catechin hydrate; 3. (-) Epicatechin; 4. Caffeic acid; 5. Rutin hydrate; 6. p-Coumaric acid; 7. trans-Ferulic acid; 8. Rosmarinic acid; 9. Quercetin; and 10. Kaempferol

Table 1: Identification of polyphenolic compounds in ethanol extract of WB using HPLC-DAD

Polyphenolic Compounds	***Content (mg/100 g of the dry extract)***
3,4-Dihydroxybenzoic acid	16.03±0.15
Catechin hydrate	15.79±0.55
(-) Epicatechin	21.63±0.07
Caffeic acid	3.17±0.05
Rutin hydrate	1.01±0.04
p-*Coumaric acid*	2.86±0.07
trans-Ferulic acid	3.85±0.15
Rosmarinic acid	4.28±0.42
Quercetin	13.32±0.02
Kaempferol	3.09±0.15

3.2 Steryl ferulates in WB n-hexan extract

Total *γ*-oryzanol-like steryl ferulate content was estimated following the method described by Kumar et al [23,25] with some modifications. The chromatographic separation of steryl ferulate in *γ*-oryzanol as standard and ethanol extract of WB is shown in Fig. 2. The content of each steryl ferulate component found in the ethanol extract of WB was calculated from the corresponding calibration curve as mentioned in Table 2. Among 5 components of oryzanol [24], 24-methylene cycloartanyl ferulate (0.03±0.01 %), Campestanyl ferulate (0.22±0.01 %), and *β*-sitosteryl ferulate (0.16±0.01 %) are present.

Table 2: Contents of steryl ferulate components in n-hexane extract of *Triticum estivum* bran.

Peaks	Standard Compounds	% of Hexane extract of WB
1	Cycloartenyl ferulate	ND
2	24-methylene cycloartanyl ferulate	0.03±0.01
3	Campesteryl ferulate	ND
4	Campestanyl ferulate	0.22±0.01
5	*β*-sitosteryl ferulate	0.16±0.01

Values are expressed as mean±RSD. RSD: Relative Standard Deviation. ND: Not Detected

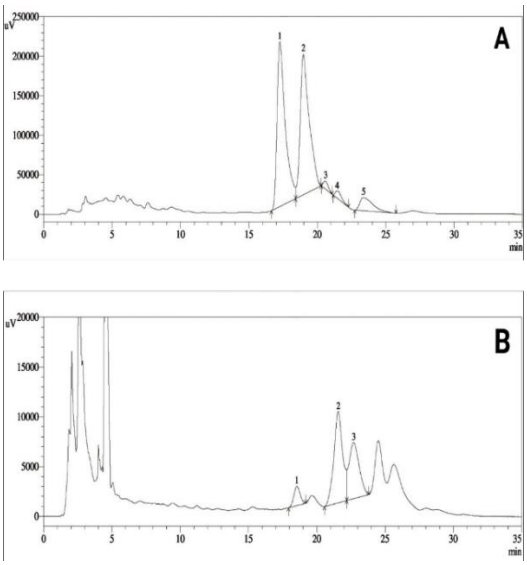

Figure 2. Chromatogram of steryl ferulate components. A) *γ*-oryzanol as standard; Peak 1. cycloartenyl ferulate; Peak 2. 24-methylene cycloartanyl ferulate; Peak 3. campesteryl ferulate; Peak 4. campestanyl ferulate Peak 5. *β*-sitosteryl ferulate B) n-hexan extract of WB; Peak 1. 24-methylene cycloartanyl ferulate; Peak 2. campesteryl ferulate; Peak 3. *β*-sitosteryl ferulate

3.2 GC-MS Analysis of WB extracts

Phytochemical analysis of both ethanol and n-hexane extract of WB was performed using GC-MS. The chromatographic separation of ethanol and n-hexane extract of WB is shown in Fig. 3 and Fig.4, respectively. The identified components are listed according to the order of their retention time. The identified components of ethanol extract of WB are listed in Table 3 and that of n-hexane in Table 4 respectively.

3.2.1 GC-MS Analysis of Triticum estivum bran ethanol extract

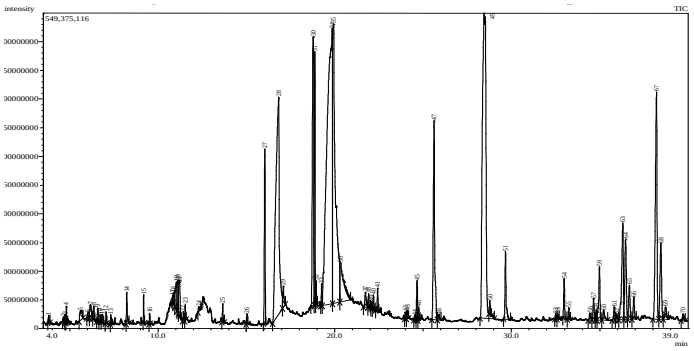

Figure 3: Chromatogram of ethanol extract of WB of GC-MS Analysis

Table 3: GC-MS Analysis of ethanol extract of WB.

SI No.	**Retention time (Min)**	**% Area**	**Tentative compound name**
1	3.805	0.09	Diglycerol
2	4.63	0.07	Cyclopentanone
3	4.742	0.08	Pyrrolidine
4	4.81	0.18	Cyclohexanone
5	5.616	0.31	2-Hydroxy-gamma-butyrolactone
6	6.03	0.13	2,5-Hexanediamine, 2,5-dimethyl-
7	6.175	0.31	Thiazole, 2-amino-5-methyl-
8	6.364	0.17	2,5-Dimethylfuran-3,4(2H,5H)-dione
9	6.584	0.15	1H-Azonine, octahydro-1-nitroso-
10	6.729	0.06	Phenol, 2-methoxy-
11	6.831	0.13	3-Butene-1,2-diol
12	7.054	0.09	Phenylethyl Alcohol
13	7.325	0.06	Methyl nicotinate
14	8.233	0.36	1-Ethyl-2-hydroxymethylimidazole

15	9.185	0.19	2-Methoxy-4-vinylphenol
16	9.518	0.06	Phenol, 2,6-dimethoxy-
17	10.82	0.07	1H-Benzotriazole, 5-methyl-
18	10.865	0.28	Apocynin
19	11.04	0.59	Beta-D-Glucopyranose, 4-O-.beta.-D-galactopyranosyl-
20	11.12	0.52	1,3,2-Dioxaphosphorinane, 2-(2-methoxyethoxy)-5,5-dimethyl-
21	11.215	0.75	d-Mannitol, 1,4-anhydro-
22	11.431	0.09	Dodecanoic acid
23	11.541	0.11	3',5'-Dimethoxyacetophenone
24	12.295	0.07	d-Glycero-d-ido-heptose
25	13.658	0.18	Tetradecanoic acid
26	15.028	0.1	Pentadecanoic acid
27	16.043	2.03	Octadecanoic acid, 3-hydroxy-2-tetradecyl-, methyl ester, (2R,3R)-
28	16.83	10.92	n-Hexadecanoic acid
29	17.089	0.33	Hexadecanoic acid, ethyl ester
30	18.784	5.23	6,9-Octadecadienoic acid, methyl ester
31	18.874	2.92	9-Octadecenoic acid, methyl ester, (E)-
32	18.944	0.21	9-Octadecenoic acid, methyl ester, (E)-
33	19.259	0.21	Methyl stearate
34	19.85	21.22	9-Octadecynoic acid
35	19.934	11.06	9-Octadecenoic acid (Z)-, hexadecyl ester

36	20.34	1.98	2-Methyl-5-(2,6,6-trimethyl-cyclohex-1-enyl)-pentane-2,3-diol
37	21.733	0.3	5,5,8a-Trimethyl-3,5,6,7,8,8a-hexahydro-2H-chromene
38	21.915	0.16	S-[2-[N,N-Dimethylamino]ethyl]N,N-dimethylcarbamoyl thiocarbohydroximate
39	22.094	0.08	Glycidyl palmitate
40	22.187	0.19	11-Eicosenoic acid, methyl ester
41	22.424	0.27	3-Octene-2,5-dione, 6,6,7-trimethyl-, (E)-
42	23.996	0.1	Linoleic acid ethyl ester
43	24.117	0.11	6,9-Octadecadienoic acid, methyl ester
44	24.54	0.07	9-Octadecenoic acid, 12-hydroxy-, methyl ester, [R-(Z)]-
45	24.659	0.52	endo-2-Methyl-2-norbornanol
46	24.742	0.17	Cyclohexylmethyl S-2-(dimethylamino)ethyl propylphosphonothiolate
47	25.623	4.09	Hexadecanoic acid, 2-hydroxy-1-(hydroxymethyl)ethyl ester
48	25.92	0.12	Bis(2-ethylhexyl) phthalate
49	28.453	15.48	E,E,Z-1,3,12-Nonadecatriene-5,14-diol
50	28.776	0.16	Octadecanoic acid, 2,3-dihydroxypropyl ester
51	29.664	1.04	cis-11-Eicosenamide

52	32.51	0.07	Palmitic acid vinyl ester
53	32.62	0.06	(Z)-5-(Pentadec-8-en-1-yl)benzene-1,3-diol
54	32.981	0.52	Phosphite, diisopropylmenthyl-
55	33.242	0.15	beta.-Tocopherol
56	34.437	0.13	i-Propyl 5,9,17-hexacosatrienoate
57	34.645	0.38	Vitamin E
58	34.804	0.19	Undec-10-ynoic acid, 3-methylbut-2-en-1-yl ester
59	34.979	0.98	(R)-2,7,8-Trimethyl-2-((3E,7E)-4,8,12-trimethyltrideca-3,7,11-trien-1-yl)chroman-6-ol
60	35.217	0.22	Trilinolein
61	35.817	0.24	(Z)-5-(Pentadec-8-en-1-yl)benzene-1,3-diol
62	35.96	0.12	(Z)-5-(Pentadec-8-en-1-yl)benzene-1,3-diol
63	36.304	2.39	2-Dodecen-1-yl(-)succinic anhydride
64	36.462	1.76	Campesterol
65	36.673	0.67	Ergostanol
66	36.928	0.38	Stigmasterol
67	38.208	5.4	*γ*-Sitosterol
68	38.456	1.73	Stigmastanol
69	38.72	0.31	Methoxyolivetol
70	39.718	0.13	16-Allopregnen-3.beta.,7.alpha.-diol-20-one

From these GC-MS chromatograms and peak report of WB ethanol extract, a large number of secondary metabolites have been identified that include Ethyl linolenate, phtysterols, components of oryzanol like steryl ferulate: Campesterol, Stigmasterol, *β*-sitosterol, *γ* -sitosterol, lower levels of apocynin, vitamin E, *β*-tocopherol, and so on.

3.2.1 GC-MS Analysis of Triticum estivum bran n-hexane extract.

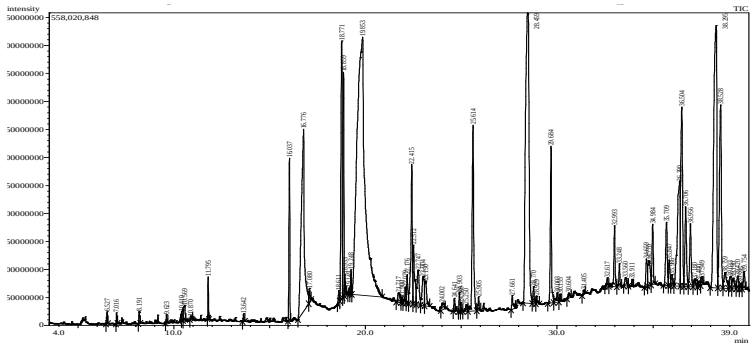

Figure 4: Chromatogram of n-hexane extract of *Triticum estivum* bran of GC-MS Analysis.

From these GC-MS chromatograms and peak report of WB n-hexane extract, a large number of secondary metabolites have been identified that include phtysterols, lower levels of *β*-tocopherol, components of oryzanol like steryl ferulate: campesterol, stigmasterol, *β*-sitosterol, *γ* -sitosterol, and so on.

Table 4: GC-MS Analysis of n-hexane extract of WB.

SI No.	**Retention time (Min)**	**% Area**	**Tentative compound name**
1	6.527	0.12	Thymine
2	7.016	0.06	Phenylethyl alcohol
3	8.191	0.12	5-hydroxymethylfurfural
4	9.623	0.07	Sulfurous acid, cyclohexylmethyl hexadecyl ester
5	10.41	0.16	Naphthalene, 1,7-dimethyl-
6	10.569	0.31	Sucrose

7	10.87	0.06	Alpha.-d-glucopyranose, 4-o-.beta.-d-galactopyranosyl-
8	11.795	0.3	Phthalic acid, di-(1-hexen-5-yl) ester
9	13.642	0.06	Tetradecanoic acid
10	16.037	1.67	Octadecanoic acid, 3-hydroxy-2-tetradecyl-, methyl ester (2R,3R)
11	16.776	6.76	1,2,4-Trioxolane-2-octanoic acid, 5-octyl-, methyl ester
12	17.08	0.19	Hexadecanoic acid, ethyl ester
13	18.611	0.13	N-Nonadecanol-1
14	18.771	3.99	Cyclopropanebutyric acid, 2-[(2-nonylcyclopropyl)methyl]-, methyl ester
15	18.859	2.33	9-Octadecenoic acid, methyl ester, (E)-
16	18.933	0.19	9-Octadecenoic acid, methyl ester, (E)-
17	19.149	0.07	Octadecanoic acid, 7-hydroxy-, methyl ester
18	19.248	0.23	Heptadecanoic acid, 16-methyl-, methyl ester
19	19.853	25.04	E,E,Z-1,3,12-Nonadecatriene-5,14-diol
20	21.717	0.23	5-heptylresorcinol
21	21.9	0.08	3-Cyclopentylpropionic acid, 2-dimethylaminoethyl ester
22	22.079	0.24	Glycidyl palmitate
23	22.176	0.44	11-Eicosenoic acid methyl ester
24	22.415	2.33	2-Myristynoic acid
25	22.512	1.15	Palmidrol
26	22.747	0.93	1-Butanone, 4-nitro-1-2-oxocyclohexyl
27	23.004	0.82	1-Butanone, 4-nitro-1-2-oxocyclohexyl

28	23.15	0.52	3H,8H-Dipyrrolo[1,2-a:2,1-b]imidazole-3,8-dione, hexahydro
29	24.002	0.2	Pentyl linoleate
30	24.641	0.15	Carbamic acid, 2-(dimethylamino)ethyl ester
31	24.903	0.21	Bicyclo[10.1.0]tridec-1-ene
32	24.98	0.11	Glycidyl oleate
33	25.25	0.15	Glycidyl oleate
34	25.614	3.55	Hexadecanoic acid, 2-hydroxy-1-(hydroxymethyl)ethyl ester
35	25.905	0.21	Bis(2-ethylhexyl) phthalate
36	27.661	0.22	Cyclopropane, 1,1-dichloro-2,2,3,3-tetramethyl-
37	28.459	12.02	E,E,Z-1,3,12-Nonadecatriene-5,14-diol
38	28.77	0.26	Octadecanoic acid, 2,3-dihydroxypropyl ester
39	28.929	0.12	Triacontanoic acid, methyl ester
40	29.684	2.2	6-Octadecenoic acid
41	30.003	0.22	Tetradecanamide
42	30.155	0.1	Squalene
43	30.604	0.1	Alpha-tocospiro A
44	31.405	0.06	17-pentatriacontene
45	32.617	0.14	(Z)-5-(Pentadec-8-en-1-yl)benzene-1,3-diol
46	32.993	0.89	3-(1-Methylhept-1-enyl)-5-methyl-2,5-dihydrofuran-2-one
47	33.248	0.32	Beta-tocopherol
48	33.56	0.19	Propanoic acid, 3,3'-thiobis-, didodecyl ester
49	33.911	0.1	Cholesta-4,6-dien-3-ol, 3.beta

50	34.659	0.51	Vitamin E
51	34.77	0.72	1-Butanone, 1-bicyclo[4.1.0]hept-7-yl-
52	34.984	0.89	(R)-2,7,8-Trimethyl-2-((3E,7E)-4,8,12-trimethyltrideca-3,7,11-trien-1-yl)chroman-6-ol
53	35.709	1.22	4-Methyl-2,2,4-tris(4'-methoxyphenyl)pentane
54	35.847	0.44	3H,8H-Dipyrrolo[1,2-a:2,1-b]imidazole-3,8-dione, hexahydro
55	35.986	0.22	(Z)-5-(Pentadec-8-en-1-yl)benzene-1,3-diol
56	36.39	3.65	Butylphosphonic acid, ethyl neopentyl ester
57	36.504	3.65	Campesterol
58	36.706	1.58	Ergostanol
59	36.956	1.16	Stigmasterol
60	37.18	0.19	7,8-Epoxylanostan-11-ol, 3-acetoxy-
61	37.4	0.11	16-Allopregnen-3.beta.,7.alpha.-diol-20-one
62	37.549	0.17	Ergost-7-en-3-ol, (3.beta)
63	38.295	9.4	Gamma-sitosterol
64	38.528	4.2	Stigmastanol
65	38.759	0.5	Cyclopropa[5,6] stigmast-22-en-3-ol, 3',6-dihydro-, (3.beta.,5.beta.,6.alpha.,22E)-
66	39.033	0.29	Stigmasta-5,24(28)-dien-3-ol, (3.beta.)-
67	39.19	0.29	Beta-amyrin
68	39.42	0.26	Beta-sitosterol
69	39.595	0.11	4,22-Stigmastadiene-3-one
70	39.754	0.32	33-Norgorgosta-5,24(28)-dien-3-ol, (3.beta)

3.2 Antioxidant activity of WB extracts

Antioxidant activity study was performed on WB ethanol and n-hexane extracts using Nitric Oxide Radical Scavenging Assay and DPPH (2,2-diphenyl-1-picryl-hydrazyl-hydrate) free radical Scavenging Assay method. IC_{50} values were calculated in comparison to the concentration of standard or bran extract required to scavenge 50 % of the free radicals.

3.2.1 Nitric Oxide Radical Scavenging Activity

In this study, Sodium nitroprusside was used, which produces nitric oxide radicals that have a strong oxidizing ability and can alter cellular structure as well as function. The scavenging activity of WB extracts on nitric oxide production was determined following previously mentioned methods [10, 19] and graphically represented in Figure 5.

Both ethanol and n-hexane extract of WB exhibited significant nitric oxide radical scavenging activity, resulting in the reduction of the NO- concentration in the assay medium. The graph shows that the scavenging activity of WB extracts on Nitric oxide production was found to increase in a concentration-dependent manner. The IC_{50} values for nitric oxide scavenging ability of WB extracts are listed in **Table 5.**

Table 5: IC_{50} values for nitric oxide scavenging ability of WB extracts and ascorbic acid as standard.

Sample	IC_{50} (µg/mL)
WB n-Hexane extract	55.51
WB ethanol extract	51.38
Ascorbic acid	25.64

Among 2 extracts of WB, ethanol extract has lower IC_{50} value of 51.38 µg/mL with significant nitric oxide radical scavenging potential compared to the IC_{50} value of WB n-Hexane extract.

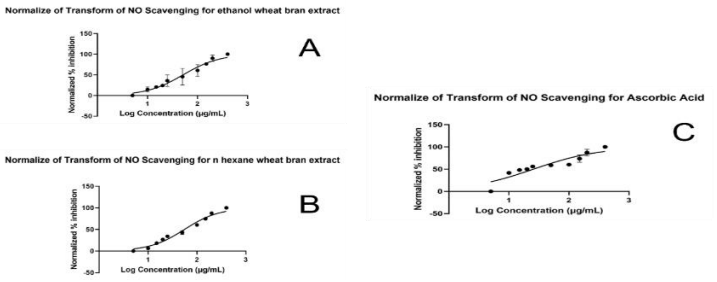

Figure 5: Nitric oxide scavenging ability of WB extracts and ascorbic acid as standard.

3.2.2 DPPH Free Radical Scavenging Activity

In the DPPH assay, 2,2-diphenyl-1-picrylhydrazyl, DPPH free radical forms a violet-colored solution, which is subsequently reduced in the presence of antioxidant to a colorless solution, 1,1-diphenyl-2-picryl hydrazine in a concentration-dependent manner. The scavenging activity of WB extracts on DPPH free radical was determined following previously mentioned methods [10, 19] and graphically represented in Figure 6.

Both ethanol and n-hexane extract of WB exhibited significant DPPH free radical scavenging activity, resulting in a colorless solution. Graphically, the DPPH free radical scavenging activity of WB extracts and Ascorbic acid as standard were found to be increased in a concentration-dependent manner. We list the IC_{50} values for the DPPH free radical scavenging potential of WB extracts in Table 6. The ethanolic and n-hexane extract of WB has an IC_{50} value of 39 µg/mL and 42.99 µg/mL, respectively, whereas the standard ascorbic acid has an IC_{50} value of 14.57 µg/mL.

Table 6: IC_{50} values for DPPH free radical scavenging ability of *T.estivum* bran extracts and Ascorbic acid as standard.

Sample	IC_{50} (µg/mL)
WB n-Hexane extract	42.99
WB ethanol extract	39.00
Ascorbic acid	14.57

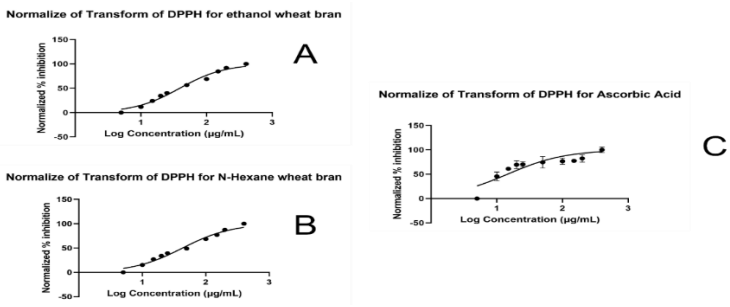

Figure 6: DPPH free radical scavenging ability of *T. estivum* bran extracts and Ascorbic acid as standard.

3.2.3 *α-amylase inhibitory activity*

Alpha-amylase inhibitory activity of the WB extracts was determined following previously mentioned methods [13] and graphically represented in Figure 7. At lower concentrations, both of the extracts showed no significant difference in the inhibition of *α*- amylase. Graphically, *α*-amylase inhibitory activity of WB extracts and acarbose as standard were found to be increased in a concentration-

depended manner. The IC_{50} values for α-amylase inhibitory potential of WB extracts are listed in **Table 7.**

Table 7: IC_{50} values for α-amylase inhibitory activity of *T. estivum* bran extracts and Acarbose as standard.

Sample	IC_{50} (µg/mL)
WB n-Hexane extract	41.45
WB ethanol extract	61.97
Acarbose	35.80

Both ethanol and n- hexane extract of WB has higher IC_{50} value of 61.97 µg/mL and 41.45 µg/mL respectively in comparison to the IC_{50} value of Acarbose (35.80 µg/mL) as standard.

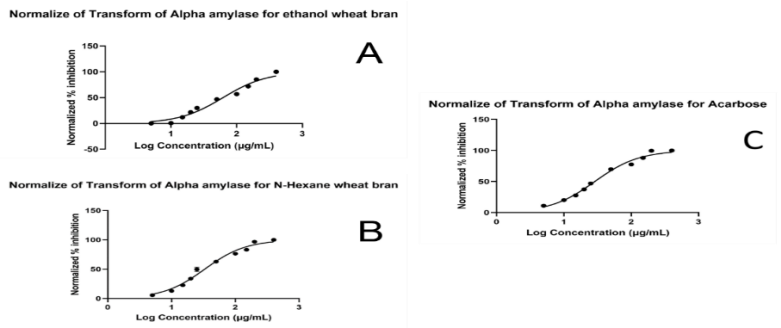

Figure 7: α-amylase inhibitory activity of WB extracts and Acarbose as standard.

4. Discussion

The aim of the study is to identify and determine the content of polyphenol in WB through HPLC and GC-MS and measure its antioxidant and anti-diabetic potential. Antioxidant activity was analyzed using nitric oxide radical scavenging assay and DPPH (2,2-diphenyl-1-picryl-hydrazyl-hydrate) free radical scavenging assay on both ethanol and n-hexane WB extracts. Anti-diabetic potential of WB extract was measured by its inhibitory effect on α-amylase.

HPLC profiling of WB ethanol extract reveals that it contains 3,4-dihydroxybenzoic acid, catechin hydrate, (-) epicatechin, caffeic acid, rutin hydrate, *p*-coumaric acid, trans-ferulic acid, rosmarinic acid, quercetin and kaempferol, which are similar with the findings reported by Zhou et al. [2]. The content of 3,4-dihydroxybenzoic acid is highest and is 16.03±0.15 mg whereas rutin hydrate content is the lowest and 1.01±0.04 g per 100 g of dry extract among 10

identified polyphenolic compounds. The total content of selected polyphenolic compounds was 85.03 mg per 100 g of dry extract which clarifies the reason behind its antioxidant potential.

Total *γ*-oryzanol-like steryl ferulate content was estimated and among 5 components of oryzanol [21], 24-methylene cycloartanyl ferulate (0.03±0.01 %), Campestanyl ferulate (0.22±0.01 %) and *β*-sitosteryl ferulate (0.16±0.01 %) is present, and this finding is similar to the HPLC findings of Kumar et al. [17]. Kumar et al. found 3 major peaks from the HPLC chromatogram of WB oil but with a notable quantity. Previous studies of Talawar et al, [22] also reported higher content of total *γ*-oryzanol-like steryl ferulate compared to the reports of Moreau et al. [23] and Rebolleda et al. [9]. The previous report also summarized that *γ*-oryzanol-like steryl ferulate is associated with several significant beneficial health effects such as antioxidant properties, hypocholesterolemic effect etc. [24].

Phytochemical analysis of both ethanol and n-hexane extract of WB was performed using GC-MS. GC-MS chromatograms and peak report of WB ethanol extract, ethyl linolenate, phtysterols, components of oryzanol like steryl ferulate: Campesterol, Stigmasterol, *β*-sitosterol, *γ* -sitosterol, lower levels of apocynin, vitamin E, *β*-tocopherol, and many more are identified, whereas from GC-MS chromatograms of WB n-hexane extract, phtysterols, lower levels of *β*-tocopherol, components of oryzanol like steryl ferulate: campesterol, stigmasterol, *β*-sitosterol, *γ* -sitosterol, and many more are identified. The presence of oryzanol like steryl ferulate gives clarity to the reports of HPLC profiling of steryl ferulate. Between ethanol and n-hexane extract of WB, n-hexane extract contains higher amount of steryl ferulates (18.67 % area) than that of in ethanol extract (9.27 % area) which is less than half of the n-hexane extract of WB.

Reactive nitrogen species causes cellular damage and dysfunction and thus leads to tissue toxicity and inflammatory conditions. Suppression of $NO^{\cdot}$ release or scavenging of $NO^{\cdot}$ can reduce the load of reactive nitrogen species. Both extracts reduced the amount of nitrite generated from sodium nitroprusside and the scavenging potential was found to increase in concentration dependent manner.

DPPH (2,2-diphenyl-1-picrylhydrazyl), is a stable free radical and in the DPPH assay, DPPH free radical forms a violet-colored solution which is subsequently reduced to 1,1-diphenyl-2-picryl hydrazine (colorless solution) in the presence of antioxidant either due to transfer an electron or hydrogen atom to DPPH. Both ethanol and n-hexane extract of WB exhibited significant DPPH free radical scavenging activity resulting in colorless solution. DPPH free radical scavenging activity of WB extracts and ascorbic acid, as standard, were found to be increased in a concentration-depended manner. The ethanolic and n- hexane extract of WB has IC_{50} value of 39 µg/mL and 42.99 µg/mL respectively, whereas the standard ascorbic acid has IC_{50} value of 14.57 µg/mL. Lower value of IC_{50} of WB ethanol extract indicates that it contains greater quantity of phytochemicals with antioxidant properties than in the n-hexane extract. IC_{50} value of both extracts are not too high

in comparison with that of ascorbic acid, suggesting the presence of significant antioxidant potential of WB.

With the development of modern medicine, many naturally occurring medicinal plants have been identified as a good source of beneficial and nutritional health effects as well as pharmacological activities. α- amylase is one of the important digestive enzymes, found in saliva and pancreatic juice, involved in hydrolyzing glyosidic bond thus breaking down insoluble starch molecules into smaller absorbable molecules such as glucose, dextrin, maltose. Inhibitors of α-amylase delay or inhibit the breakdown of starch by blockade of site of the α-amylase. Alpha-amylase inhibitors play significant role in lowering postprandial blood glucose level. We observed that at lower concentrations, both of the extracts showed no significant difference in the inhibition of α- amylase. With the increase in the concentration of WB extracts, α-amylase inhibitory activity of *T. estivum* bran extracts and acarbose as standard were found to be increased in a concentration-depended manner. Both ethanol and n- hexane extract of WB has higher IC_{50} value of 61.97 µg/mL and 41.45 µg/mL respectively in comparison to the IC_{50} value of acarbose (35.80 µg/mL) as standard. IC_{50} value of n-hexane extracts is not too high as opposed to that of acarbose, suggesting that it can be given attention for α-amylase inhibitory potential.

5. Conclusions

HPLC-profiling showed the presence of several phenols, including ferulic acid and caffeic acid, which are associated with antioxidant and anti-inflammatory activities. Total γ-oryzanol-like steryl ferulate content was estimated, and among 5 components of oryzanol, 24-methylene cycloartanyl ferulate, campestanyl ferulate, and β-sitosteryl ferulate were identified. Both ethanol and n-hexane extract of WB exerted antioxidant activities. Out of two extracts, WB n-hexane extract displayed moderate inhibition of the α-amylase enzyme. In conclusion, the presence of a notable number of antioxidants in WB may considered suitable for addition to diet as an alternative means of preventing chronic diseases such as cardiovascular disease, cancer, and type 2 diabetes.

Author Contributions: Conceptualization-MA, MAA, NS; resources- MAA, NS; experiments- MA, NA, MJR, KSA, HPLC analysis- KSA, HH; data analysis- MAA, HH, NS; writing—original draft preparation-MA, NA, MJR; writing—review and editing- MAA, NS, MJR. All authors have read and agreed to the published version of the manuscript.

Funding:

This research work received no dedicated funding from agencies in public, private or non-profit sectors. Experiments were performed in the Department of Pharmaceutical Sciences at North South University, Bangladesh.

Institutional Review Board Statement:

This study is only based on *in vitro* experiments. No animals were used in any experiment.

Data Availability Statement:

All data are availed in the result section of this manuscript.

Acknowledgments:

The authors are thankful to the authority of Department of Pharmaceutical Sciences, North South University, Bangladesh for the providing facilities for present work.

Conflicts of Interest:

The authors declared no potential conflict of interests with respect to the research, authorship, and/or publication of this paper.

References

1. Pizzino, G., Irrera, N., Cucinotta, M., Pallio, G., Mannino, F., Arcoraci, V., Squadrito, F., Altavilla, D., Bitto, A. Oxidative stress: harms and benefits for human health. *Oxid. Med. Cell Longev*. 2017; 2017: 8416763.

2. Zhou, K., L. Su, and L.L. Yu, Phytochemicals and antioxidant properties in WB. *J. Agric. Food Chem.* 2004. 52(20): 6108-14.

3. Awah, F.M., Antioxidant activity, nitric oxide scavenging activity and phenolic contents of *Ocimum gratissimum* leaf extract. *J. Med. Plants Res.* 2010; 4(23): 2479-2487.

4. Onipe, O.O., Jideani A.I.O., Beswa D., Composition and functionality of WB and its application in some cereal food products. *Int. J. Food Sci. Technol.* 2015; 50(12): 2509-2518.

5. Wilson, T. A., Nicolosi, R. J., Woolfrey, B., & Kritchevsky, D. Rice bran oil and oryzanol reduce plasma lipid and lipoprotein cholesterol concentrations and aortic cholesterol ester accumulation to a greater extent than ferulic acid in hypercholesterolemic hamsters. *J. Nutr. Biochem.* 2007; 18(2):105-112.

6. Yasukawa, K., Akihisa, T., Kimura, Y., Tamura, T., Takido, M. Inhibitory effect of cycloartenol ferulate, a component of rice bran, on tumor promotion in two-stage carcinogenesis in mouse skin. *Biol. Pharm. Bull.* 1998; 21(10): 1072-1076.

7. Zhou, K. and L. Yu, Effects of extraction solvent on WB antioxidant activity estimation. *LWT - Food Sci. Technol.* 2004; 37(7): 717-721.

8. Hakala, P., Lampi, A. M., Ollilainen, V., Werner, U., Murkovic, M., Wähälä, K., Karkola, S., Piironen, V. Steryl phenolic acid esters in cereals and their milling fractions. *J. Agric. Food Chem.* 2002; 50(19): 5300-5307.

9. Rebolleda, S., José, M. L. G., Sanz, M. T., Beltrán, S., Solaesa, Á. G. Bioactive compounds of a wheat bran oily extract obtained with supercritical carbon dioxide. Foods, 2020; 9(5): 625.

10. Berger, A., Rein, D., Schäfer, A., Monnard, I., Gremaud, G., Lambelet, P., Bertoli, C. Similar cholesterol-lowering properties of rice bran oil, with varied gamma-oryzanol, in mildly hypercholesterolemic men. *Eur. J. Nutr.* 2005. 44(3): 163-173.

11. Son, M. J., Rico, C. W., Nam, S. H., Kang, M. Y. Effect of oryzanol and ferulic acid on the glucose metabolism of mice fed with a high-fat diet. *J. Food. Sci.* 2011; 76(1): H7-H10.

12. Peyrot des Gachons, C., Breslin P.A. Salivary amylase: digestion and metabolic syndrome. *Curr. Diab. Rep.* 2016; 16(10): 102.

13. Kazeem, M.I., Adamson, J.O., Ogunwande, I.A. Modes of inhibition of alpha -amylase and alpha -glucosidase by aqueous extract of *Morinda lucida* Benth leaf. *Biomed. Res. Int.* 2013; 2013: 527570.

14. Kaur, N., Kumar, V., Nayak, S. K., Wadhwa, P., Kaur, P., Sahu, S. K. Alpha-amylase as molecular target for treatment of diabetes mellitus: a comprehensive review. *Chem. Biol. Drug Des.* 2021; 98(4): 539-560.

15. Tu, J., Chen, J., Zhu, S., Zhang, C., Chen, H., Liu, Y. Inhibition of wheat bran and it's active components on α-glucosidase *in vitro*. *Pharmacogn. Mag.* 2013; 9(36): 309-314.

16. Ahmed, K., Jahan, I., Jahan, F., Hosain, H. Antioxidant activities and simultaneous HPLC-DAD profiling of polyphenolic compounds from *Moringa oleifera* Lam. *Food Res.* 2021; 5(1): 401-408.

17. Kumar, G.S., Krishna, A.G. Studies on the nutraceuticals composition of wheat derived oils wheat bran oil and wheat germ oil. *J. Food Sci. Technol*. 2015; 52(2): 1145-1151.

18. Krishna, A. G., Khatoon, S., Shiela, P. M., Sarmandal, C. V., Indira, T. N., Mishra, A. Effect of refining of crude rice bran oil on the retention of oryzanol in the refined oil. *J. Am. Oil Chem. Soc.* 2001; 78(2): p. 127-131.

19. Alam, M.A., Ghani, A., Subhan, N., Rahman, M.M., Haque, M.S., Majumder, M.M., Majumder, M.E.H., Akter, R.A., Nahar, L. Sarker, S.D. Antioxidant and membrane stabilizing properties of the flowering tops of *Anthocephalus cadamba*. *Nat. Prod. Commun.* 2008; 3(1): 1934578X0800300114.

20. Banerjee, S., Chanda, A., Ghoshal, A., Debnath, R., Chakraborty, S., Saha, R., Das, A. Nitric oxide scavenging activity study of ethanolic extracts of from two different areas of kolkata. *Asian J. Exp. Biol. Sci.* 2011; 2: 595-599.

21. Narayan, A.V., Barhate R.S., Raghavarao K.S.M.S. Extraction and purification of oryzanol from rice bran oil and rice bran oil soapstock. *J. Am. Oil Chem. Soc.* 2006; 83(8): 663-670.

22. Talawar, S. T., Harohally, N. V., Ramakrishna, C., Suresh Kumar, G. Development of wheat bran oil concentrates rich in bioactives with antioxidant and hypolipidemic properties. *J. Agr. Food Chem.* 2017; 65(45): 9838-9848.

23. Moreau, R.A., Powell, M.J., Hicks, K.B. Extraction and quantitative analysis of oil from commercial corn fiber. *J. Agr. Food Chem.* 1996; 44(8): 2149-2154.

24. Ramazani, E., Akaberi, M., Emami, S. A., Tayarani-Najaran, Z. Biological and pharmacological effects of gamma-oryzanol: an updated review of the molecular mechanisms. *Curr. Pharm. Des.* 2021; 27(19): 2299-2316.

Guide for Authors

Journal of Biosciences and Experimental Pharmacology is a peer-reviewed journal that covers all aspects of Life sciences. Categories of contribution for the journal are Communications, Full length Research article, Review articles, and Progress reports. All types of articles should represent novel research and significant advances in the field of life science. Only manuscripts in English are accepted. Contributors should bear in mind the interdisciplinary nature of the readership, always emphasizing the importance of the topic to the life science research community on the whole. Reprints and PDF files can be ordered when the proofs of a manuscript are returned to the publisher. Reprint rates are available from the Editorial Office on request.

Manuscript Submission

The manuscript should be submitted online *via* e-mail to editor or the online submission service. In order to submit a manuscript you will need a single Microsoft Word, RTF, or PDF file that contains the text, all figures and tables, and any Supporting Information associated with the manuscript. MS Word templates for Research article, Reviews, Progress Reports, and Communications are available on request to editor by e-mail or the homepage in the section "Author Guidelines". Please use these templates for submission of your contribution.
Journal of Biosciences and Experimental Pharmacology does not publish manuscripts that have already appeared in print or electronically (including those deposited in preprint archives).
The author must inform the editor of manuscripts submitted, soon to be submitted, or in press at other journals that have a bearing on the manuscript being submitted to *Journal of Biosciences and Experimental Pharmacology*. In particular, authors should reveal all sources of funding for the work presented in the manuscript and should declare any conflict of interest. To ensure continuity of contact details, the corresponding author of a manuscript should hold a permanent academic and or research position. Exceptions may be made at the discretion of the Editorial Office.

Confirmation of Receipt/Assessment

Authors of all articles will receive acknowledgement of receipt of their manuscript (by email). All contributions are subject to assessment by the editors and/or refereeing.

Manuscript for Production

If a manuscript is accepted, the file supplied at manuscript submission (or revision if applicable) will be used for production. The data therefore must be the FINAL version. Costs for any additions or further changes made during correction of the page proofs may be charged to the author. **Tables** should be included in the text files and follow the example laid out in the template. **Vector graphic images** such as plots, graphs, and line diagrams (including chemical structures) should be imported into a Word file. Original files of graphical items prepared using ChemDraw or Photoshop may also be included. **Bitmap graphic images** such as photographs and electron microscope images should be saved as TIFF files; each figure part must have a resolution of at least 300 dpi (1000 pixels wide when the image is printed at a single column width).

Supporting Information in the form of additional figures, experimental details, and so on may accompany a manuscript, and will be published online only. This material will not be edited, so should be error free. Supporting Information pages must be prepared as a single MS Word document and should be submitted as a separate file with all figures incorporated into the text.

Guidelines for the Preparation of Manuscripts

Authors are requested to take special care with the following points when preparing manuscripts for Journal of Bioscience and Pharmaceutics:

a) **Manuscripts** should be typed with double-line spacing (about 60 characters per line and about 26 lines per page; large script; Greek letters in the character font Symbol; special characters must be clearly recognizable; sub- or superscripts, italics, or boldface should be clearly distinguishable); this holds for all parts of the manuscript, including those that will be printed in smaller type, and also for the printed version of an electronic manuscript. Page Layout should be A4 size (8.27" x 11.69") of each page. All pages, including those with the references, tables, and legends, must be numbered (Page: 1, Page: 2…) consecutively.

American-style English spelling should be used throughout the manuscript.

b) **The title**, which should be as succinct as possible. The first letters of all words, except coordinating conjunctions, articles, and prepositions, should be capitalized. No references should be used.

Then follows the first name, other initials, and surname of each author, and an asterisk to indicate each corresponding author. Use digit superscript number (X [1], Y [2], Z [3] …) to indicate the affiliation(s) of the author(s)).

The names of all authors according to research group (with academic title and all first names as initials), the complete postal address, and e-mail address of the corresponding author(s) appear after the author byline. For all other authors, only the address of their academic institution or company is required.

c) References

References must be numbered in order of appearance in the text (including citations in tables and legends) and listed individually at the end of the manuscript. We recommend preparing the references with a bibliography software package, such as EndNote, Reference Manager or Zotero to avoid typing mistakes and duplicated references. Include the digital object identifier (DOI) for all references where available.

Citations and references in the Supplementary Materials are permitted provided that they also appear in the reference list here. In the text, reference numbers should be placed in square brackets [ ] and placed before the punctuation; for example [1], [1–3] or [1,3]. For embedded citations in the text with pagination, use both parentheses and brackets to indicate the reference number and page numbers; for example [5] (p. 10), or [6] (pp. 101–105).

1. Author 1, A.B.; Author 2, C.D. Title of the article. *Abbreviated Journal Name* **Year**, *Volume*, page range.
2. Author 1, A.; Author 2, B. Title of the chapter. In *Book Title*, 2nd ed.; Editor 1, A., Editor 2, B., Eds.; Publisher: Publisher Location, Country, 2007; Volume 3, pp. 154–196.
3. Author 1, A.; Author 2, B. *Book Title*, 3rd ed.; Publisher: Publisher Location, Country, 2008; pp. 154–196.
4. Author 1, A.B.; Author 2, C. Title of Unpublished Work. *Abbreviated Journal Name* year, *phrase indicating stage of publication (submitted; accepted; in press)*.
5. Author 1, A.B. (University, City, State, Country); Author 2, C. (Institute, City, State, Country). Personal communication, 2012.
6. Author 1, A.B.; Author 2, C.D.; Author 3, E.F. Title of Presentation. In Proceedings of the Name of the Conference, Location of Conference, Country, Date of Conference (Day Month Year).
7. Author 1, A.B. Title of Thesis. Level of Thesis, Degree-Granting University, Location of University, Date of Completion.
8. Title of Site. Available online: URL (accessed on Day Month Year).

d) **Tables** should be provided with a brief legend (use the word "Table" throughout the text unabbreviated) and should only be subdivided by three horizontal lines (head rule, neck rule, foot rule). Tables with only one or two columns and columns with only one or two entries are to be avoided. For footnotes in Tables, Roman lowercase letters followed by a closing parenthesis are to be used. All tables are to be numbered (Arabic numerals) in the sequence in
which they are referred to in the text. Physical data for several compounds should be summarized in a Table; otherwise, a footnote is sufficient.

e) **Each figure** and scheme should have a caption, and these should be listed together in numerical order after the references. All figures and schemes should be mentioned in the text in numerical order. For peer-review, it is preferred to have the figures and schemes appear as they are mentioned in the text. Different types of atoms in structural chemistry figures should
be clearly distinguishable (by different graphical shading). Use the full word "Figure" in all parts of the manuscript.

Symbols of physical quantities, but not their units (e.g., ***T*** (for temperature, in contrast to T for the unit Tesla), but K as unit; ***J***, but Hz; a, but nm), stereochemical information (cis, *E*, *R*, etc.; D), locants (*N*-methyl), symmetry groups and space groups (C_{2v}), and prefixes in formulae or compound names such as *t*Bu and *tert*-butyl must be in italics, and formula numbers in boldface (Arabic numerals and, if necessary, Roman lowercase letters). Labels of axes are to be separated from their units by a slash: e.g., *T*/K; the ordinate should be labeled parallel to the axis.

f) **Equations** should be labeled with consecutive number and mentioned by label in the text, for example, "Equation (1).

g) **Physical data** should be quoted with decimal points and negative exponents (e.g., 25.8 J K^{-1} mol^{-1}), and arranged as follows where possible — but in any event in the same order within the manuscript.

h) **Nomenclature, symbols, and units**: The rules and recommendations of the International Union of Pure and Applied Chemistry (IUPAC), the International Union of Biochemistry (IUB), and the International Union of Pure and Applied Physics (IUPAP) should be adhered to. The Latin names of biological species and genera should be written in italics, with the full name always used when it appears for the first time in the text (e.g., *Homo sapiens*); the abbreviated form (e.g., H. sapiens) may be used thereafter.

i) **Supporting Information and Acknowledgements**: A Supporting Information notice and the Acknowledgements can be inserted after the main text and experimental section of the manuscript.

j) **Manuscripts containing animal experiments** must include a statement in the Experimental Section to state that permission was obtained from the relevant national or local authorities. The institutional committees that have approved the experiments must be identified and the accreditation number of the laboratory or of the investigator given where applicable. If no such rules or permissions are in place in the country where the experiments were performed, then this must also be clearly stated.

k) **Manuscripts with experiments with human subjects or tissue samples from human** subjects must contain a disclaimer in the Experimental Section to state that informed signed consent was obtained from either the patient or from next of kin.

Electronic Proofs

One of the corresponding authors will receive galley proofs. As a corresponding author, the contacted author is responsible for ensuring that all necessary authors are aware the proofs are ready for review. Please avoid having multiple authors access the proofs simultaneously. Corrections should be returned to the editor within three days.

Submission Checklist

You can use this list to carry out a final check of your submission before you send it to the journal for review. Please check the relevant section in this Guide for Authors for more details.

Ensure that the following items are present:

One author has been designated as the corresponding author with contact details:

• E-mail address
• Full postal address

All authors and their affiliations including the address of the affiliations should be listed

All necessary files have been uploaded:

Manuscript: The Manuscript file should be uploaded to the Editorial System in a Word .doc or .docx file format

• Include keywords
• All figures (include relevant captions)
• All tables (including titles, description, footnotes) should be editable (not an image) and uploaded in a .doc or .docx file format
• Ensure all figure and table citations in the text match the files provided
• Indicate clearly if color should be used for any figures in print

Graphical Abstracts / Highlights files (where applicable)
Supplemental files (where applicable)

Further considerations

• Manuscript has been 'spell checked' and 'grammar checked'
• All references mentioned in the Reference List are cited in the text, and vice versa
• Permission has been obtained for use of copyrighted material from other sources (including the Internet)
• A competing interests statement is provided, even if the authors have no competing interests to declare
• Journal policies detailed in this guide have been reviewed
• Referee suggestions and contact details provided, based on journal requirements

Call for Paper

The *Journal of Biosciences and Experimental Pharmacology* provides rapid publication of articles in all areas of Pharmaceutical Sciences. The Journal welcomes submission of manuscripts that meet the general criteria of significance and scientific excellence. Papers will be published approximately one month after acceptance. *Journal of Biosciences and Experimental Pharmacology* will be published twice a year and all articles are peer-reviewed. The following types of papers are considered for publication:

- Original articles on basic and applied research.
- Critical reviews, surveys, opinions, commentaries and essays.

Our objective is to inform authors of the decision on their manuscript(s) within four weeks of submission. Following acceptance, a paper will normally be published in the next issue.

Open Access

One key request of researchers across the world is unrestricted access to research publications. *Journal of Biosciences and Experimental Pharmacology* is fully committed Open Access Initiative by providing free access to all articles (both Abstract and full PDF text) as soon as they are published. We ask you to support this initiative by publishing your papers in this journal.

Invitation to Review

Journal of Biosciences and Experimental Pharmacology is looking for qualified reviewers as members of its review board team. *Journal of Biosciences and Experimental Pharmacology* will serve as a great resource for researchers and students across the globe. We ask you to support this initiative by joining our Reviewer's team. If you are interested to serving as a reviewer, please send us your resume to journalbep@gmail.com.

Publication Alert

We will be glad to send you a publication alert showing the table of content with link to the various Abstracts and full PDF text of articles published in each issue.